

Structural evolution and active structures of Dezful Embayment in Zagros foreland basin deduced from balanced cross section and SAR interferometry

Yu-Ting Tai¹、Jyr-Ching Hu¹、Kuang-Yin Lai²、Ping-Jung Hsieh²

(1)Department of Geosciences, National Taiwan University、(2)Exploration and Development

Research Institute, CPC Corporation

Zagros foreland basin is about 1400 km long, 100-300 km wide, from southeast of Iran to eastern Turkey. This basin was formed since Miocene due to the oblique convergence between Arabian and Eurasian plates. The present-day convergent rate of two plates is about 20-30 mm/yr. The structural development and sedimentary environments greatly contribute to the formation of petroleum system in Zagros basin. At least 60 oil and gas fields have been found by the end of 2009. Therefore, realizing the structural evolution is beneficial to explore petroleum system. Here, we apply Move 2018 to restore the cross section in Dezful embayment to examine the reasonableness and understand the process of structural evolution. In addition, we project the seismic data and GPS data to understand the active structures in this region. Moreover, by using InSAR technique, the surface deformation could be observed appropriately. According to the result of restoration, major faults develop both in-sequence and out-of-sequence thrusting, the shortening is approximately 33 km and the long-term shortening rate would be 1.5 mm/yr parallel to the profile. The most active structure is Mountain Front Fault which accommodated 9.6 km shortening and led Kamarun Anticline to become fault-propagation fold. The GPS result projected to the profile shows Zagros foredeep fault accommodates an insignificant shortening in comparison with whole shortening rate of ~2 mm/yr across the foreland basin. We project earthquake data to correlate the seismicity with the active structures, the high seismicity is located near Mountain Front fault extended to the basement at depth about 20 km. We use multi-temporal InSAR to monitor the deformation patterns in main structures in foreland basin. The preliminary result shows the significant gradient of LOS velocity across the Zagros Foredeep fault, thus we suggest that this structure is active due to the creeping of weak detachment.

Keywords: Dezful embayment, restore cross section, detachment, InSAR, SBAS

The clumped-isotope geochemistry of exhumed marbles from the Hoping area, eastern Taiwan

Yi-Chia Lu¹、En-Chao Yeh²、Ling-Wen Liu¹、Thi-Mai Nguyen²、

Pei-Ling Wang³

(1)Department of Geosciences, National Taiwan University、(2)Department of Earth Sciences, National Taiwan Normal University、(3)Institute of Oceanography, National Taiwan University

The carbonate clumped-isotope thermometer has emerged as an innovative method to constrain the cooling rates and retrograde metamorphic histories of marble. The ‘apparent equilibrium blocking temperature’ recorded by the clumped isotopic composition of marble represents the results of deformation, water–rock reactions, and diffusion-controlled atomic mobility. For a better understanding of the thermal evolution demonstrated by marbles in the Hoping area, a total of 13 calcite marbles were sampled for bulk isotopic ($\delta^{13}\text{C}$ and $\delta^{18}\text{O}$) and clumped isotopic analyses ($\Delta 47$). Grain size, deformation, mineralogy, and element compositions of marbles were also determined via the observation of oriented thin sections, X-ray diffraction analysis (XRD), and energy dispersive spectroscopy (EDS) by Scanning Electron Microscope (SEM). Our results show that the estimated clumped temperatures of calcite marbles in the Hoping area range from 200 °C to 330 °C, which are not correlated with the grain sizes, deformation, and elemental compositions. Noteworthy, the $\Delta 47$ -based apparent temperature of calcite marble experiencing exhumation-controlled cooling rates should range between ~150 °C and 200 °C theoretically, which are lower than the estimated clumped temperatures for the calcite marble in the Hoping area. A plausible magma intrusion event and/or high uplifting rate could cause a higher $\Delta 47$ -based apparent temperature, but a further examination is still needed.

Keywords: Hoping area, marble, carbonate clumped-isotope thermometer

Slip inversion on the creeping thrust fault using geodetic data and repeating earthquakes

Wei Peng¹、Mathilde Radiguet²、Erwan Pathiere²、Kate Huihsuan Chen³

(1)Department of Earth Sciences, National Taiwan Normal University; Institut des Sciences de la Terre in Grenoble, France、(2)Institut des Sciences de la Terre in Grenoble, France、(3)Department of Earth

Sciences, National Taiwan Normal University

The Chihsang segment of Longitudinal Valley Fault (LVF) is characterized by both rapid surface creep and creeping at deeper depth. However, the slip inversion of the interseismic creep rate obtained using geodetic measurements does not have a good resolution at depth below 15 km, which indicates that the understanding of along-dip variation of aseismic creep is still very limited. In this study, we apply a static joint inversion that combines both geodetic data (GPS and InSAR) and seismic data (repeating earthquake) to better understand the interseismic creep. By taking advantage of the repeating sequences majorly occurring at depths below 15 km, we are able to explore more about the along-dip variation of aseismic creep. Using the data from 2007 to 2011, our slip model reveals an anti-correlation spatially between the interseismic slip and co-seismic slip of the 2003 M6 event. We also find that the mainshock of the 2003 M6 event occurred on the boundary between areas with high and low interseismic slip. This study provides a new approach of modeling the static creeping behavior, constrained using geodetic and seismic data, which might further improve the time-dependent seismic hazard.

Keywords: interseismic deformation, Chihshang fault, static inversion

Natural and experimental evidence of thermal pressurization and frictional melting during the 1999 Mw 7.6 Chi-Chi earthquake

Wen-Jie Wu¹、Li-Wei Kuo²、Chia-Wei Kuo³、Wei-Hsin Wu¹、

Hwo-Shuenn Sheu⁴

(1)Department of Earth Sciences, National Central University、(2)Department of Earth Sciences, National Central University; Earthquake-Disaster & Risk Evaluation and Management Center, National Central University、(3)Center for Advanced Model Research Development and Applications, National Central University、(4)National Synchrotron Radiation Research Center

Frictional melting and thermal pressurization (TP) can reduce the resistance of fault surfaces and thus govern rupture dynamics and energy partitioning. The hydraulic properties of surrounding rocks, relevant to the efficiency of fluid drainage during sliding, play a critical role in driving either frictional melting or TP in the principal slip zone. Frictional melting and TP have been documented to occur within the principal slip zone of the Chelungpu fault during the 1999 Mw7.6 Chi-Chi earthquake, but the triggering mechanism to which remains unclear. Here, we (1) conduct rotary shear friction experiments on saturated gouges from the Taiwan Chelungpu-fault Drilling Project (TCDP) under varied fluid drainage conditions and (2) compare the experimental products with the principal slip zones of the TCDP. All rotary shear experiments are performed at 1-m/s slip velocity, 18-MPa normal stress, and ~3-m displacement. Scanning electron microscope, focused ion beam-transmission electron microscope, synchrotron X-ray diffraction are conducted for microanalysis. Mechanical data shows that plateau-like peak friction (0.15~0.25) is followed by an ultralow steady-state friction (0.03~0.07) under undrained condition. Peak and steady-state friction are 0.4~0.5 and 0.08, respectively, under drained condition. The formation of distinct shear localization and amorphous materials indicates that frictional melting occurred under drained condition. In contrast, distributed shear and the absence of amorphous materials within the slip zone is recognized under undrained condition. Our experimental observation is consistent with the reported natural observation, suggesting the presence of heterogeneous fluid drainage along the fault zone during coseismic slip. Taken together, we conclude that both frictional melting and TP were operated on gouge because of the variation of fluid drainage and promote the slip in this position during the 1999 Chi-Chi earthquake.

Keywords: frictional melting, thermal pressurization, fluid drainage, Chelungpu Fault, Chi-Chi earthquake

利用曾文溪沿岸階地及碳 14 定年法分析台灣西南部崙後斷層及

口宵里斷層之活動特性

石智偉¹、黃文正¹、波玫琳¹、邱奕維¹、曾雅筑²、劉彥求³

(1)中央大學應用地質研究所、(2)臺灣師範大學地球科學系、(3)經濟部中央地質調查所

崙後斷層與其東側的口宵里斷層位於台灣西南部的台南嘉義一帶，兩者為比鄰的南北走向逆移斷層，前者向東傾，後者向西傾。該區的 GPS 資料顯示跨兩斷層具有每年約 1.5 公分的縮短量，本研究利用流貫本區的曾文溪，其沿岸的階地對比分析，探討崙後斷層及口宵里斷層的活動性及構造關係對此縮短量的可能貢獻。首先利用高精度數值模型進行地形判釋及測繪河階地，再輔以野外調查及 C-14 定年相互對比，並透過地質資料繪製地質剖面，藉以瞭解兩條斷層之關聯與活動特性。本研究根據地形資料分析將階地依相對於現生河道高程的高低分成七階，由高至低分別為 T1 (8 ka)、T2、T3 (3-4 ka)、T4a、T4b(2 ka)、T4c T5，綜合目前所獲得之 C-14 定年結果及前人定年資料，崙後斷層上盤 T4b 階地年代為 1878-1998 cal BP，下盤 T4b 階地年代為 1640-1820 cal BP，且階地高程相似，故推斷崙後斷層可能在 2 ka 以來無活動跡象。口宵里斷層上盤崙後斷層西側的 T3 階地年代為 3820-3446 cal BP，東側的 T3 階地年代則為 3005-3212 cal BP，階地高程差約 20-25 公尺，指示口宵里斷層於全新世內有活動，與其於劉陳尾截切約三千年前形成的階地之證據相符，然而 T3 階地可用定年資料橫跨兩條斷層，因此無法明確得知其抬升量是受崙後斷層或口宵里斷層所主導。為解釋其對於該區的縮短量，本研究綜合上述之野外觀察與定年資料，可得出兩種解釋，其一為崙後斷層因淺部傾角過高而鎖住無法繼續活動，形成口宵里背衝斷層向東逆衝；另一解釋為，因緊鄰崙後斷層西側的烏山頭背斜折曲至臨界點產生破裂，而形成向東逆衝的口宵里斷層，截切崙後斷層並切穿地表河階沉積物。

中文關鍵字：曾文溪、河階地、烏山頭背斜、崙後斷層、口宵里斷層、斷層活動性

GPU acceleration on geodynamic simulation via OpenACCEh Tan¹、Chase J. Shyu¹、Fang-Yi Lee²、Chih-Chin Lee¹

(1)Institute of Earth Sciences, Academia Sinica, Taiwan、(2)Institute of Oceanography, National

Taiwan University

Numerical simulation on geodynamic processes is computationally expensive. Pursuit of higher resolution and more accurate physical simulation requires more and more computation power. The speed improvement of CPUs has stalled in recent years. Moreover, the speed of memory access has improved only slowly in decades, which further reduces the performance of the simulation. The advance of GPGPU (General Purpose computing on GPU) can help to solve the performance problem. GPU provides quick memory access and fast context switch to hide memory access latency while keeps the computation units busy. Traditionally, the GPU and CPU have separated memory space. Programmers have to transfer data between GPU and CPU manually before and after the computation. The newer generation of Nvidia GPU provides unified memory space to avoid manual data transfers. Additionally, we can port the CPU codes to GPUs using a few lines of OpenACC directives. In the end, we completely ported out simulation code to GPU and achieved a 40x speed-up, compared to a single CPU performance. We will details the porting strategy and compare the similarity of OpenACC to OpenMP.

Keywords: GPU, numerical method, OpenACC

井下地震儀觀測 Pd 與 M_L 之關係

于子桓¹、林彥宇¹、陳達毅²

(1)中央大學地球科學系、(2)中央氣象局

地震預警系統已廣泛應用在台灣、日本及美國等地，為地震發生時拯救生命財產的一大利器。目前使用之地震預警系統以地表測站觀測資料為基準，利用 P 波位移波形前三秒之最大振幅推估地震規模(以下簡稱 Pd 值)，進而使用此資訊配合強地動衰減式估算各地震度。然地表站觀測波形可能會受到場址效應的影響，增加估計規模的誤差導致震度估計有所偏差，而井下測站儀器避開了鬆軟之淺層構造，大大降低場址效應的影響，可以有效的增加地震預警的準確性及效率。截至目前為止中央氣象局已於全台灣佈設了 52 個井下地震儀測站，其中包含強震站以及寬頻站。本研究蒐集 2018 年井下地震儀之強震地震資料共 522 個地震(966 筆垂直紀錄)，得到芮氏規模大於 4 之地震，其震源距 50 公里內的 Pd 與規模之迴歸式為 $\log(Pd) = -2.11\log(R) + 0.99M - 4.12$ 。此迴歸式得到的預測規模 M_{pd} 與觀測之芮氏規模 M_L 有良好的相關性，其關係式為 $M_L = 1.03M_{pd} - 0.02$ ，標準差為 0.15 低於前人的研究 0.18~0.23，未來將投入中央氣象局地震預警系統測試。

中文關鍵字：地震預警系統、Pd、井下地震儀



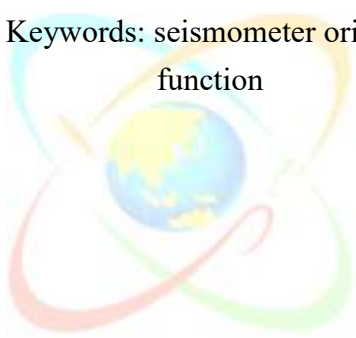
A comparison of methods for calibration of seismometer orientation

Wen-Tzong Liang¹、Chu-Te Chen¹、Teh-Ru Alex Song²

(1)Institute of Earth Sciences, Academia Sinica, Taiwan、(2)Seismological Laboratory, Department of Earth Sciences, University College London

Many seismological researches rely on precise seismometer orientation. To understand the performance of currently available methods based on teleseismic P-wave, Rayleigh wave, and receiver functions respectively, we have applied them to well calibrated broadband seismic stations in Taiwan. In general, seismic waveform data collected for distant earthquakes distributed at various back-azimuth is required for higher precision and accuracy. It seems that the P-wave particle motion can give a good result if the noise level is acceptable whereas the back-azimuth coverage does not change the orientation significantly. We are going to apply these methods to open data that is collected in Taiwan to enable a complete metadata for borehole or ocean bottom seismometers.

Keywords: seismometer orientation, observational seismology, seismogram, receiver function



Observations of separating first P arrivals as induced by mantle wedge fast anomalies beneath NE Taiwan

Yen-Hung Yu¹、Po-Fei Chen¹

(1)Department of Earth Sciences, National Central University

Using data from the Formosa Array (FMA), a dense seismic network covering North Taiwan with roughly 140 broadband stations, we observed that an earthquake (25.02°N, 121.86°E, 138 km) exhibits distinct two arrivals of P waves (two phases) for stations just above it. Having determined the two phase delayed times for FMA, results show a spatial radiation pattern decreasing from 1.6 seconds to zero outward the epicenter. In addition, this event is located on the Ryukyu subduction zone, where the Philippine Sea Plate subducts beneath the Eurasian Plate, and both the slab and mantle wedge exhibit the feature of fast P wave anomalies, which is also mentioned by previous publication of high resolution tomography on NE Taiwan (Su et al., 2019). Then, we conducted a study of tracing rays, and visualized them on the 2 D cross sections with multiple azimuth. Therefore, we find a positive correlation between the duration of delayed times and the length of rays passing through the fast P anomaly in the mantle wedge. As a result, we conclude that the two phase arrivals are induced by the fast anomaly in mantle wedge beneath NE Taiwan. Moreover, after comparing the data and ray paths of other adjacent events with weaker two phase arrivals, we can further confirm the conclusion. To figure out the causes of the two phase arrivals, the simulations of wave propagations will be simulated in the future.

Keywords: Formosa Array, northeastern Taiwan, anomalous waveform effects

3-D plate interactions beneath Taiwan orogeny from source-side seismic tomography

Po-Li Su¹、Hsin-Hua Huang²、Justin Yen-Ting Ko¹

(1)Institute of Oceanography, National Taiwan University、(2)Institute of Earth Sciences, Academia Sinica, Taiwan

We conducted unconventional joint local and teleseismic traveltime tomography, source-side seismic tomography, for improving regional 3-D P -wave velocity (V_p) structure beneath the Taiwan region down to ~400 km. The teleseismic data in this study are traveltime residuals of local earthquakes determined at distant stations instead of those from teleseismic events to local stations in the traditional teleseismic tomography. This provides a larger amount of the teleseismic data than before and a better raypath coverage at the upper mantle depths, benefiting from a much larger number and a more even distribution of the local earthquakes compared to those of broadband stations only placed on the surface in the study area. Our results show clear geometry of the subducting Eurasian Plate (EP) and Philippine Sea Plate (PSP) beneath Taiwan. In the south, the top interface of the high- V_p anomaly interpreted as the subducting EP extends eastward and downward to reach a depth of 450 km at a longitude of about 123°E. From central to northern Taiwan, the deeper part of the EP subducting beneath the PSP is progressively deformed, while the PSP continuously collides with the shallow part of the EP on the west and gradually subducts northward. The subducting EP becomes sub-vertical beneath northern Taiwan and seems to be detached as the PSP subducts below a depth of about 80 km.

Keywords: Taiwan orogeny, seismic tomography, subduction, tectonics

Three-dimensional Scattering Dominated Attenuation Models in Southern California

Yu-Pin Lin¹、Thomas H. Jordan²

(1)Institute of Earth Sciences, Academia Sinica, Taiwan、(2)Department of Earth, Planetary and Space Sciences, University of California Los Angeles, USA

Seismic attenuation is not only a powerful tool to constrain the physical state of the Earth's materials but also a crucial component to improve the accuracy of the ground motion simulations at higher frequencies ($f > 1$ Hz). Lin and Jordan (2018) indicated that the attenuation at high frequencies is frequency dependent with a power-law rate $\alpha=0.4$ and dominated by scattering from small-scale crustal heterogeneities in Southern California. In this study, we inverted the spectral-amplitude residuals between observations and synthetics for 3-D P - and S -wave attenuation structures from 660 regional earthquakes ($3 \leq M \leq 5.7$) recorded at 281 broadband stations of the Southern California Seismic Network (SCSN). The synthetic spectral amplitudes accounted for geometrical spreading, source excitation, and frequency dependence of Q . The 3-D Q_P and Q_S variations are inverted by the spectral ratios measured in the band 1-10 Hz. Results from independent inversions of the P and S datasets are strongly correlated. Our results show weaker attenuation in two more homogeneous batholithic blocks including Peninsular Ranges and southern Sierra Nevada and stronger attenuation in the vicinity of the San Andreas Fault and the Garlock Fault systems, which is dominated by the elastic waves scattering from the fracture structures around the faults. The Salton Trough displays the strong attenuation, which consistent with the high heat flow in the Salton Sea area. However, the low Q_P/Q_S indicates that the elastic scattering still dominates the attenuation observations in this region.

Keywords: seismic attenuation, elastic scattering, Southern California

Source investigation for earthquakes along Flores Thrust, IndonesiaDimas Sianipar¹、Bor-Shouh Huang²、Kuo-Fong Ma³

(1)Taiwan International Graduate Program (TIGP) Earth System Sciences, Academia Sinica and National Central University; Agency for Meteorology, Climatology, and Geophysics of the Republic of Indonesia (BMKG), Jakarta, Indonesia、(2)Institute of Earth Sciences, Academia Sinica, Taiwan、(3)Institute of Earth Sciences, Academia Sinica, Taiwan; Earthquake-Disaster and Risk Evaluation and Management Center (E-DREaM), National Central University

The south-dipping, low-angle Flores Thrust in Indonesia hosted damaging $M_w > 6$ earthquakes, including the 1992 M_w 7.7 Flores earthquake-tsunami and most recent the 2018 Lombok earthquake sequence that claimed more than 500 casualties and resulted in severe damages. However, the characteristics of the earthquake ruptures and their relations to regional tectonic were poorly investigated. Here we study the source time functions and possible rupture models of ten M_w 6.2+ earthquakes along Flores Thrust through finite fault inversions. Our inversions were constrained with the teleseismic body- and surface-waves and the updated information of the seismicity from both global and Indonesia regional seismic networks. The model uncertainties were computed by performing statistical jackknife tests. We find that cascading asperities ruptured neighbor fault patches in western Flores Thrust, including the 2002-2009 Sumbawa sequence (5 events) and 2018 Lombok sequence (3 events). The ruptures were often initiated from the mid-crust and propagated unilaterally. We discuss the idea that this cascading feature of moderate magnitudes (M_w 6-7) might be related to fault immaturity. The cluster of M_w 6-7 cascading earthquakes implies that the western Flores fault prohibited the growth of a single large earthquake ($M_w > 7$). We further discuss the rupture characters of the fault (e.g., initiation, the rupture speed, stress drop) by comparing the western and eastern Flores Thrust. The nature of shallow rupture of M_w 6-7 beneath the northern coast of island arcs favors the high seismic and tsunami hazard to the region. Thus, this study is essential to provide the rupture characteristics and asperity locations along the Flores Thrust necessary to evaluate the region's earthquake and tsunami hazard.

Keywords: asperities, finite-fault, Flores Thrust, rupture, source-time-functions

Linking K-feldspar $^{40}\text{Ar}/^{39}\text{Ar}$ geochronology with textures and compositions

Yu-Ling Lin¹、Tung-Yi Lee¹、Ching-Hua Lo²、Sarah C. Sherlock³、
Yoshiyuki Iizuka⁴、Tadashi Usuki²、Long-Xiang Quek¹、Punya Charusiri⁵

(1)Department of Earth Sciences, National Normal Taiwan University、(2)Department of Geosciences,
National Taiwan University、(3)School of Physical Sciences, Faculty of Science, Technology,
Engineering and Mathematics, The Open University, Milton Keynes, United Kingdom、(4)Institute of
Earth Sciences, Academia Sinica, Taiwan、(5)Department of Geology, Faculty of Science,
Chulalongkorn University, Thailand

K-feldspar $^{40}\text{Ar}/^{39}\text{Ar}$ geochronology has drawn a lot of attention for its moderate closure temperature in thermal history reconstruction and common occurrence in most lithologies. However, the complexity of K-feldspar $^{40}\text{Ar}/^{39}\text{Ar}$ step heating age spectrum raises difficulties in its age interpretation. The two plateau-like segments shape, one type of the K-feldspar spectra, was inferred as the result of excess argon contamination in the past. This study finds an alternative plausible scenario for such spectrum shape through petrologic and EPMA analyses on K-feldspars in a sheared leucogranite sample from the Mae Ping shear zone, NW Thailand. This leucogranite had rounded and fractured perthitic K-feldspar phenocrysts embedded by albite, and the largest grain can be up to 3 cm in length. Fine-grained K-feldspars at the pressure shadows and boudin necks of albite fishes have distinct textures and chemical compositions from phenocrysts. Two-feldspar thermometers suggest lower equilibrium temperatures of 266°C for the K-rich fine-grained K-feldspar, and higher equilibrium temperature around 373°C for Na-rich phenocrysts. Modeling with multi-diffusion size extractor indicates a high closure temperature of 350°C for the old, high temperature segment while a low closure temperature of 160°C for the young, low temperature segment. Therefore, the K-feldspar $^{40}\text{Ar}/^{39}\text{Ar}$ age spectrum with two plateau-like segments may result from the two major distinct diffusion domain sizes associated with Na-rich phenocrysts and K-rich recrystallized fine grains.

Keywords: K-feldspar, $^{40}\text{Ar}/^{39}\text{Ar}$ dating, EPMA, diffusion domain, closure temperature

Age and geochemical characteristics of the Cenozoic volcanic rocks in Pacitan area, East Java

Lediyantje Lintjewas¹、Yu-Ming Lai²、Iwan Setiawan³、Hao-Yang Lee⁴、
Andrie Al Kausar¹、Yoshiyuki Iizuka⁴、Long-Xiang Quek²

(1)Department of Earth Sciences, National Taiwan Normal University; Research Center of
Geotechnology, LIPI, Indonesia、(2)Department of Earth Sciences, National Taiwan Normal
University、(3)Research Center for Geotechnology, Indonesian Institute of Sciences、(4)Institute of
Earth Sciences, Academia Sinica, Taiwan

The subduction of Indian-Australian oceanic crust beneath the Eurasian plate produced the Cenozoic volcanoes on Java Island at the SE Sundaland. Two Cenozoic arc chains are identified on Java: The Late Eocene-Early Miocene volcanic arc that formed the Southern Mountains known as the 'Old Andesite'; another is the modern volcanic arc that has been active since the Late Miocene and erupted in the central part of Java Island. The Pacitan area is a part of the Southern Mountains, and this study focuses on the volcanic rocks in this area to recognize the magmatic stages and identify the geochemical variations from different stages. We identify two magmatic period in the area, Late Oligocene (26.0-26.7 Ma) and Middle Miocene (12.0-13.0 Ma) using the zircon U-Pb method. Our age results are younger than the previous results from the K-Ar method (28 Ma and 15-19 Ma, respectively). The Late Oligocene volcanic rocks vary from andesite to dacite, and are comparable to medium to low-K calc-alkaline volcanic rocks. The Middle Miocene volcanic rocks vary from basalt to dacite, and comparable to high-K calc-alkaline to tholeiitic volcanic rocks. Nb/U–Nb, Ce/Pb–Ce diagrams, and the depletion of HFSEs (Nb, Ta, and Ti) shows arc characteristics in these volcanic rocks. The LILEs (such as Cs and Rb) and Pb enrichment in the Late Oligocene rocks are significantly lower than those in the Middle Miocene rocks. These results may be because of the different effects of the subduction-related fluids between these two stages in Java Island.

Keywords: Java island, Southern Mountain, Cenozoic magmatism, Old Andesite, Zircon U-Pb dating.

萜類化合物與古植物學鑑定化石樹脂植物來源

張世正¹、張英如¹

(1)臺灣海洋大學地球科學研究所

化石樹脂是古代的植物分泌物也是琥珀以及柯巴的總稱，經過長時間掩埋、溫度以及壓力作用下所形成的脂狀物，其中萜類化合物組成記錄著植物來源之訊息，可做為化石樹脂之生物指標，故可藉由有機地球化學分析方式，探討其植物來源。本研究利用傅立葉紅外光衰減全反射光譜(Fourier transform infrared - attenuated total reflection spectroscopy, FTIR-ATR)以及熱裂解氣相層析質譜儀(Pyrolysis Gas chromatography-mass spectrometry; PY-GC-MS)分析來自拉脫維亞、緬甸、馬達加斯加、多明尼加以及印尼之化石樹脂。FTIR-ATR 的初步成果顯示於 2955 cm^{-1} 以及 2870 cm^{-1} 甲基以及亞甲基的對稱收縮訊號，1700 cm^{-1} 有來自醛、酮的 C=O 拉伸的訊號，1600 cm^{-1} 則為 C=C 官能基訊號，1451 cm^{-1} 以及 1385 cm^{-1} 則有來自環己烷甲基之 C-H 鍵的彎曲震動，1150 cm^{-1} 到 1050 cm^{-1} 有 C-O 伸縮震動且拉脫維亞在此有一特徵峰 “Baltic shoulder”，馬達加斯加的樣本於 887 cm^{-1} 則有 exocyclic methylene。PY-GC-MS 的初步成果顯示，拉脫維亞的樣本含有顯著 succinic acid 化合物以及 abietan、pimaran 的二萜類化合物(diterpenoid)，植物來源可能為金松科的裸子植物；緬甸的樣本則含有 fichtelite、phyllocladane type 二萜化合物且缺少 labdane，植物來源高機率為南洋杉科；多明尼加以及馬達加斯加則含有 enantio labdane 的化合物，其植物來源可能為被子植物中的豆科植物；印尼的化石樹脂成分含有倍半萜類(sesquiterpenoid)的 cadelene 以及三萜類的 α -amyrin、 β -amyrone，由於缺少二萜類成分，故可推論本研究之印尼化石樹脂其植物來源可能為被子植物中的龍腦香科(Dipterocarpaceae)。本實驗可得知利用萜類化合物以及其官能基鍵結可有效分析化石樹脂的植物來源。

中文關鍵字：化石樹脂、萜類化合物、傅立葉紅外光衰減全反射光譜、熱裂解氣相層析質譜儀

Geochemistry of pore water around the Keelung Submarine Volcano, off northern Taiwan and its hydrothermal implication

Feng-Hsin Hsu¹、Chih-Chieh Su¹、Hsio-Fen Lee²、Yu-Shih Lin³、

Song-Chuen Chen⁴、Yunshuen Wang⁴

(1)Institute of Oceanography, National Taiwan University、(2)National Center for Research on Earthquake Engineering, National Applied Research Laboratories、(3)Department of Oceanography, National Sun Yat-sen University、(4)Central Geological Survey, Ministry of Economic Affairs

The Keelung Submarine Volcano (KLSV), located in the near-shore area of northern Taiwan, is the seaward extension of the Northern Taiwan Volcanic Zone, with most of the gas emissions concentrate around the northern border of the volcanic cone. In this study, we focused on the geochemistry of pore water with two sediment cores collected from both northern and southern borders of KLSV. Results showed that they were not only characterized by gas enrichment, but also revealed specific geochemical features of pore water, implying a significant influence of hydrothermal fluid. The elevated DIC and TA, lowered pH, and much heavier $\delta^{13}\text{CDIC}$ implied the high flux of volcanic CO_2 input. The downward decreasing of Mg^{2+} (<5 mM below 120 cm) and Cl^- (< 200 mM below 120 cm) in pore waters indicated an obvious mixing between seawater and hydrothermal fluid relative to the phase separation reaction. Based on two end-member mixing model of Mg^{2+} , the highest fraction of hydrothermal fluid is estimated to be 92.2%. Furthermore, extremely high concentrations of Li^+ were observed in pore waters (>2.0 mM), which means the sampling locations are related to high-temperature (>350 °C) rock/sediment-fluid interaction. The end-member values of volcanic fluid are estimated to be 2.12~3.35 mM with an average of 2.52 ± 0.29 mM, which is close to the estimates of hydrothermal field in the Okinawa Trough. All the geochemical results in pore water reflected the importance of secondary modification processes after high-temperature water-rock interaction, especially the interaction between hydrothermal fluid and sediment.

Keywords: Keelung Submarine Volcano, sediment-hosted hydrothermal system, pore water

Sources and budget of dissolved inorganic carbon in the deep water of the southern Okinawa Trough

Yu-Shih Lin¹、Li-Hung Lin²、Tefang Lan²、Chih-Chieh Su³、
Hsiao-Fen Lee⁴、Bo-Shian Wang⁵、Song-Chuen Chen⁶、Yunshuen Wang⁶、
Wei-Jen Huang¹

(1)Department of Oceanography, National Sun Yat-sen University、(2)Department of Geosciences, National Taiwan University、(3)Institute of Oceanography, National Taiwan University、(4)National Center for Research on Earthquake Engineering, National Applied Research Laboratories、(5)Taiwan Ocean Research Institute, National Applied Research Laboratories; National Academy of Marine Research、(6)Central Geological Survey, Ministry of Economic Affairs

The West Philippine Sea (WPS) intermediate water enters the Okinawa Trough via the near-bottom layer of the Kerama Gap. This overflow ventilates the deep basin (≥ 1000 m) of southern part of the trough, where southwestward currents near the seafloor have been documented. Hence, the deep water in the southwest corner of the Okinawa Trough (southern Okinawa Trough, SOT) likely records the cumulative input of materials from different sources since the water leaves the Kerama Gap, and can be used to assess the basin-scale inventories of these sources. In this study, we measured the dissolved inorganic carbon (DIC) concentration, stable carbon isotopes of DIC ($\delta^{13}\text{CDIC}$), and helium isotopes ($^3\text{He}/^4\text{He}$) of the SOT deep water collected in locations both with and without active venting. Compared to the WPS water of the same potential density, most SOT samples exhibit a significant level of excess DIC, elevated $^3\text{He}/^4\text{He}$ ratios, and depletion in $\delta^{13}\text{CDIC}$ values. A mixing model that takes all three parameters into account was developed to quantify the contribution of different sources. It was found that the measured $\delta^{13}\text{CDIC}$ values can be better reproduced when methane oxidation, a process that produces ^{13}C -depleted DIC, was included as a source. Model outputs show that hydrothermal discharge was the main source ($51\pm 25\%$) of excess DIC, followed by diagenesis ($33\pm 29\%$), and methane oxidation ($16\pm 16\%$). Ongoing work includes assessing the budget of DIC and other carbonate chemistry parameters in the deep basin.

Keywords: dissolved inorganic carbon, hydrothermalism, diagenesis, methane oxidation, back-arc basin, southern Okinawa Trough

新竹客雅溪 2017 年河水與底泥汙染物質的時空分佈

魏國彥¹、黃許麗娟²、顏春蘭³

(1)臺灣大學地質科學系、(2)工業技術研究院綠能與環境研究所、(3)環保署環境檢驗所

客雅溪流經新竹科學園區與新竹市區，環保署為監測工業排放與生活污水的汙染潛勢在 2017 年分三次採集該溪河水與底泥，進行主次要與微量元素的分析，並對結果做主變量分析，從 55 個水與底泥標本中辨識出四個相似的元素組合，各組合依序解釋了多變量數據資料中的最大量變方，其百分比依序大約為：38%、20%、15%、7%。其元素組合、分佈及意義分述於下：

第一組合（鉍、鈷、鐵、鎳、鈇）解釋了最大量的數據變方，時空分佈也最廣，暗示有污染源存在於客雅溪上游與下游，而河川出海口的底泥有較高含量的此組合元素暗示河口的污水處理廠處理未完全，仍有汙染潛勢。

第二組合（銅、鎳、汞、鎳、磷、鎳、鎢、銻、鈦）以銅、鎳為最大宗，主要分佈於中、上游，暗示來自客雅溪上游與南門溪的工業。

第三組合（硼、鋰、鋇、鈣、銀）指出現於河川中游的底泥，推測與該地的紙廠早年排放有關。

第四組合（錫、鋅、銻、鎘）只發現於中游的頂點區域，暗示來自鳳凰橋以上更上游的工業排放，且與新竹科學工業園區無關。

2017/10/11 科學園區可能排出銻 In、錫 Sn（第四組合元素）。同日中山橋水樣亦含較高之銅 Cu、汞 Hg、鎳 Ni、磷 P（第二組合），可能係生活廢水及其他汙染源所造成。兩者分別暗示科學園區及其他廠商/廢水處理廠商可能利用 10 月 10 日國定假期執法空窗期偷排廢水。

2017 年客雅溪雖出現各汙染物質，但其濃度並未超出河川水水質與底泥品質的管制標準，表示只有輕度汙染。

上述這一套在定點、不定期採集河水與底泥標本進行化學與統計分析的方法不失為一個監測工業都市河川汙染的良好方法。

中文關鍵字：重金屬、都市河川、汙染監測、主變量分析

解密太平洋最大規模史前遺址

沈川洲¹、Felicia Beardsley²、宮守業³、Yusuke Yokoyama⁴、劉司捷¹、
姜宏偉¹、Zoe T. Richards⁵、Jean-Paul A. Hobbs⁶

(1)臺灣大學地質科學系、(2)College of Arts and Sciences, University of La Verne, USA、
(3)國立自然科學博物館、(4)Atmosphere and Ocean Research Institute, Tokyo University, Japan、
(5)Department of Aquatic Zoology, Western Australian Museum, Australia、(6)School of Biological
Sciences, Queensland University, Australia

現代人(智人, *Homo sapiens*) 出走非洲後, 最後抵達太平洋島嶼, 幾千年來, 發展出多樣的文化, 現今許多海島上還保存許多史前遺蹟, 例如復活節島上的巨石人像群、科斯雷島上的珊瑚金字塔等, 而在密克羅尼西亞的波納佩島(Pohnpei) 的東部海岸, 則有一座稱為南馬都爾(Nan Madol) 的廢棄古城, 占地約 18 平方公里。由於它是以超過 100 座皆使用柱狀玄武岩和珊瑚砌造而成的人工島與運河所組成, 因此也被暱稱為「太平洋的威尼斯」。這個人類在太平洋上最大規模的遺址, 於 2016 年 7 月由聯合國教科文組織正式認定為世界文化遺產。

南馬都爾是紹德雷爾王朝(Saudeleur Dynasty) 的首都, 自 1965 年第一批碳十四定年報告出爐, 迄今已累積超過 50 年的定年資料。據此推論該王朝可能興建於 1100-1200 年之間; 並在 1500-1600 年間, 因王朝被推翻, 遭到棄用而荒廢。但是確切的建造和廢棄時間, 學界則尚無定論。

為了解開南馬都爾的謎團, 我們團隊在 2016 年 7 月和 2018 年 1 月, 於 14 個有代表性的人工島上採集超過 150 個珊瑚標本, 篩選 148 個新鮮標本進行鈾釷定年。結果顯示南馬都爾的建造經過兩期大型工程, 第一期約在 900-1100 年之間, 規模較大的第二期則約落在 1150-1350 年。3 個最年輕的標本年齡為 1403±4 年、1410±9 年、及 1411±3 年, 顯示該城最後工程時間約在 15 世紀初。

國王居住的 Pahnkadira 島, 測定的 11 個珊瑚年齡落在 930-1403 年之間, 且分布狀況與所有標本的年齡特性一致; 有 4 個標本在 930-1140 年之間, 6 個標本集中在 1220-1340 年, 最年輕的標本則是 1403±4 年。珊瑚鈾釷年齡與過去發表的遺址碳十四年齡分布相符, 說明珊瑚年齡應可代表南馬都爾的歷史。

綜合分析後推論, 該址的大規模建造約始於 10 世紀, 比過去的認知早了 200 年, 第二次大型工程在 12 世紀中葉到 14 世紀, 持續約 200 多年。王朝崩落, 南馬都爾被棄用的時間應在 15 世紀初期, 比先前的推估早了 100-200 年。

中文關鍵字: 太平洋的威尼斯、南馬都爾、鈾釷定年

左營舊城附近區域的古環境變遷研究

游玉璇¹、齊士崢¹、顏君毅²、吳柏霖²、陳佳宏¹

(1)高雄師範大學地理學系、(2)東華大學自然資源與環境學系

國立成功大學考古學研究所在 2019 年的「高雄市左營區鳳山縣舊城(城內空間)考古調查發掘暨展示研究計畫」中，於小龜山西南側探坑裡發現清代鳳山舊城的夯土磚土城結構與上覆的人為擾動層間，有一厚度約半公尺的塊狀砂層，由此所採集的碳屑年代約為距今二百年前，故推論砂層的堆積年代應是在土城廢棄到新建砵石城之間。由於此砂層無明顯層理並夾有許多貝殼、碳屑和陶片碎塊，疑似為洪水事件所造成，並且也與南部地區盛傳的「加藤港」古海嘯事件年代相近，因此本研究透過地質鑽探取得的六支 8 公尺長岩芯，進行沉積特徵判釋、粒徑分析、micro XRF 分析、岩象分析和放射性碳十四定年等工作，解釋沉積環境變化及進行古環境指標分析，重建左營舊城區域的古環境變遷過程、解釋環境變遷的原因，進一步探討土城上覆的砂層來源、成因，以及討論是否和《台灣采訪冊》記載「加藤港暴漲」事件有關。

中文關鍵字：左營舊城、古環境變遷、加藤港暴漲



台北陽明山夢幻湖沉積物所紀錄的古湖沼變遷

汪良奇¹

(1)中正大學地球與環境科學系

本研究分析於 2017 年鑽取於陽明山國家公園夢幻湖長達 300 公分沉積物內的花粉與炭屑紀錄，以重建該區古植群與古火災紀錄。根據岩性、放射性碳十四定年、與花粉含量結果推測，岩心下部 120 公分厚（180-300 公分）的沉積物為單次事件所堆積，可能與在 4360 cal BP 所發生的山崩或土石流事件有關。花粉以禾本科與莎草科花粉為主，顯示夢幻湖周圍自 4360 cal BP 以來為陸生草地植物與濕生草地植物相互演替，森林覆蓋度低。台灣水韭孢子在 1950-1530 cal BP 與近 1000 cal BP 連續存在於沉積物內，顯示當時穩定淺水溼地狀態。炭屑分析顯示較為頻繁火災主要出現在 4000 cal BP 之前與 2000 cal BP 以來，可能反應相對乾燥的氣候。

中文關鍵字：花粉、碳屑、古火災



重建一萬一千年來三星妹池之古氣候

劉邦權¹、汪良奇¹、Ludvig Löwemark²

(1)中正大學地球與環境科學系、(2)臺灣大學地質科學系

三星妹池位於宜蘭縣南澳鄉，為三星池旁的濕地。海拔 2100m，鄰近山地植群隨海拔高度變化明顯分帶。分別為高山植被帶（3500m 以上）、亞高山植被帶（3000~3500m）、上部山地植被帶（2000~3000m）、山地植被帶（1000~2000m）及下部山地植被帶等。由於百年來森林砍伐，目前三星妹池周圍森林樹種組成以人工造林的紅檜與扁柏為主。

本研究使用三星妹池中 2.5 公尺的沉積物，沉積物中花粉含量豐富，並擁有良好定年控制的 11 個 ¹⁴C 定年資料以及 16 個 ²¹⁰Pb 的定年資料，顯示三星妹池為研究並分析過去一萬一千年來台灣東北部的環境變化的良好地點。其中 ¹⁴C 定年使用日曆年校準曲線 INTCAL20，校正後的年代為 cal BP (0 cal BP=1950 AD)。花粉圖譜使用深度對應花粉百分比製作，花粉百分比則是陸生花粉總數為分母。

除了使用花粉資料以外，本研究也使用碳屑資料，根據前人研究，碳屑可以反應當地的火災事件，透過 CharAnalysis，可以將連續碳屑資料中的火災事件以及火災頻率計算出來。

使用 stratigraphically constrained cluster analysis 分析花粉百分比，可劃分為五個孢粉帶，其中 Zone 3 可分為兩個子帶。(Zone 5：11130-10420 cal BP、Zone 4：10420-7960 cal BP、Zone 3-B：7960-4000 cal BP、Zone 3-A：4000-3410 cal BP、Zone 2：3410-790 cal BP、Zone 1：790 cal BP-現代)。結果顯示，三星妹池沉積物內所保存花粉約有 42 種，其中木本植物以 *Alnus*、*Quercus*、*Tusga*、*Pinus*、*Trochodendron* 為常見樹種，草本植物與蕨類則以 *Cyperaceae*、*Poaceae*、*Monolete* 及 *Trilete* 最為常見。

本研究中使用主成分分析花粉百分比，可以得出 PC1 這個指標，代表溫度。根據主成分分析結果、各孢粉帶的組合以及碳屑分析的結果，可以得知在 11140 cal BP 後，氣溫逐漸降低，濕度一直都很低，且有火災事件的發生。直到 10400 cal BP，氣溫持續降低且溼度還是很低，在 9900 cal BP，達到最冷的時期，後持續變暖變濕到 7900 cal BP，而這段時間中都無火災事件。而 7900-4000 cal BP 持續了一段穩定且溫暖且潮濕的時期但這段期間內無火災事件。直到 4000 cal BP 有溫度急遽下降後急遽上升但濕度維持在高值，溫度較 4000 cal BP 之前高，且溼度依然很高，而這段期間內無火災事件。3410 cal BP 後氣溫維持穩定但濕度降至極低，此時火災事件頻率增加，而濕度則是 1620 cal BP 後開始維持定值。到了接近現代，火災事件有大幅增加的趨勢。

中文關鍵字：氣溫、濕度、花粉、孢粉分析、孢粉帶

迭代邊界回歸面地面點標記法對無人機載光達地面點雲分類的影響

孫正璋¹、詹瑜璋²、張國楨³、江晉霆²、胡植慶⁴

(1)中央研究院地球科學研究所、臺灣大學地質科學系、(2)中央研究院地球科學研究所、

(3)臺北科技大學土木工程系、(4)臺灣大學地質科學系

隨感測器技術進步與小型化，高性能的光達系統可掛載至小型無人機上，相對於以過往空載光達的資料，點雲密度增加超過百倍，可使地形與地上物的測繪更加細緻，但如此綿密的點雲資料已可以觀察到垂直方向上的測量誤差分布，需要不同的演算法來取得地面點雲。

本研究為了處理前述的點雲特性，設計了迭代邊界回歸面地面點標記法，結合使用移動窗格、迭代坡度擬合、地面點雲候選標記等三個步驟，給予每個點評分，在最終以視覺化呈現後，設定一門檻後即可將地面點雲選出。

研究區域選擇宜蘭縣大同鄉梵梵地區，擁有竹針葉混淆林、邊坡、柏油路面、河灘地等多種地形提供分析，以無人機載光達系統並以仿地飛行方式對地區進行測繪，進行標準化的前處理後，即以迭代邊界回歸面地面點標記法對點雲進行標記。

演算法中移動窗格對於不同的地形有明顯不同的表現，本次研究將取兩種地形：混淆林區與邊坡進行演示，設定從 0.5 米至 2 米共三種不同的移動窗格尺寸，對點雲進行標記，並且以不同的門檻值選取地面點雲後，將地面點雲製作成不同尺度的 DEM 呈現。

根據前述流程後處理的結果發現，針對坡度變化不大、有樹林存在的地區，較大的移動窗格對地面點選取的較佳，較可包容因樹木等實體阻擋導致部分區域無測量點的「房屋效應」狀況；而對於短距離內坡度變化較大的地形，則以較小的移動窗格進行分析標記，較可以正確標記坡度變化的邊緣附近的地面點。最終取點的門檻值也對於地形有所不同，針對密林區，因有房屋效應的影響，在過程中特定窗格可能會發生標記錯誤的狀況，但因有移動窗格掃描分析，選用較高的門檻值即可濾除這些不正確標記的點雲；在地形坡度變化較大的地區，則可以降低門檻值，以保留更多邊緣細節。

在移動窗格大小的選取、門檻值選取與處理時間之間取得平衡是重要的課題，未來工作希望對於不同地形特性的點雲資料進一步分析，找出最佳化的參數，提供地形分析、防災、地質判釋等多樣的應用。

中文關鍵字：點雲、地面點雲分類、光達、無人機

無人機光達點雲資料評估及差異分析

陳奕霖¹、張國楨¹、曾俊偉²

(1)臺北科技大學土木與防災所、(2)行政院農委會林業試驗所

近年來由於遙測技術的進步，測量方式由傳統的水準儀及全測站測量一分鐘3個點演變至利用雷射掃瞄測距一秒鐘量測數十萬個點的光達技術；以往光達掃瞄儀本體重量且體積大，需要搭配航空飛機執行測量任務，不僅花費時間長、空間上的限制也多，於是發展出能搭載在無人飛行載具(Unmanned Aerial Vehicle)無人機光達，以求更快速且便利的測量，並能夠將空間資料收集的精確及完整，彌補空載光達在細微處辨識不足的地方。

本研究位置位於宜蘭的丸山遺址，使用無人單旋翼直升機 VAPOR55 及無人多旋翼直升機 DJI M600 Pro 分別搭載 RIEGL VUX-1、miniVUX-2 進行光達掃瞄作業。完成掃瞄後首先針對不同光達掃瞄出來的點雲進行空間上的精度評估及分析，探討不同無人機光達之間所存在的差異；而後利用點雲建製數值地形模型，了解無人機光達在使用不同 DTM 製作軟體上所形成的差別。

透過本研究的空間資料取得及分析比較，可以得知不同無人機光達在各無人飛行載具上的特性，針對研究區域提供精確、高解析度之數值地形模型，提供易於辨識的地形、地貌，進而評估無人機光達在土地使用概況、維護管理、防災規劃及後續地形差異監測等狀況。

中文關鍵字：無人機光達系統、點雲差異、精度分析、數值地形模型

井下原地深層地熱流體取樣設備：GTFSampler

謝佩珊¹、林鎮國¹、張裕德¹、呂學諭²、楊燦堯³

(1)工業技術研究院材料與化工研究所、(2)中正大學地球與環境科學系、(3)臺灣大學地質科學系

本團隊已成功研發一套井下原地(in-situ)深層地熱流體取樣設備，名為 GTFSampler (Geothermal Fluid Sampler)，並建立流體分樣與組成分析流程。GTFSampler 主要由一個不鏽鋼取樣瓶與一組氣體驅動閥門(shut-in valve)所組成，並安裝在不鏽鋼保護護套中；氣體驅動閥門與不鏽鋼管連接，不鏽鋼管除了用來懸吊取樣器，另一個重要功能為由地表控制管內氣壓，來打開與關閉氣體驅動閥門，進行流體取樣；GTFSampler 另有搭配一支留點溫度計，以量測記錄井下最高溫度。GTFSampler 已於 2013-2014 在宜蘭清水地熱 IC-19 號井深度 800 m 處測試，進階改良版亦於 2020 年於清水 IC-13 號井深度 1100 m 處測試，以上測試皆成功取得原地地熱流體，並完成地化組成分析。為了要確認取出的原地深層地熱流體保留了位於該深度的特性，本團隊利用 IC-19 號井的地熱流體地化組成分析結果，來計算 800 m 取樣深度的理論熱力學平衡溫度，並與留點溫度計實際量測的溫度進行比對。比對結果顯示，清水 IC-19 號井在噴流狀態下 800 m 處的現地量測溫度落在約 190~198°C，而理論計算溫度則落在約 185~210°C，相符的結果證實了 GTFSampler 取樣地熱流體的代表性。測試結果另顯示在閉井狀態下無法獲得合理的理論平衡溫度，推測是閉井時井內流體所產生之自然對流，影響了該深度的地熱流體原始化學組成，故建議進行原地深層地熱流體取樣時，應在噴流狀態下進行。目前 GTFSampler 的最深成功取樣深度為 1100 m，應可推進到 2000 m 深，但限於目前所使用的 O-ring 耐溫限值，取樣環境溫度極限為 250°C。GTFSampler 除了應用在地熱資源開發，也可在一般溫度的井下進行深層流體原地取樣，應用的領域包括：二氧化碳地質封存、核廢料地質處置、地下水探勘等。

中文關鍵字：井下取樣、地熱流體、清水地熱

斜張型盆地油氣田地質模型建立方法

馮力中¹、王銘浩²、蕭從文¹

(1)台灣中油探採事業部、(2)Schlumberger

在全球的產油盆地中，斜張型盆地已發現大量的油氣田，是非常具油氣潛能的盆地類型，亦是台灣中油公司核心探勘目標之一。油氣田從發現進入生產階段，須藉由建立地質模型來描述油氣田儲集層分布，估計油氣蘊藏量，再依據模型佈置適當的生產井位，以最佳化油氣生產。

本研究以斜張型盆地油氣田為例，依據鑽井、震測資料建立地質模型。建模步驟主要為依據震測解釋之地層面與斷層面建立構造模型，按照測井對比之分層將構造模型分為四個地層區間，在水平與垂直方向上建立構造模型之網格，接著將屬性適當地填入構造模型的網格中。本研究利用(1)井資料統計；(2)震測逆推等兩種方法建立屬性模型，包含：岩性、孔隙度、滲透率與含水飽和度等屬性。岩性係依據測井曲線分為砂岩、致密砂岩與頁岩等三種岩性，從變異圖(variogram)統計結果設定其垂直與水平方向之延伸範圍，井資料統計方法在垂直方向可提供穩定的統計結果，但水平方向因控制點太少而無法取得合適的延伸範圍，僅能以經驗方式設定水平方向參數。利用震測逆推方法從震測振幅反推 P 波阻抗屬性，得到 P 波阻抗高者多為砂岩，P 波阻抗低者多為頁岩之關係，可用來做為岩性分布之趨勢，並改善水平方向變異圖之統計結果，依據此趨勢體計算岩性模型，接著按砂岩、致密砂岩與頁岩所對應的孔隙度分布，以岩性模型為趨勢計算孔隙度模型，再以孔隙度模型為趨勢計算滲透率模型，最後以滲透率模型為趨勢計算含水飽和度模型。

本研究建立之地質模型提供油氣田構造、岩性、孔隙度、滲透率與含水飽和度等三維模型，提供後續蘊藏量評估及油氣田開發模擬所需之數據，設計適當之開發計畫，期能降低鑽井成本並增加油氣田採收率。

中文關鍵字：地質模型、震測逆推、儲集層

整合井測與震波逆推方法應用於查德礦區 A 區塊

伍允豪¹、李健平¹、邱維毅¹、洪作緒¹、李沅銘¹

(1)臺灣中油公司探採研究所

非洲查德礦區為本公司積極探勘、佐證可採蘊藏量的海外經營礦區，並已進入開發生產階段。本計畫主要研究礦區中的 A 區塊，根據先前已有的探勘資料及近期新鑽探佐證與生產井的結果，經由多礦物組成分析、岩石物理模擬、類神經網路模擬橫波、岩石物理模板等井測資料分析，並利用新鑽井之鑽遇地層深度與井測進行合成震波比對、震測重新解釋、震波逆推（包含重合前/後及確定性/隨機性）等方法，進行滾動式更新地質模式。並搭配探勘資料庫設計與建立，以增加油藏量評估的可信度，結果可作為查德礦區生產開發與探勘永續經營方針訂定之重要依據。

中文關鍵字：井測分析、震波逆推、岩石物理模擬



利用高解析反射與折射震測來探測池上斷層幾何形貌

陳昱菘¹、郭陳浩¹、黃俊銘¹、郭炫佑¹

(1)中央大學地球科學系

池上斷層位於臺灣東部，為花東縱谷斷層系統的南段，全長約四十七公里，是臺灣地表潛移速率最明顯、快速的一條斷層。此區域是台灣活動斷層活躍的區域，先前已有不少的大地測量以及地球物理資料，然而先前的反射震測資料因震源與佈設展距限制，最多僅可看到 300 公尺深的資料。

2020 年 11 月，本團隊池上斷層實施反射與折射震測測線三條，利用反射震測獲取板塊邊界較深的構造影像及池上斷層幾何形貌，另一方面使用折射震測計算近地表的速度構造，實驗設計使用集線式受波器陣列 240 部以及震盪震源車施測，受波器間距為 4 公尺。其中 A 測線(錦園村)東西向穿越池上斷層，B 測線(萬安村)東西向佈置於斷層上盤，C 測線使用新式受波器 SmartSolo 以南北向連接 A、B 兩測線之間，測站間距為 10 公尺。值得一提的是，C 測線為本團隊首次使用攜帶式無線短周期地震儀於震測實驗上，擺脫以往線材約束，難以克服地形限制等問題，實為本團隊實驗技術突破的里程碑。

A 測線剖面沉積層的中間有凹陷的情形，且在凹陷處東側有疑似兩條破裂以及褶皺的情形。B 測線剖面的沉積層較為混亂，且在剖面東側相對於西側有明顯的抬升，判斷應是受力形成的隆起，且可看到斷層破裂到深處。而 C 測線剖面在淺處能看到有明顯的凹陷，且在深部也能看到有層面的訊號，整體資料能看到的構造相比更多，最多可看到的反射訊號可達約 900 公尺。

中文關鍵字：池上斷層、花東縱谷斷層、折射震測、反射震測

Carbon dioxide degassing around the Chihshang Fault and its implications for exploring earthquake generation process

Ching-Chou Fu¹

(1)Institute of Earth Sciences, Academia Sinica, Taiwan

Measurement of CO₂ degassing at the Chihshang Fault (CSF) in the Longitudinal Valley of eastern Taiwan was performed systematically with a high spatial resolution from a few tens to hundreds of meters. The distribution of CO₂ flux in the area appears as halo anomalies along with the fractures due to crustal leaks. The result revealed that CO₂ flux in the soil gas show anomalous values at the specific positions, and the trace of these anomalous values is coincident with the N-S trending CSF. The flux values of CO₂ in the study area ranged from 0.1 to 26.6 gm⁻²d⁻¹ indicate that faults can facilitate the upward flow of CO₂, with flux rates being greater where the higher densities of fractures occur. Further repeated or continuous measurements of CO₂ flux are critical for improving understanding of the dynamic processes on fault/earthquake generations and seismic activities during the pre-, co-, and post-seismic periods.

Keywords: CO₂ degassing, Chihshang Fault, earthquake generation



New approach in multi-scale adaptive mesh construction of 2D/3D Taiwan Models and traveltimes tomography

M. Syahdan Akbar Suryantara¹、How-Wei Chen¹

(1)Department of Earth Sciences, National Central University

Traveltimes tomography has been used for years. However, low resolution features due to structured mesh system usually prohibit its applicability of accommodating realistic suggestion and potentially large error involved during interpretation stage. Therefore, to avoid this limitations, unstructured adaptive mesh system is needed. A new approach for seismic traveltimes tomographic inversion or potentially suitable for other geophysical problems is tested. The goal is to reduce the geophysical uncertainty when merge different types of data which carry various degree of errors while incorporate accurate geographic information into the model. Shortest path ray tracing is implemented for unstructured Delaunay triangulation mesh system. Un-structured mesh system is designed follow Adaptive Mesh Refinement (AMR) scheme with intension to preserve multi-scale features of the model including topography, bathymetry, geological boundary, active fault traces, sensor location and available information of different velocity models. We show that such an unstructured adaptive mesh system can preserve detailed features of 2D Earth surface and then extend to 3D model of Taiwan. The implementation strategy in mesh generation process follow atomic meshing algorithm. Atomic lattice construction algorithm uses designate control points, its density distribution and cell size to perform refinement within particular regions to preserve discontinuous features. Automatic initialization of control points is based on the nominal distance field that derived from the gradient of a particular physical feature such as velocity or topography variations. In the region where the gradient is high, the cell size become smaller than those region where gradient is low. Forward seismic ray tracing for such mesh system also shows better coverage and accuracy. Consequently, incorporate all proposed approaches can produce more reliable traveltimes inversion result at the end.

Keywords: unstructured mesh, adaptive mesh system, atomic meshing, seismic ray tracing, traveltimes inversion

板岩片岩交界帶附近邊坡穩定與岩體工程特性探討 -

以南橫公路摩天下馬沿線為例

羅百喬¹、羅偉¹、潘立慈¹、李紫彤²、陳玟伶²、王泰典²、謝有忠³

(1)臺北科技大學資源工程研究所、(2)臺灣大學土木工程學系、(3)經濟部中央地質調查所

本文針對近年來南橫公路摩天下馬沿線之邊坡經常性崩塌路段，配合多時期遙測影像邊坡崩塌分佈篩選及查核邊坡失穩類型，再輔以路線地質測繪與岩體特性調查，進行板岩與片岩交界帶附近邊坡失穩與岩體工程特性的關係探討。研究成果顯示，大南澳片岩與板岩交界帶之岩體 Q 值低於兩側圍岩，岩體破碎，為邊坡岩體滑動、岩屑崩滑以及落石好發處，Q 值評分因子中以 RQD 以及 Jr 差異較明顯。而板岩層中，板岩、千枚岩及變質砂岩交界帶，其岩體工程特性變化一般不及褶皺出露處明顯；另，中視尺度褶皺軸部斷層、層間剪裂、密集裂隙等調適構造則造成岩體破碎，易成為岩屑崩滑、落石的發生源。片岩層中不連續面組之持續性不佳或呈波浪狀，填充物蝕變程度不高；中視尺度褶皺軸部與邊坡崩塌位置的關聯性不及板岩層。大比例尺路線地質圖以及褶皺各部岩體工程特性經詳細地質評估及採岩體評分法量化分級，有利於板岩與片岩交界帶邊坡穩定及大地工程等課題深入評估。

中文關鍵字：板岩、片岩、Q 法、岩體評分、岩性交界

公路邊坡破壞模式與因應治理方式－以中橫 63.4K 為例

康耿豪¹、黃明萬¹、施乃慈²、戴仲平³、呂正安³

(1)合昱工程顧問有限公司、(2)中興測量有限公司、(3)交通部公路總局第二區養護工程處

中橫公路受民國 89 年九二一地震與民國 93 年敏督利風災重創道路橋梁，該路段邊坡極為破碎，二十年內歷經重複致災後更顯地質脆弱，當地仍存有多處邊坡坍滑或崩落等災害點，常因強降雨、颱風、地震等造成山崩及土石流等誘發邊坡災害不斷，危及用路人安全。

本研究以中橫公路 63.4k 為例，利用多期航空照片、無人載具影像進行分析，輔以現地調查，該路段主要因上、下方邊坡的坑溝侵蝕，坑溝向源侵蝕及溝壁側向侵蝕以致溝壁坡面局部崩塌，提供土石料源影響下方道路安全；養護管理上透過邊坡分級列為優先關注邊坡，防災管理上則將該路段列為重點監控路段，配套有積極性預警、警戒及行動作為，搭配道路復建，以提升道路長期抗災應變能力。

中文關鍵字：邊坡破壞、中橫公路



Stochastic-based approach to uncertainty quantification of large-scale landslide

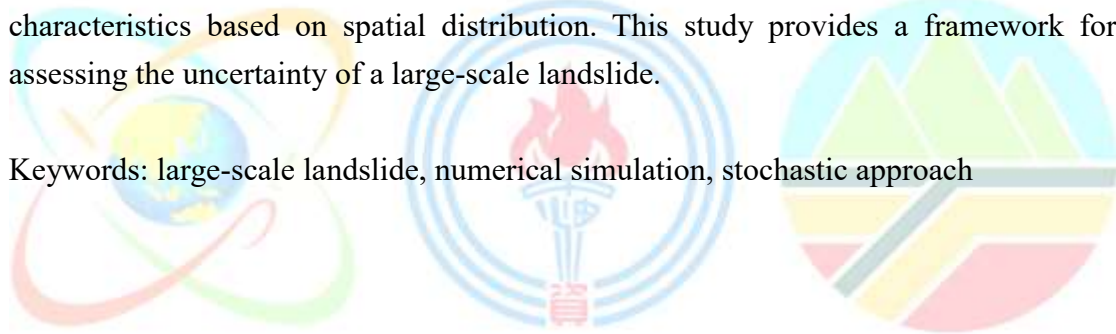
Kim-Tu Tran¹、Chuen-Fa Ni¹、I-Hsien Lee²

(1)Graduate Institute of Applied Geology, National Central University、

(2)Center for Environmental Studies, National Central University

Most assessments of landslide hazards are implemented by building the landslide occurrence risk maps. The levels of uncertainty in investigating the landslide occurrence depend on many significant factors, such as the model of the landslide area, the quality of data. The study presents a case study of the Lantai deep-seated landslide of the Taipingshan National Forest Recreation Area in northern Taiwan. The integration of the digital elevation model (DEM) and the numerical simulation is conducted to establish the three-dimension model, which allows evaluating deterministically landslide hazards based on the stochastic approach. According to the previous researches, the geological profile and hydrogeological profile are selected. Due to the limitation of the data, the study uses the naturally susceptible properties of material characteristics based on spatial distribution. This study provides a framework for assessing the uncertainty of a large-scale landslide.

Keywords: large-scale landslide, numerical simulation, stochastic approach



岩坡上楔型岩塊定位技術結合數位實境開發與應用

陳玟伶¹、李紫彤¹、王泰典¹

(1)臺灣大學土木工程學系

本文運用先進測繪技術，針對岩石邊坡建立數值表面模型，發展一套半自動辨識岩楔空間位置程序：透過不連續面判釋技術取得坡面上不連續面位置資料，藉由對應的數學式計算加以將不連續面分組而後區隔同組不同道平面，據以估計坡體中等值不連續面空間分佈，並研判各平面之相交性，完成邊坡岩楔自動萃取、可能墜落岩楔識別以及其潛在運動方向分析等作業，可於數值表面模型中定位潛在岩楔位置，提供露頭調查成果視覺化展現；繼而將岩坡數值模型中可能墜落岩楔視為特徵單元，應用數位實境技術介接岩楔幾何特性及空間分佈，作為監測作業觀察不連續面持續度延伸、開張狀況變化，以及數值模擬分析評估岩楔穩定度成果之檢核比對，架構岩坡數位實境監測平台雛型。本文並透過台 2 線濱海公路鼻頭路段、台 8 線中橫公路天祥附近邊坡測試所提技術，成效良好並具實務應用性。

中文關鍵字：不連續面、楔型岩塊、視覺化



精細測繪應用於落石邊坡脆弱度評估

李紫彤¹、陳玟伶¹、楊宜蓉¹、鄭富書¹、王泰典¹、劉曉樺²、
曹孟真³、黃奉琦⁴

(1)臺灣大學土木工程學系、(2)聯合大地工程顧問股份有限公司、(3)臺北科技大學資源工程所、
(4)財團法人台灣營建研究院

岩坡與地工構造物所處環境多為半無限域空間，結構具高度靜不定特性，破壞前異狀徵兆出現位置難於透過解析力學模態預測；加之岩坡失穩常具突發性，以致傳統點狀或線狀配置的監測作業效果受限。

在落石災害管理中，透過遙測分析敏感性及潛在落石位置至關重要，然將落石分析結果套用至真實邊坡時，難以客觀的定義危險區。本研究將 UAV 或地面光達點雲產製的高精度數值地形應用於視覺化不連續面調查、岩體評分以及數位實境地貌變異分析，應用於台灣東部天祥明隧道附近落石邊坡，透過點雲判釋露頭不連續面位態技術及檢定方法，檢核數值地形的適用性；基於點雲判釋不連續面結果，自動萃取關鍵岩楔，繼而應用岩體評分法-Q-slope 評估坡面脆弱度；最後採視覺化展現監測結果，達到整合岩盤工程地質調查成果、精緻化場址分區、三維視覺化模型展示以及大量數據彙整分析，提昇岩體工程特性調查評估、分析設計、建造以至於運營維管的精度與效能。

中文關鍵字：精細測繪、脆弱度、擴增實境、落石監測

以物理實驗探討微振動訊號與倒懸岩楔穩定性之間的關係

楊宜蓉¹、李紫彤¹、王泰典¹

(1)臺灣大學土木系工程學系

倒懸岩楔失穩墜落為邊坡路段以及坑道崖壁中最常發生的自然災害事件，此災害分佈範圍廣、突發性強且危害性大，然而山崩前兆並不明顯，導致早期預警技術一直難以實現。本研究首次引進微振動訊號特徵概念於邊坡穩定度預警系統中，並設計實驗室物理實驗，探討岩楔穩定性與微振動訊號之間的關係。發現岩楔處於穩定狀態時，微振動訊號頻譜呈分散狀，主要頻率對應振幅峰值不突出；當岩楔穩定度趨向些微不穩定狀態時，頻譜隨即有集中、頻率變小的趨勢，其最大振幅則大幅增加。此趨勢出現的時間，遠早於岩楔崩壞事件的發生時間。比起以往的山崩預警方法，利用微振動訊號分析，可以更早偵測到邊坡岩楔穩定性出現的細微變化，亦可以清楚辨識出高風險岩楔位置。此研究有利於日後評估邊坡路段致災風險以及偵測岩楔失穩位置，提供更早的災害預警，給予更充裕的時間施做邊坡安全補強作業，達到山崩早期預警的實質效果。

中文關鍵字：微振動訊號、穩定性評估、山崩早期預警



水下表面波震測施作參數規劃與低頻震源設計初探

林俊宏¹、吳孟哲¹、洪湘詒¹

(1)中山大學海洋環境及工程學系

我國近年來離岸工程的發展越發興盛，由港灣、海纜至風機基礎，乃至於箱網養殖之錨碇，皆與海床之工程性質息息相關，而為有安全穩定之設計，海床的工程性質調查扮演非常重要的角色，影響層面包括場域選擇、興建施工及運維。就現階段之應用而言，海洋地球物理技術主要在規劃階段協助調查工作，除了底床深度調查外，以反射震測類之聲學技術進行底床下之地質狀況調查(如底層剖面儀)為一重要應用，其可定性的顯示底床下方地質之不連續面，配合少數之鑽孔資料協助對地質之判讀，然而此些反射震測類之調查技術無法提供底床之工程性質。水下表面波震測可定量的提供海床之剪力波速，其可直接反映海床之強度、剪力模數、承载力等供地工設計使用之參數。國內目前尚未有相關技術之應用，作者為發展此量測系統，先行透過數值模擬探討水深、土壤參數以及不同施作方法對於水下表面波之行為影響，並據此評估較為合適的試驗系統規格與施作方法，透過數值模擬之初步研究結果顯示，震源應至少能產生最低頻率 5 Hz 之訊號，而接收器亦須至少能接收 5 Hz 之訊號，以收錄到足夠反映底床性質之特徵頻率段；另外，施作中採用定置式地聽器固定於海床上可有最佳收錄效果，若採用水聽器組成之 streamer，則建議離海床最遠不可高於 6 公尺(或是小於所收到蕭特爾波最大波長的 1/4)；而在資料前處理上，當震源遠離海床時，波傳路徑複雜，需將時間域非蕭特爾波的部分濾除可得到較佳之頻散曲線分析成果。而針對低頻率水下震源之開發，初步測試結果顯示，低頻含量與敲擊源之質量有關，質量越高低頻含量越高，將據此進行後續水下低頻震源設計。

中文關鍵字：水下表面波震測、施作參數、低頻震源

勵進南海首航之空氣鎗陣列近場訊號分析

鄧家明¹、林聖心¹、陳鼎仁¹、邱朝聰¹、葉一慶²、許樹坤²

(1)臺灣海洋科技研究中心、(2)中央大學地球科學系

在 2019 年 3 月勵進科學首航航次期間，與國立中央大學地球科學系合作，遠征前往南海中洋脊附近進行研究。在此航次期間，使用約 2 公里 (132 頻道數) 長的受波器浮纜，蒐集約 900 公里長的震測資料，震源系統所使用的空氣鎗為 SECREL 公司出產的 G. Gun II，較方便維護與操作，因此能夠在航次期間為了不同探測目標，在甲板上更換空氣鎗容積配置。此外，雖然空氣鎗容積僅有 1240 in³，但仍清楚的看到沉積層影像中的斷層與基盤等構造。其原因為此震源系統能量較集中，主要透過混合空氣鎗陣列容積與平行鎗簇的方式，提高 P/B (Peak to Bubble) 值，得到更清晰的沉積地層剖面。以南海首航 LGD1901-02 測線的震源訊號資料為例，從分析 4 串鎗簇近場之疊合訊號得知，其 P/B 值約介於 3.84-4.76 之間。進而，模擬遠場之直達波訊號，可發現其氣泡訊號幾乎消失，P/B 值約介於 21.99-32.63 之間。由此可知，此套震源系統能夠有效去除氣泡影響，提供乾淨的訊號。進而，統計此測線的整體 P/B 值，得知 P/B 值集中，67-70% 的 P/B 值落在 1 個標準差值內，且 95% 以上的 P/B 值落在兩個標準差值內，此數據顯示空氣鎗陣列震源訊號品質穩定。因此，使用此分析方式，不僅能夠證明此空氣鎗陣列配置的震源訊號品質，亦希望未來能夠將空氣鎗陣列調整至最佳配置，對於台灣周遭海域能源或地質災害潛勢的調查，提供學研界高品質的震測資料。

中文關鍵字：空氣鎗震源、長支距多頻道震測、勵進研究船

Tectonics of the Hualien Ridge and offshore extension of the Milun Fault

Lien-Kai Lin¹、Shu-Kun Hsu¹、Ching-Hui Tsai²、Yi-Ching Yeh¹、

Shiou-Ya Wang¹、陳冠廷¹、陳松春³、林筱珊²

(1)Department of Earth Sciences, National Central University、(2)Center for Environmental Studies, National Central University、(3)Central Geological Survey, MOEA, Taiwan

Located in eastern Taiwan, the Longitudinal Valley is generally considered as the collisional suture between the Philippine Sea and the Eurasian plates. To the northeast, the Philippine Sea Plate is generally considered to have subducted beneath the Ryukyu Arc. The corner between the eastern Taiwan and the Ryukyu Arc system is the transition from the plate collision to plate subduction of the Philippine Sea Plate. In consequence, the tectonics is complicated and the earthquakes are rather frequent. In this study, we use marine geophysical data to study the submarine Hualien Ridge that is situated in this plate collision/subduction transition. The Hualien Ridge is the offshore portion of the inland Milun Tableland; the Milun Tableland is uplifting and is bordered in the west by the active Milun Fault. Our results show that the Hualien Ridge can be tectonically divided into the active southern Hualien Ridge and the inactive northern Hualien Ridge. Several active faults trending $\sim N30^{\circ}E$ exist in the southern Hualien Ridge; some faults could be linked to the active faults in the Milun Tableland. The structures in the southern Hualien Ridge and the Milun Tableland display a pop-up structure that is subject to the oblique compression from the northwestward collision of the Philippine Sea plate. Moreover, the $\sim N30^{\circ}E$ trending structural faults are the results of the transpressional fault system. However, the Milun Fault, the western boundary of the fault system, probably terminates near $24^{\circ}04'N$, where a pronounced bathymetric structure trending $N300^{\circ}$ exists. On the other hand, in the northern Hualien Ridge we can only observe several blind normal faults covered by ~ 100 m thick sediments. Overall, The distinct separation of tectonic activity in the Hualien Ridge marks the transition from the actively plate colliding (convergence) to inactively convergence or partially subduction of the Philippine Sea Plate relative to the Eurasian Plate.

Keywords: Hualien Ridge, collision, subduction, sparker reflection seismic, Milun Fault

台灣北部貢寮外海之地質構造研究

林怡玟¹、許樹坤¹

(1)中央大學地球科學系

台灣東北海域在造山活動結束後轉為山脈垮塌，而形成一系列東北-西南方向的正斷層構造。而在台灣貢寮地區的逆斷層，澳底斷層、蚊子坑斷層及枋腳斷層似乎與海域上的線型特徵有相關性，推測斷層可能有往外海延伸。為了了解海陸斷層間的關聯，以及這些斷層在海域中是否為活動斷層，使用火花放電反射震測來針對貢寮外海地區做探討，此系統適合淺海區域，且對於淺層構造可以有很高的解析度。

在震測剖面中，此區大致上的形貌為東西兩側基盤較高，中間為堆滿沉積物的盆地。資料中可觀察到兩大重點，一是盆地中的沉積層有層序地層的特徵、二是盆地西側邊界的斷層構造。在剖面中可清楚辨識出一侵蝕面，在此不整合面上可觀察到許多水道切蝕填充的樣貌，因其深度大約在 100-200 公尺深，與一萬八千多年前的末次最盛冰期海水面下降 120 公尺左右相近，推測可能為當時所產生的侵蝕面。除此侵蝕面外，也依據震測相的差異定義出沙波基底面、海進面、上一期的最大海泛面及聲學基盤面。而在構造上，可看到一斷距大的高角度正斷層，此斷層有切穿基盤且在近海床的地層也有明顯的錯動。目前懷疑此斷層是因為張裂環境而形成的正斷層斷塊，在斷塊的頂部皆可看到明顯的強反射層。認為這個強反射是在受造山作用影響時，此區域擠壓而抬升，因此在基盤位置堆積了許多粗顆粒的沉積物。後期，造山活動結束改為張裂環境，受沉降作用的影響而形成這些正斷層與盆地。

中文關鍵字：台灣北部海域斷層、火花放電反射震測、層序地層、末次最盛冰期侵蝕面

以反射震測資料探討台灣西南海域南海大陸斜坡之氣窗分布與特性

韓為中¹、陳麗雯²、劉家瑄³

(1)臺灣中油公司探採研究所、(2)海洋委員會國家海洋研究院、(3)臺灣大學海洋中心

本研究藉由分析反射震測資料，探討臺灣西南海域變形前緣西側南中國海大陸斜坡之流體移棲構造分布與特性，由西而東包含九龍海脊、馬蹄鐵海脊、指標海脊及福爾摩沙海脊等 4 個天然氣水合物探勘好景區。震測資料指出本區有密集的海底仿擬反射(BSR)與亮點(bright spots)分布，過往研究亦發現活躍的海床滲漏徵兆，顯示動態的地下流體移棲與聚集特性。研究成果指出除傾斜地層與斷層外，氣窗(gas chimneys)亦是本區重要的流體移棲管道。本研究辨識了共 36 處氣窗，並依其在天然氣水合物儲集系統中所扮演的角色將其分為 2 種類型：第一型氣窗穿過天然水合物穩定帶基底，對於水合物生成甚或海床滲漏有直接貢獻；第二型氣窗則被沉積物深埋，其和水合物生成及海床流體滲漏無直接關聯。此二類型氣窗的空間分布與沉積環境特徵高度相關，暗示沉積作用控制了本區氣窗的發育過程。

中文關鍵字：反射震測、天然氣水合物、氣窗



從地震地層學探討南台灣新近紀以來沉積環境與構造運動之

演變關係

牟敦堅¹、黃瑞澤¹

(1)福爾摩沙能源股份有限公司

近年來台灣有關造山運動時空演化之研究數量很多，依據沉積環境、核飛跡定年、岩屑分析、二次移置化石、前陸盆地構造下沉速率等證據，都不約而同指出台灣的造山運動是在中新世晚期開始，而後在上新世早期抬升加劇。

台灣新近紀的造山運動肇因於菲律賓海板塊與東亞大陸板塊的碰撞。此類劇烈的構造活動，一般都會影響周邊沉積盆地的形貌和沉積環境。原先被動大陸邊緣陸棚上的沉積界面坡度，因碰撞帶地形大幅且快速地抬升而變陡。而突增的侵蝕力，也進而在陸棚外緣與大陸斜坡上深切出海底峽谷。印度板塊在漸新世開始和亞洲大陸發生劇烈的碰撞，巴基斯坦南部印度河口外海域盆地裡的地震剖面上，在漸新統以後的層序裡，經常可見在前置堆積三角洲前緣的深海環境中，存在許多深切的峽谷，這是一個構造運動與沉積環境演變之間因果關係的已知例證。

透過台灣中油公司過去發表的震測資料，讓我們觀察到在海域的台南盆地內，中新統頂部發育有顯著的交角不整合，其後的年輕地層裡，則開始出現深切的海底峽谷與深水相厚層泥岩。陸上的嘉南平原地下，從上新世烏嘴層至更新世中期的崁下寮層，也存在著為數眾多、切深規模數百米以上、唯有在侵蝕基面落差大的大陸斜坡深海環境下，方克生成的峽谷構造。這些地震剖面中看到的地層現象與其對應年代，和前述南台灣造山運動於中新世晚期後加劇的結論基本一致。

中文關鍵字：地震地層學、沉積環境、海底峽谷、造山運動

泥岩中的斷層帶特性研究：來自車瓜林斷層的見解

陳新翰¹、黃文正¹、邱奕維¹、曾雅筑²、劉彥求³

(1)中央大學應用地質研究所、(2)臺灣師範大學地球科學系、(3)經濟部中央地質調查所

在過往的研究中，有關斷層在泥岩中的產狀特性報導相較為少，本研究以車瓜林斷層為例，對其進行野外地表地質調查、地質剖面清理以及鑽井施作，透過由公釐至公里等級不同中視尺度的觀察，紀錄跨泥質斷層帶的構造變化及特性。車瓜林斷層位於台灣西南部的泥岩區，為古亭坑層中的層間斷層，是一條東北-西南走向現今活躍的左移逆斷層。車瓜林斷層自大廊亭山至千秋寮一帶可以於野外良好追跡約 5 公里，出露寬度約 10-30 公尺，產狀為黃褐色與深黑色泥質條帶所交織的寬帶，顏色上與斷層帶兩側的灰色泥岩有所差異。然而斷層帶中的細部組構在泥岩表面清理的前後有顯著的差異，故本研究選定車瓜林斷層的兩個露頭分別進行地質剖面及鑽井的施作，以剔除斷層帶受地表風化的因子。

地質剖面及鑽井的結果顯示，斷層帶中的變形產狀與岩性相關，我們可以將斷層帶中的岩體區分為三個單元，分別為完整砂岩段、破碎砂岩角礫及含黑色條帶的泥岩。完整砂岩段中破裂面不發達並可見層面；在破碎砂岩角礫，數公釐至數公分的砂質碎片呈角礫狀散佈於泥質基質中；而斷層帶中的泥質岩內則出現寬數公釐的密集黑色條帶狀構造並夾有角礫狀泥質碎屑。於斷層露頭的泥質岩多呈鱗片狀，表面帶有擦痕且破裂面方向具有一致性，將泥質手樣本進行拋光後可觀察到內部夾有大量角礫狀的泥質及砂質碎屑，碎屑長軸呈現具有方向性的排列。在泥岩斷層帶中難以觀察到如脆性斷層帶中變形集中於窄帶的斷層核心及斷層破壞帶，泥岩斷層帶中的變形傾向於相較平均分布於整個斷層帶中，寬度可達數十公尺，然而其中仍存在變形較集中的區域。泥岩中所出現的黑色條帶成因繁多，本研究推測其主要受斷層的剪切作用所形成，但在缺少微觀的觀察狀況下，難以確定其變形機制及礦物組構以探討斷層行為，仍需後續的研究使泥岩斷層帶的構造意義能更加完備。

中文關鍵字：車瓜林斷層、古亭坑層、中尺度地質構造

Inversion of tectonic stress and magma pressures using dikes orientation

Frantz Maerten¹、Laurent Maerten¹、Romain Plateaux²

(1)YouWol、(2)Independent Researcher

In volcano-tectonic regions, stress field variations result from tectonic stress loading and the pressurized 3-D shallow magma chambers. However, the interactions between pressurized magma chambers and tectonic stress remains poorly studied in the context of tectonic stress inversion. Indeed, in classic formulation of stress inversion techniques, which include the inversion of the reduced stress tensor that comprises the stress orientation and stress ratio, it is implicitly assumed that discontinuities cannot open or close, implying that the volumetric part of the regional stress has no influence on the slip direction and magnitude. Therefore, in the case of magma chambers and/or dikes, such classic technic cannot be applied as the volumetric part can no longer be neglected.

In this contribution, we describe a newly developed stress inversion technique that assumes that the heterogeneous stress field around volcanoes, which can be represented by the observed dikes, is a result of the mechanical interaction between the pressurized magma chamber geometry (discontinuities), the traction free Earth surface and the far field tectonic stress. The method, based on the 3-D Displacement Discontinuity Method (DDM thereafter) for homogeneous elastic half-space (successor of Poly3D and iBem3D), automatically finds the optimum far field tectonic stress and magma pressure parameters that best reproduce the observed dikes.

As magma chambers can be regarded as pressurized cavities, DDM results have been validated against known 3D analytical solution for pressurized tube-like cavity. The effectiveness of this stress inversion approach is then demonstrated through natural examples of two different volcanic systems, namely the Spanish Peak (U.S.A) and the Galapagos Islands.

Keywords: stress inversion, geomechanics, excess pressure, magma chambers

空中磁力探測於中央山脈東翼之磁力異常特徵

陳棋炫¹、董倫道²、林蔚²、林昶成¹、張育仁¹、陳勉銘¹

(1)經濟部中央地質調查所、(2)工業技術研究院材料與化工研究所

本研究討論以南橫東段區域之中央山脈東翼為主，磁力資料以 4 年分區施測完成，探測面積達 2,100 平方公里，範圍涵蓋臺灣東部四大主要地質區，由西向東依序為脊樑山脈板岩帶(含東板岩帶)、脊樑山脈片岩帶、花東縱谷地質區及海岸山脈地質區。測線間距為 500 公尺，沿約略垂直區域地質構造走向方位角 110°飛行，共計完成 220 條測線，測線及檢核線總長度達 4,923 公里。空中量測到的磁力資料，經過突波移除、基站修正、國際地磁參考場移除、高度修正及調平及歸極換算等資料處理程序，製作網格間距為 100 公尺，經歸極換算之全磁力強度圖。

由於磁場力資料反映地下空間磁力特性之總和效應，經由對資料網格進行濾波、向上延伸、計算趨勢面及微分等程序，可區分相對深層、相對淺層及輔助磁力構造等解釋。利用低通濾波截切波長 5 公里、及向上延伸高度 1 公里，反映相對深層之高磁力體，在片岩區約成塊狀分布；片岩帶往西與板岩帶交界附近，有一向東突出之弧形條狀高磁構造，包圍一區磁力異常低磁體。而利用高通濾波截切波長 2 公里，及以全磁力強度扣除向上延伸 250 公尺之趨勢圖，觀察相對淺部之磁力異常，可發現在片岩帶內有一明顯之南北向線型界線，左右兩側有不同之高磁構造特徵，可能代表層界或構造界線；深層所發現之弧形高磁構造，於淺部之高磁特徵更加顯著，被高磁包圍之淺部的低磁異常帶，與地表溫泉露頭分布接近，初步推論高磁可能與火成岩相關，而低磁異常帶可能與岩體消磁現象有關。中央山脈東翼的細部地質調查方興未艾，利用快速且大面積量測之空中磁力探測，有機會協助判釋過去未釐清之地下地質構造。

中文關鍵字：空中磁力探測、中央山脈東翼、全磁力強度、歸極換算

利用名竹盆地的長期地電阻施測估算區域地下水位及

水文地質相關參數

張竝瑜¹

(1)中央大學地球科學系

本研究通過在名竹盆地乾濕季重複進行時序的地電阻測量，推導出各地電阻測量剖面在垂直方向上的相對飽和度和深度變化。藉由 Brooks-Corey 公式估算了地下水位深度，與可能的比出水率。將鄰近新民觀測井水位的兩處測線所推算水位進行比較後，我們發現使用 Brooks-Corey 公式估算之空氣進入張壓(air-entry suction)的高程，較觀測的地下水位深度的高程平均淺了約 0.5 米。因此在本研究中的所有測站，可根據此一資料進行深度校正得到各測線位置乾濕季地下水位分布及變化。經推算，名竹盆地的地下水位深度約為 6.7 米至 16.7 米。總體而言，乾旱和濕潤季節的地下水位高程均呈現出從上游到下游逐漸降低的趨勢。在 1 月到 3 月的乾季，地下水位的高程因補注量減少而顯著下降。而由 6 月至 9 月主要雨季時間，地下水位高程逐漸上升。但是，如果我們比較由最乾的 3 月進入較濕的 3 月所施測之區域地下水位變化，約在 Min_02，Min_03 和 Min_05 測站附近，存在一南北方向的水位差較低的區域，其幾何分佈大致垂直於河流的方向。而由 Brooks-Corey 公式模型，估算的比出水率約在 0.08~0.16 之間，調查區上游段和濁水溪河道附近地區有較高的比出水率。而單以最乾的 3 月而言，比出水率亦顯示前述的南北向構造，這表明可能存在大致南北方向，導因於集集地震期間斷層活動帶造成的淺部水文地質結構。值得未來加強研究和討論。

中文關鍵字：地電阻、地下水、濁水溪、名竹盆地

土場仁澤地熱區之三維地電阻模型初探

董倫道¹、郭泰融¹、林蔚¹、張佑銓¹、曾振韋¹、林朝彥²、陳棋炫²、
林昶成²

(1)工業技術研究院材料與化工研究所、(2)經濟部中央地質調查所

宜蘭土場仁澤是受矚目的地熱區，民國 60 年代便進行過地熱探勘，並曾經設有小型發電試範系統，後因土石流事件而中斷發電試驗。國內自 2006 年重啟地熱開發以來，土場仁澤地熱區也是重點地熱開發的區域，為瞭解此地熱區的可能地熱構造，本研究進行了寬頻大地電磁探測。測點分布在以土場仁澤為中心，半徑約 5 km 範圍內，共計 32 個測點，涵蓋牛鬥斷層南北兩側地質區，頻率範圍約介於 10 kHz 至 0.001 Hz 間。探測資料經前處理後，使用 ModEM 軟體進行三維逆推，三維模型的地形部份採用海科中心 200 m 的數值模型來模擬地形及海水水體。本研究三維網格的水平間距為 125 m，以模擬起伏地形及側向電阻變化造成的靜態效應；垂直網格間距為 20 m，以降低高頻訊號的模擬誤差；水平及垂直方向三維模型尺寸則分別為 716 km 及 791 km 以降低低頻訊號的模擬誤差。此外，為了降低三維逆推過程的記憶體需求及縮短計算時間，本研究採用非對角線阻抗資料，且每個對數週期擷取 4 個記錄，共選取 28 個頻率作為三維逆推的輸入資料；並採取階段逆推程序，以避免落入局部低區，經反覆測試及運跑後，獲取能符合觀測資料的合理的三維地電阻模型。由初步地電阻模型並參考相關資訊後顯示，熱水可能沿北北東方向導水通道自深部上湧，在土場仁澤地熱區深度約 1 km 內形成約 20 ohm-m 上下的帶狀低電阻區，該低電阻帶的形成推測與熱水換質的低電阻礦物有關，而牛鬥斷層北側的梵梵溫泉亦有類似的帶狀低電阻構造，但兩者間隔著牛鬥斷層，很可能地熱構造並不相連通，但由於牛鬥斷層北側的測點分布不多，故本地熱區詳細的地熱構造，仍有待後續更多資訊之整合後加以評析。

中文關鍵字：土場仁澤、地熱、大地電磁、三維地電阻模型

台灣高精度地震動地圖製作

趙書賢¹、林哲民¹、黃雋彥¹

(1)國家地震工程研究中心

地震動地圖（Shake Map）能夠在地震後呈現地震動強度值（如地表運動峰值及不同週期的反應譜值等）的空間分佈狀況，第一時間可提供災損之推估及緊急應變措施之擬定，後續亦可供任意目標工址結構進行耐震能力評估之參考，因此其為地震防災研究與應用的重要工具之一。高精度地震動地圖的製作，仰賴精準的地震源參數與有限斷層模型、精準與足夠的地震動觀測資訊、精準的地震動預估式、及精準的空間內插與外插方式等四大重要元素。本研究旨在發展於建置台灣地震動地圖時用來進行空間內插與外插的空間相關性函數，並以台灣即時強地動觀測站（約一百餘站）的觀測資訊及所發展的空間相關性函數建置地震動地圖，接著再以非即時強地動觀測站的觀測資訊，評估所建置之地震動地圖的精確度，及探討即時強地動觀測站數量、不同地震動預估式、以及空間內插方式等對地震動地圖精確度的影響。本研究的成果可供未來震後第一時間及觀測資訊收集完整後建置高精度的台灣地震動地圖，以利地震防災相關的研究與應用。

中文關鍵字：地震動地圖、地震動預估式、空間相關性函數、空間內插與外插



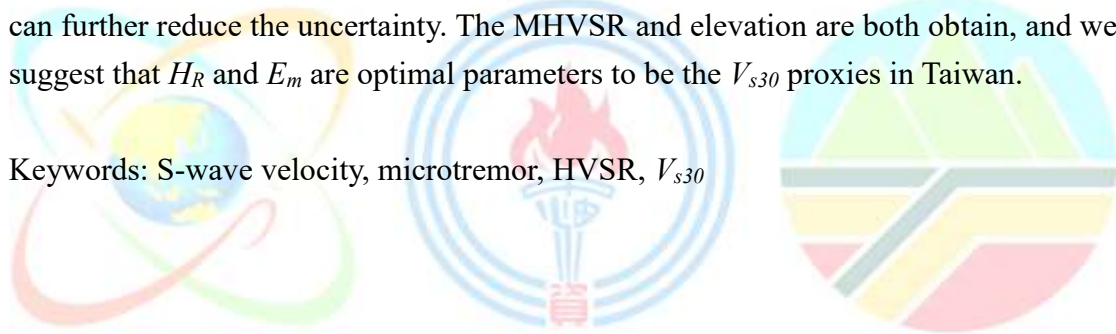
Development of new parameter (H_R) as a proxy for site conditions (V_{s30})

Chun-Te Chen¹、Chun-Hsiang Kuo²、Che-Min Lin³、Jyun-Yan Huang³、
Kuo-Liang Wen²

(1)Institute of Earth Sciences, Academia Sinica, Taiwan、(2)Department of Earth Sciences, National Central University、(3)National Center for Research on Earthquake Engineering

The average S-wave velocity (V_s) in the upper 30 m (V_{s30}) is a vital site parameter widely used for many purposes like microzonation, ground motion prediction equation (GMPE), and building codes. In this study, we used a newly developed V_s database inverted by Microtremor Horizontal-to-Vertical Spectra Ratio (MHVSR) including more than 3500 V_s profiles, to develop a new parameter H_R as a proxy for site condition (V_{s30}) in Taiwan. The parameter H_R instead of the predominant frequency (f_{peak}) as a proxy for V_{s30} reduces the standard deviation and leaves out human judgment and challenging to identify the predominant frequency of MHVSR. Both H_R and modified elevation (E_m) as predictor variables are adopted to regress a predicted equation for V_{s30} can further reduce the uncertainty. The MHVSR and elevation are both obtain, and we suggest that H_R and E_m are optimal parameters to be the V_{s30} proxies in Taiwan.

Keywords: S-wave velocity, microtremor, HVSR, V_{s30}



Modal frequency and damping ratio of TAIPEI 101:**The response to environmental factors**

Yaochieh Chen¹、Philippe Guéguen²、Bor-Shouh Huang³、Chin-Jen Lin³、
Win-Gee Huang³、Chin-Shang Ku³、Kate Huihsuan Chen⁴

(1)Department of Earth Sciences, National Taiwan Normal University; ISTerre, Universitaire de Grenoble, Grenoble 38000, France、(2)ISTerre, Universitaire de Grenoble, Grenoble 38000, France、
(3)Institute of Earth Sciences, Academia Sinica, Taiwan、(4)Department of Earth Sciences, National Taiwan Normal University

Continuous monitoring the state of buildings provides the information for structural health condition, integrity and reliability. Ambient vibration available of being recorded continuously in time, has been widely used to measure the dynamic properties of the buildings through modal frequencies approaches (e.g., Clinton et al., 2006; Nayeri et al., 2008; Ditommaso et al., 2010; Mikael et al., 2013). Over the past two decades, the globally rapid urbanization demands for the better technology and practice for long-term monitoring of high-rise buildings with seismic vulnerability. The behavior of high-rise building is strongly controlled by wind loads, mass of the building, design of damper and internal structure. The damping ratio of a tall building is found to be generally nonlinear with vibration amplitude under strong winds. As recognized as the tallest building in the world from 2004 to 2010, the TAIPEI 101 is located at the place where earthquakes and strong typhoons frequently occurred. Previous study investigated how the TAIPEI 101 responded to large earthquakes and typhoons (Chen et al., 2013; Li et al., 2011). The long-term history of the vibration characteristics of the TAIPEI 101 however, remain explored. In this study, we aim at using one-year continuous data from sensors on 90th floor to establish the characteristics of natural frequency and damping ratio of TAIPEI 101 and further, discuss the possible controlling factors.

Using the four components of seismograms in both bending (BLE, BLN) and torsion (BRN, BRZ) modes recorded at the 90th floors, we computed Random Decrement Technique to identify the identify three modes of fundamental frequency. We found that the frequency and damping behavior of horizontal components is relatively stable with similar amplitude for three different frequency modes. In horizontal components, the normalized frequency and damping is relatively high between June and September. When we further compare the frequency behavior of the building with the precipitation, air pressure, relative humidity, temperature, wind velocity and wind direction recorded at nearby weather station, we found that the frequency increases with increasing humidity/temperature and decreasing air pressure/wind velocity. In addition to the control of environmental parameters, we also

demonstrated a logarithmic relationship between frequency and amplitude in all components and modes. The damping however, seems to reveal higher order dependency on the amplitude in specifically BLN and BRN components.

Keywords: TAIPEI101, modal frequency, damping ratio



Shallow subsurface structure in the Hualien basin and relevance to the damage pattern and fault rupture during the 2018 Hualien earthquake

Chun-Hsiang Kuo¹、Masumi Yamada²、Ikuo Cho³、Che-Min Lin⁴、
Ken Miyakoshi⁵、Yujia Guo⁵、Takumi Hayashida⁶、Yasuhiro Matsumoto⁷、
Yin-Tung Yen⁸、Keng-Chang Kuo⁹

(1)Department of Earth Sciences, National Central University、(2)Disaster Prevention Research Institute, Kyoto University, Uji, Japan、(3)National Institute of Advanced Industrial Science and Technology, Tsukuba, Japan、(4)National Center for Research on Earthquake Engineering, Taiwan、(5)Geo-Research Institute, Osaka, Japan、(6)Building Research Institute, Tsukuba, Japan、(7)Kozo Keikaku Engineering Inc., Tokyo, Japan、(8)Sinotech Engineering Consultants, Inc., Taiwan、(9)Kaohsiung University of Science and Technology

The 2018 Mw6.4 Hualien earthquake generated a large peak-to-peak velocity of over 2 m/s, with a period of 3 s at the south end of the Milun fault, which resulted in the collapse of five buildings. To investigate the shallow subsurface soil structure and evaluate possible effects on the ground motion and building damage, we performed microtremor measurements in the Hualien basin. Based on the velocity structure jointly inverted from both Rayleigh-wave dispersion curves and microtremor horizontal-to-vertical spectral ratio data, we found that the shallow subsurface structure generally deepens from west to east. Close to the Milun fault, the structure becomes shallower, which is consistent with faulting during the 2018 earthquake and the long-term tectonic displacement. There is no significant variation for the site conditions in the north–south direction that can explain the large peak ground velocity in the south. As a result of the dense measurements in the heavily damaged area, where three high-rise buildings totally collapsed, these locations have the average S-wave velocity of the upper 30 m (AVS30) values and are relatively high compared to the more distant area from the Milun River. This is somewhat unusual, because lower AVS30 values indicating softer ground conditions are expected close to the river. We did not find any characteristic subsurface soil structure that may contribute to the building collapses. The large 3 s pulse was probably generated by source effects, rather than subsurface soil amplification.

Keywords: 2018 Hualien earthquake, microtremor measurement

台北都會區大氣中細懸浮微粒化學組成成分

林家恩¹、潘詩諭¹、練建國¹、紀凱獻¹、蕭大智²

(1)陽明交通大學環境與職業衛生研究所、(2)臺灣大學環境工程研究所

台灣將近七成人口居住於城市大都會區，而當人口密度提高時，人類活動所產生的污染排放量越多，比如在固定污染來源的空氣染物排放、因為車輛所造成的尾氣污染物以及其他可能影響空氣品質的沙塵暴事件等。而在空氣中的 PM2.5 為目前當今較被大眾關注的污染物，其本身附著在微粒上的化學成分會對人體健康產生危害如：多環芳香烴(PAHs)具有致畸性和致癌性以及金屬(trace metal)易造成神經和免疫系統的破壞等。本研究於台北都會測站進行實驗，分析大氣中 PM2.5 濃度以及化學成分，並探討日夜間及平假日變化外，同時也考慮事件日(境外長程傳輸 LRT 以及本土污染 LP)及無事件日(normal)的發生；並進一步使用正矩陣因子法(Positive Matrix Factor, PMF)解析其污染物來源，最後以吸入性終生致癌增量風險(ILCR)來評估台北都會測站大氣中 PM2.5 所造成之健康風險。

研究結果顯示：都會測站於日夜間 PM2.5 濃度分別為 12.9 ± 5.64 ($\mu\text{g}/\text{m}^3$)和 10.4 ± 5.16 ($\mu\text{g}/\text{m}^3$)；而平假日的 PM2.5 日平均濃度則分別為 12.2 ± 4.96 ($\mu\text{g}/\text{m}^3$)、 10.3 ± 3.47 ($\mu\text{g}/\text{m}^3$)。比較有無事件日發生時，在 non-event 時 PM2.5 日平均濃度為 9.70 ± 3.62 ($\mu\text{g}/\text{m}^3$)，而當在 event 發生時，LRT 的 PM2.5 濃度為 15.6 ± 5.45 ($\mu\text{g}/\text{m}^3$)、LP 則為 21.7 ± 4.48 ($\mu\text{g}/\text{m}^3$)。而 PAHs 濃度在日夜間分別為 4.96 ± 6.48 ($\text{ng BaPeq}/\text{m}^3$)和 4.02 ± 7.89 ($\text{ng BaPeq}/\text{m}^3$)；平假日則為 2.89 ± 2.36 ($\text{ng BaPeq}/\text{m}^3$)和 3.27 ± 1.84 ($\text{ng BaPeq}/\text{m}^3$)；非事件濃度為 3.02 ± 2.50 ($\text{ng BaPeq}/\text{m}^3$)、LRT 為 2.51 ± 0.293 ($\text{ng BaPeq}/\text{m}^3$)以及 LP 為 3.53 ($\text{ng BaPeq}/\text{m}^3$)，且在 PAHs 的物種分布中，不管是日夜間、平假日還是有無事件日發生都以高環數占比最高，特別是當 LP 發生時高環數占比又再增多，其主要與存在高環數物種的 BghiP 濃度較高有關。最後在水溶性陰陽離子之分布，不管在日夜間、平日假日還是有無事件日發生，主要離子皆包含 SO_4^{2-} 、 NH_4^+ 、 NO_3^- ；金屬元素之分布則都以 Na、Fe、K 為主。使用 PMF 進行解析本研究之都會測站大氣污染來源，解析結果得出 3 種主要污染貢獻來源，分別為交通車輛之汽油引擎 (73.7%)、交通車輛之柴油引擎(12.2%)、燃煤電廠(12.2%)。最後暴露於都會測站 PAHs 之吸入性終生致癌增量風險(ILCR)之評估結果為日間($1.69 \pm 9.73 \times 10^{-5}$)、夜間($1.35 \pm 1.11 \times 10^{-5}$)；平日($1.66 \pm 6.63 \times 10^{-5}$)、假日($1.41 \pm 1.17 \times 10^{-5}$)；而在不同情境下 normal ($1.46 \pm 8.38 \times 10^{-5}$)、LRT ($1.47 \pm 2.67 \times 10^{-5}$)、LP(2.60×10^{-5})，其暴露風險皆介於可容忍之限值 ($10^{-6} \sim 10^{-4}$)。

中文關鍵字：細懸浮微粒、多環芳香烴、痕量金屬、健康風險

PM_{2.5} and hazardous air pollutants: characteristics, source apportionments, and their health impacts

Ngo-Tuan Hung¹、Wei-Ting Hsu²、Yu-Hsuan Yang¹、Yina Lee¹、
Pei-Chun Tsai¹、Wen-Chi Pan¹、Kai-Hsien Chi¹

(1)Institute of Occupational and Environmental Health Sciences, National Yang-Ming Chiao-Tung University、(2)Institute of Occupational and Environmental Health Sciences, National Yang-Ming Chiao-Tung University; International Health Program, National Yang-Ming Chiao-Tung University

Different sources of air pollution can affect the composition of PM_{2.5} which in turn differently influence human health. In this research, we aim to study the sources of ambient PM_{2.5} in Taiwan and how they affect the human health. We focused on PCDD/Fs composition of PM_{2.5} for source apportionment analysis.

Air pollution was collected using high volume instrument at different places including industrial, urban, LRT, cooking areas. PM_{2.5} samples then underwent extraction and purification processes to obtain and separate different compositions. Organic compounds (PAHs, PCDD/Fs) were analyzed using GSMS, metal elements were quantified using ICP-MS, and ion chromatograph (IC) was employed to study ion composition. Source apportionment was done using PCA, PMF, and Bivariate Polar Plot coupling with cluster analysis. We conducted cytotoxic research for different sources of PM_{2.5} on cell model and epidemiological research to study association between concentration of PM_{2.5} from different sources and mortality.

PM_{2.5} and PCDD/Fs were highly correlated. Major sources of PM_{2.5} and PCDD/Fs in Taiwan were industrial activities, traffic activities, and also LRT (North of Taiwan). In Taiwan as a whole, 71.2% of PCDD/Fs originated from stationary sources. Long-range transport could bring air pollution from the Northern continent or Indochina peninsula to Taiwan depending on the season. Cytotoxic research found that highest concentration of PM_{2.5} does not correspond to high toxicity. About 150% elevation of ROS and positive genotoxicity was observed after exposure with organic compound of cooking samples. Epidemiological research found that higher concentration of PM_{2.5} and PCDD/Fs in the ambient air positively associated with mortality. PM_{2.5} from stationary sources had higher impact on CVD (0.8% increase each $\mu\text{g}/\text{m}^3$ PM_{2.5}) and respiratory diseases mortality (2.0% increase each $\mu\text{g}/\text{m}^3$ PM_{2.5}) comparing to traffic originated PM_{2.5} (0.4% and 0.6% increase respectively).

Keywords: PM_{2.5}, PCDD/Fs, source apportionment, health risk

Linking the Wrangellia flood basalts to the Galápagos hotspot

J. Gregory Shellnutt¹、Jaroslav Dostal²、Tony Lee¹

(1)Department of Earth Sciences, National Taiwan Normal University、

(2)Saint Mary's University, Department of Geology

The Triassic volcanic rocks of Wrangellia erupted at an equatorial to tropical latitude that was within 3000 km of western North America. The mafic and ultramafic volcanic rocks are compositionally and isotopically similar to those of oceanic plateaux that were generated from a Pacific mantle plume-type source. The thermal conditions, estimated from the primitive rocks, indicate that it was a high temperature regime ($TP > 1550^{\circ}\text{C}$) consistent with elevated temperatures expected for a mantle plume. The only active hotspot currently located near the equator of the eastern Pacific Ocean that was active during the Mesozoic and produced ultramafic volcanic rocks is the Galápagos hotspot. The calculated mantle potential temperatures, trace elemental ratios, and Sr-Nd-Pb isotopes of the Wrangellia volcanic rocks are within the range of those from the Caribbean Plateau and Galápagos Islands, and collectively have similar internal variability as the Hawaii-Emperor island chain. The paleogeographic constraints, thermal estimates, and geochemistry suggests that it is possible that the Galápagos hotspot generated the volcanic rocks of Wrangellia and the Caribbean plateau or, more broadly, that the eastern Pacific (Panthalassa) Ocean was a unique region where anomalously high thermal conditions either periodically or continually existed from ~230 Ma to the present day.

Keywords: Wrangellia, Triassic, Galápagos hotspot, Caribbean plateau, ultramafic volcanic rocks

Secular variation of Early Cretaceous granitoids in Kyushu, SW Japan: The role of *mélange* rocks as a possible magma source

Kenshi Suga¹、Meng-Wan Yeh¹

(1)Department of Earth Sciences, National Taiwan Normal University

The Early Cretaceous volcanic-arc granitic rocks from Kyushu, SW Japan are contemporaneous with the granitic rocks of the Yanshan Orogeny (SE China) along the eastern Eurasian continental margin. The secular geochemical variations of the whole-rock major elemental and Sr–Nd isotope data of the Early Cretaceous granitic rocks from Kyushu, SW Japan, as well as the zircon and apatite saturation temperatures, shows distinct changes during the Albian (~115 to ~100 Ma) as: (1) the mASI value of the rocks (i.e., Shiraishino granodiorites) decreases below 1, (2) the Sr–Nd isotopic data are relatively constant [$^{87}\text{Sr}/^{86}\text{Sr}_i = 0.70471$ to 0.70573 ; $\epsilon\text{Nd}(t) = +0.2$ to $+1.9$] within different rock types including granites, granodiorites, tonalites, and adakitic rocks (i.e., the Shiraishino granodiorites), following the increase of $^{87}\text{Sr}/^{86}\text{Sr}_i$ and decrease of $\epsilon\text{Nd}(t)$ from Berriasian, and (3) higher maximum temperatures at ~105 Ma. The secular changes indicate that important geodynamic changes occurred in the arc system of SW Japan as it changed from subduction-accretion during the Jurassic to continental arc during the Early Cretaceous. Thermodynamic partial melting modeling demonstrates that the Albian granitic rocks can be derived from *mélange* rocks, such as chlorite-actinolite schists, at moderate depth and variable redox conditions. It is concluded that the genesis of the Early Cretaceous granitic rocks from Kyushu, SW Japan, may be related to upwelling of the asthenosphere and hot corner flow into the mantle wedge caused by slab rollback, which followed a shallowing of the subduction angle and subsequent flat-slab subduction during the Late Jurassic. The resultant heat induced the partial melting of the *mélange* rocks that formed on and were transported from the subducted plate interface. Reference: Suga, K., Yeh, M.W., 2021. *Front. Earth Sci.* 8:95.

Keywords: granitoids, *mélange*, arc magma, partial melt, Early Cretaceous, SW Japan, Yanshan orogeny

Geochemical investigation of mafic–ultramafic rocks from the Archean Olondo greenstone belt on the Aldan Shield, Siberian Craton

Tran Thi Duyen¹、Kuo-Lung Wang¹、Victor P. Kovach²、
Alexander B. Kotov²、Sergey Velikoslavinsky²、Hao-Yang Lee¹、
Yoshiyuki Iizuka¹、Li-Wei Kuo³、Der-Chuen Lee¹

(1)Institute of Earth Sciences, Academia Sinica, Taiwan、(2)Institute of Precambrian Geology and Geochronology, Russian Academy of Sciences、(3)Department of Earth Sciences, National Central University

The Archean Olondo greenstone belt (OGB) is located in the Aldan shield, which is the largest basement of Siberia craton. Well-preserved abundant mafic-ultramafic rocks make the OGB unique to other greenstone belts worldwide. The ultramafic rocks are mainly dunites with minor serpentinites. They are highly refractory, showing U-shape Rare Earth element patterns with positive to negative Nb anomalies. Platinum Group Element chemistry suggests they are residual mantle phase. Re-Os isotope compositions yield mantle model age (TMA) of 2960-3020 Ma. These isotopic and geochemical features suggest that the OGB dunites are mantle residual after a high degree of partial melting (>30%) then interacted with subduction-related melt/fluid. The OGB mafic rocks (komatiitic and tholeiitic basalts) have been metamorphosed from greenschist to amphibolite facies. Komatiitic basalts are slightly depleted in both LREE and HREE, suggesting a garnet-bearing source. Tholeiitic basalts are divided into three groups: depleted, undepleted, and enriched tholeiites. The depleted group is proposed similar to that of modern N-MORB but lower trace-element abundance, whereas the enriched group is more like that of modern boninite. The undepleted group has flat patterns, close to the primitive mantle. The compositional variation of these mafic rocks is comparable to that of Suprasubduction Zone ophiolites. $\epsilon\text{Nd}(t)$ values of the OGB mafic rocks range from +0.1 to +3.9, with no variation of Nd isotope compositions among different rock types. The lower ϵNd values with negative Nb-Ta-Ti anomalies could result from either subduction component or crustal contamination. However, Nb depletion is also revealed in residual dunites, which are unable to be affected by crustal processes. These overall geochemical data suggest that plate- and plume-tectonic processes could be involved in the OGB formation and evolution during Mesoarchean. Therefore, typical modern plate tectonics are likely to operate at 3 Ga.

Keywords: Archean greenstone belt, plate tectonics, geochemistry, mafic-ultramafic rocks

High temperature-low pressure metamorphic evolution associated with continental crust extension in the Kinmen Island, Taiwan

Tsung-Han Huang¹、Ching-Hua Lo¹、Tadashi Usuki¹、Meng-Wan Yeh²、
Yoshiyuki Iizuka³

(1)Department of Geosciences, National Taiwan University、(2)Department of Earth Sciences,
National Taiwan Normal University、(3)Institute of Earth Sciences, Academia Sinica, Taiwan

The Kinmen Island is situated at southeast coast of the Cathaysia block, where the continental lithosphere was under thinning to almost rifting during the Cretaceous due to the long-lasting slab rollback of Paleo-Pacific plate. Such crustal thinning history was recorded by metamorphic evolution accompanying the exhumation of the high-grade metamorphic rocks in the island. Petrographic and microstructure analyses of highly-deformed orthoschists revealed four episodes of metamorphism (M1, M2, M3, M4). M1 shows granulite-facies mineral assemblage of cordierite + K-feldspar + biotite within the microlithon domain. M2 records amphibolite facies mineral assemblage of garnet + biotite + muscovite whereas the mica folia define the subhorizontal matrix foliation. M3 is only developed within narrow NNE-SSW striking upright shear zones as sillimanite replaced muscovite and crosscutted biotite. M4 shows typical greenschist facies assemblage with albite replacing K-feldspar and clay mineral after cordierite. The presence of cordierite would indicate low pressure but high temperature conditions for M1 granulite-facies metamorphism. The following retrograde metamorphism of amphibolite-facies registered in the subhorizontal foliation to greenschist-facies metamorphism under low pressure yet high temperature conditions coincide to the upwelled asthenosphere beneath the highly-extended continental lithosphere. The evolution path may reflect the lithosphere thinning along the southeast coastal region of Cathaysia block during the late Cretaceous.

Keywords: Kinmen Island, metamorphism, lithosphere thinning

Supercontinent breakup mechanisms inferred from the thermal state of Large Igneous Provinces

M.P Manu Prasanth¹、J. Gregory Shellnutt¹、Tung-Yi Lee¹

(1)Department of Earth Sciences, National Taiwan Normal University

The primary magma solutions and mantle potential temperatures (TP) determined for flood basalts of LIPs that are associated with Pangea and its breakup. Among the Pangean LIPs the Oslo rift, Permian Emeishan LIP, and Siberian trap are consistent with a mantle plume thermal regime. The early-Permian Himalayan LIP exhibit ambient mantle TP and consistent with melt derivation from a shallow mantle source. The Post-Pangean LIPs, however, exhibit complex TP relations, and such complexities in the mantle source can be correlated with the dispersal stages of Pangea. The TP estimates on 200 Ma. Central Atlantic Magmatic Province (CAMP) and Miocene Columbia River Basalt are consistent with non-plume sources and the slightly elevated TP relative to the ambient mantle is attributed to the process like continental insulation and subduction delamination. The Early Jurassic Karoo-Ferrar LIP, Early Cretaceous Etendeka LIP, and Paleocene North Atlantic LIP (NALIP) exhibit both mantle plume and ambient mantle thermal regimes. The TP estimates of Deccan LIP (DLIP) and Madagascar LIP are consistent with a mantle plume related origin. The mantle plume-related LIPs and the LIPs that exhibit both lithospheric and sub-lithospheric components point out that they were emplaced into an already thinned lithosphere. Despite the mantle plume origin, the plume-induced continental rifting is absent in the Pangean LIPs like Siberian trap and Emeishan. The LIPs like Himalayan, CAMP, and Columbia River Basalt Group exhibit significant melt generation and continental rifting without mantle plumes. The Karoo-Ferrar LIP, Etendeka LIP, and NALIP show evidence for prior thinned lithosphere and lithosphere-controlled rifting events before the onset of plume magmatism. We posit, based on the thermal state of the LIPs, that mantle plumes act as the source of thermal energy rather than the primary driving mechanism of supercontinent rifting, which is controlled by lithospheric processes.

Keywords: Large Igneous Province, mantle potential temperature, mantle plumes

Tectonic implications of Mesozoic magmatism to initiation of Cenozoic Basin Development within the passive South China Sea margin

Meng-Wan (Mary) Yeh¹、Mai-Hue Anh²、Yu-Lu Chan¹、Tong-Yi Lee¹

(1)Department of Earth Sciences, National Taiwan Normal University、

(2)Institute of Earth Sciences, Academia Sinica, Taiwan

The South China Sea (SCS) is one of the most active exploration regions for oil and gas over the past decades. This marginal sea situated within three major tectonic plates of the Eurasian, Indo-Australian and Philippine plate that exhibited various types of plate boundaries and complex tectonic evolutions due to subsequent subduction and convergences of numerous micro blocks and accretionary prisms during the Cenozoic time. In order to decipher the evolution and their tectonic framework, correlation between the temporal and geographical distribution of Cenozoic magmatism, and the development histories of major basins within and surrounding the SCS were conducted. Four major tectonic episodes can be recognized. (Charvet) The SE ward younging trend of A type granite and high-K calc-alkaline magmatic rock in SE Asia during Paleogen indicated the initiation of continent extension by eastward retreating of subduction of the Pacific plate to Asia. This also induced episodic rifting within the basins along the Asia continental shelf NW of SCS marked by rift onset unconformities. The SCS begin to spread in N-S direction from the NE region along the E-W trending ridge (C11-7) around 34-33 Ma possibly response to southward slab pull during the subduction of proto-South China Sea oceanic crust, which is also marked by the beak up unconformity within surrounding basins. (3) The left lateral shearing activity of the Red River Shear zone (27~16 Ma) due to collision of India into Eurasia trigger a southward ridge jump event (C6b~5c) and the development of the SW sub-region of SCS. The clockwise rotation of Indochina accompanying the left-lateral shearing event induced asymmetric graben and half graben development within the basins west of the SCS. (4) The SCS seized spreading around 15.5 Ma as the Pacific sea plate continued subducted westward. However, this compressional setting reinforced the subsidence of basins to the maximum depth till Pliocene.

Keywords: South China Sea, Mesozoic magmatism, basin development, tectonic reconstruction

無人機攝影測量於狹長區域之地形建置精度評估

翁瑋辰¹、張國楨¹、曾俊偉²

(1)臺北科技大學土木與防災所、(2)行政院農委會林業試驗所

無人機的攝影測量與傳統的攝影測量相比可以更有效率且快速的獲得高解析度的遙測影像，然而在於大面積的狹長地形中進行空中三角測量的作業，將會因為地形起伏不同、拍攝時間不同，會形成有連接點匹配不足的問題，位於海岸線的沙灘上更是難以尋找地形特徵點。本研究透過對地面控制點(Ground Control Point)之佈設方法與在於影像上尋找特徵點來建置模型。地面控制點之佈設本研究配合使用虛擬基準站之網路化即時動態定位(Virtual Base Station RTK, VBS-RTK)量測其砂土點位及岸上人工建物之座標，藉此進一步比較正射影像(Orthoimage)及數值地表模型(Digital Surface Model, DSM)，以了解無人飛行載具於狹長地形區域之建模精度並評估誤差。

本研究區域位於苗栗縣竹南鎮至通霄鎮之海岸線，模型之控制點佈設以每500 m 佈設一地面控制點，在航道交界處則於測繪軟體上點選連接點。其中位於竹南縣海岸段之海岸地形砂岸居多，特徵物較少建置之模型之精度較差，而位於後龍段之海岸線則因海角樂園至白沙屯段擁有許多人工建物，而海岸也並非只有單純之砂質海灘，有混合一些卵礫石屬於混合形砂灘，而特徵物比竹南段多因此建置之模型精度較為良好。由本研究可了解影像之特徵共軛點，及地面控制點之佈設對於狹長地形攝影測量之重要性。

中文關鍵字：共軛點、地面控制點、數值地表模型

基於 PPK 技術之無人機攝影測量之地形建模精度評估

陳冠榕¹、張國楨¹、曾俊偉²

(1)臺北科技大學土木工程系、(2)行政院農委會林業試驗所

近年來遙測軟硬體技術不斷演變，無人機的發展也跟著越來越進步，且成本也隨之降低許多，只要使用單點定位無人機搭配地面控制點以及軟體，即可在短時間內取得目標區域內的數值地形模型。而為了在複雜地形建置更精準的模型，差分定位也越來越常使用於無人機上，如使用 RTK 進行實時差分，可以立即取得飛機的精準位置，但本方法容易受地形遮蔽及通訊品質等影響，致使無人機於作業過程中無法直接精確定位。而 PPK 則是使用了後處理差分技術，較不受地形影響，作業半徑大約可延伸至 50km，因此適合用來使用於大範圍的帶狀區域使用，如公路、鐵路等。

本研究之研究區域位於花蓮縣瑞穗鄉吉蒸牧場，拍攝面積約 1 平方公里，測區內地勢平坦且空曠無遮蔽物，飛行及測量條件良好。本研究使用的無人飛行載具分別為 DJI Phantom 4 RTK，以及搭載了非量測性數位相機與外掛 Reach M2 定位模組之 DJI Matrice 600 Pro 多軸飛行器，分別進行了兩期及一期的航拍任務、飛行高度為離地 100 及 200 公尺，並比較以 RTK、PPK，以及使用單點定位等不同無人機定位方式下，不同技術之地形建模精度的差異。研究區現地一共佈設了 33 個地面控制點，控制點測量的部分則使用了 e-GNSS、RTK、以及快速靜態這三種方式進行量測，在進行快速靜態及 RTK 測量時，使用現地的三等衛星控制點作為基站使用。

由於不需要控制點，本研究使用了 30 個點作為檢核點使用，研究成果顯示兩期 P4RTK 在經過後處理解算後，平面誤差分別小於 5.5 公分以及 8.2 公分，而高程誤差小於 7.5 公分，M600 在排除邊界處三個點後，平面誤差小於 7.66 公分，高程誤差小於 10.06 公分。而測量的部分則是快速靜態精度最佳，RTK 次之，e-GNSS 最差；不過由於測區訊號良好且無遮蔽物，因此三種測量方式的較差不會太大。從三種測量方式的較差比較中可以看出，平面部分 RTK 與快速靜態最大較差只有 3.8 公分，e-GNSS 與快速靜態則為 7.9 公分，較 RTK 差；高程部分 RTK 與快速靜態最大較差為 7.8 公分，e-GNSS 與快速靜態則為 8.8 公分，也是 RTK 較佳。

中文關鍵字：無人飛行載具、動態後處理、數值地形模型

半動態參考框架應用在地方地籍測量之適用性研究－以高雄市為例

李建寬¹、景國恩²、陳國華³

(1)高雄市政府、(2)成功大學測量及空間資訊學系、(3)臺北大學不動產與城鄉環境學系

推動高精度大地參考框架的目的，就是為了串接控制測量和地籍測量。研究證實半動態參考框架不僅解決了靜態框架精度隨時間劣化的致命傷，其中引用大量觀測資料建置的地表變形模型，更近即時性有效化解地震效應與基準轉換殘差對大地參考框架精度的干擾問題。然而對於應用在地方地籍測量是否適用，尚未可知。高雄市轄區內擁有西部海岸平原、西部麓山帶與中央山脈等臺灣主要的地質區塊，而且還有 10 個觀測站構成的大地控制網，提供本研究所需的基礎環境。為了達到研究目的所擬定的策略，首先是以該 10 個 cGNSS 於 2013 年的公告成果作為參考依據，比較自 2013 年到 2020 年的網形變形情形，以及經半動態參考框架的地表變形模型修正後的結果。結果顯示，修正前的大地控制網確有變形現象，經半動態參考框架的地表變形模型修正後已可消除，顯見半動態參考框架可直接應用在地方控制測量。另因地方地籍測量實際存在山坡地與市區混雜情況，故本研究再以地形變化且地質活動明顯的壽山國家自然公園為例，進行實際地籍測量運用情況的測試。測試結果顯示，在精度上也完全符合現行地籍測量規範。最後，因為半動態參考框架的地表變形模型是以大量大地觀測資料為基礎，故若能增設較多的連續 GNSS 觀測站，尤其是在地質環境敏感區域附近，對於區域地表變形資訊的掌握會更精確，精度也會更為提升。至於增建數量及地點的評估建議，則有待再進一步的研究。

中文關鍵字：半動態參考框架、地籍測量

Heterogeneous power-law flow with transient creep in Southern California following the 2010 El Mayor-Cucapah earthquake

Chi-Hsien Tang¹、Sylvain Barbot²、Ya-Ju Hsu¹、Yih-Min Wu¹

(1)Institute of Earth Sciences, Academia Sinica, Taiwan; Department of Geosciences, National Taiwan University、(2)Department of Earth Sciences, University of Southern California

Rock rheology and the interaction between seismic/aseismic slip and viscoelastic flow in the lithosphere control the state of stress and strain over seismic cycles. The rheological behavior of rocks is well constrained by laboratory experiments, but the rheology in natural settings is poorly resolved. These drawbacks highlight the need for a more direct approach to explore rheology in tectonic settings. Here, we designed a kinematic inversion scheme to invert the distributed anelastic strain from geodetic data. Unlike a conventional forward model, our method does not prescribe a rheological model but directly relates surface displacements to off-fault anelastic strain. We explored the lower-crustal rheology in Southern California by using 8 years of GNSS postseismic displacements following the 2010 El Mayor-Cucapah earthquake. Our models image the viscoelastic flow in the lower crust with lateral variations of effective viscosity. A Burgers assembly with nonlinear dashpots ($n=3$) approximates the temporal evolution of stress and strain rate, indicating the activation of nonlinear transient creep and steady-state dislocation creep. The transient and background viscosities in the lower crust of the Salton Trough, where the surface heat flow is locally high, are on the order of $\sim 10^{18}$ and $\sim 10^{19}$ Pa s, respectively, about an order of magnitude lower than the surrounding regions. Our analysis shows the importance of transient creep, nonlinear flow laws, and lateral variations of rheological properties describe the entire history of postseismic deformation following the El Mayor-Cucapah earthquake.

Keywords: seismic cycle, GNSS, postseismic deformation, rheology, Southern California

Toward comprehensive geodetic rate estimation based on TEM fault model

Geng-Pei Lin¹、R. Y. Chuang¹、Kuo-En Ching²、Wu-Lung Chang³

(1)Department of Geosciences, National Taiwan University、(2)Department of Geomatics, National
Cheng-Kung University、(3)Department of Earth Sciences, National Central University

Since the island-wide seismogenic structure database and seismic hazard map were published by the Taiwan Earthquake Model (TEM) project, an attempt to incorporate geodetic data into future TEM output was made. We take the advantage of block modeling to estimate slip and deficit rate for the total 45 TEM faults. We build the model in two specific constraints: First, we maintain a uniform model resolution on the fault plane, we put fault nodes in equal distance on each fault. Because previous studies often use to reduce the number of fault nodes due to the expensive computational cost and convenience in setting block geometry. In this version, we set a node interval about 8 km along strike on each fault and at least three layers of node in depth. Second, we use inputs of knowledge-based initial locking ratios (coupling ratio). To gain a realistic model setting, we learn from published literature to set where the asperity was recognized as fully locked, and allow specific surface nodes able to creep when fault creeping was documented. For most cases, locking ratio decreasing along depth is a reasonable and typical constraint. If any fault locking behavior could be non-typical, we remove the depth-dependent constraint and allow the locking ratio on specific fault to be free. With the up-to-date GNSS velocity field, a latest version of slip rate model estimation will be presented. The modeled slip rate and slip deficit rate will be compare to geologic data and discuss the implication of the seismic potential.

Keywords: block model, slip rate, slip deficit, seismic potential

Re-estimating strain partitioning between the Timor Trough and the Wetar Backthrust

Timothy Day¹、Yunung-Nina Lin²、Yu Wang¹、Yu-Ting Kuo²、

Ira Mutiara Anjasmara³、Sin-Da Tsai⁴、Ya-Ju Hsu²

(1)Department of Geosciences, National Taiwan University、(2)Institute of Earth Sciences, Academia Sinica, Taiwan、(3)Department of Geomatics Engineering, Institut Teknologi Sepuluh Nopember, Surabaya, Indonesia、(4)Timor Map, Dili, Timor-Leste

The mechanism for strain partitioning between the frontal and the back structure, as well as the proportion of partitioning, has long been of great interest to the study of plate tectonic evolution and seismic hazard evaluation. As one of such front-rear structure pairs, the Timor Trough to the south and the Wetar Fault to the north together absorb and partition the plate convergence motion between the Australian plate and the Sunda plate along the southern rim of the Banda Sea. Earlier geodetic modeling with campaign-mode GPS observations suggests that the majority of plate motion has been taken up along the Wetar Fault, leaving the Timor Trough relative inactive and free from generating large subduction zone earthquakes. In this study, we adopt observations from continuous GPS stations (including one installed by IES in Timor-Leste since 2019) and InSAR time-series from ESA's Sentinel-1 satellites to reconstruct the 3D displacement fields on the Timor Island. With the augmentation of these continuous observations, we aim to refine the strain partitioning between the frontal and the back structure in order to assess the seismic hazard in the region.

Keywords: synthetic aperture radar, GPS, strain partitioning, plate motion, back-arc thrusting

Recent geohazards in Taiwan caught on seismic stations and multidisciplinary techniques

We-An Chao¹、the Landslide Working Group²

(1)Department of Civil Engineering, National Yang-Ming Chiao-Tung University、(2)Disaster Prevention and Water Environment Research Center, National Yang-Ming Chiao-Tung University

Mass-movement events on hillslopes are one of frequent natural geohazards causing fatalities and economic losses. The prevention and mitigation of geohazards should be based on the understanding of dynamic behavior of event. In the past decade, landslide seismology has been applied to rapidly determine information on when, where and how event occur that is useful for hazard assessments. Compared to the conventional geo-engineering-based techniques such as borehole drilling, inclinometer, GPS, and piezometer, seismological technique is low-cost and invasive tool and can be widely adopted. Here, I present the results based on a combined analysis of seismic signals, multidisciplinary geological survey and numerical simulation for a landslide event occurred in the Central Cross-Island Highway. Another landslide site (Landslide Inventory ID: DS160) has been well understood by geological, geophysical, geodetic, geotechnical, hydrological and seismological perspectives, which not only improved our understanding in landslide mechanism and but also advanced in studying the landslide forecasting. Above two case studies have successfully toward a rapid assessment of highway slope disasters and defining certain thresholds for landslide forecasting.

Keywords: landslide seismology, hazard assessment, forecasting

無人飛行載具影像技術在山崩活動性之應用

吳庭瑜¹、謝有忠¹、李祖鈺¹、孫武群¹

(1)經濟部中央地質調查所

無人飛行載具，可在野外地質調查、山崩調查等進行遠距露頭或地形觀察，此外也可利用以 SfM 攝影測量範圍成像技術進行三維地形建模，獲取正射影像與數值地表模型資料，有助於地表地形分析。

本研究前期使用 DJI PHANTOM 4 PRO (P4P) 及搭配地面基站 D-RTK 2 的 PHANTOM 4 RTK (P4RTK) 兩款搭載不同衛星定位模組之無人飛行載具，於同一地區，利用未加入地面控制點所拍攝的影像產製之正射影像成果，透過質點影像測速法 (Particle Image Velocimetry, PIV) 進行分析並探討兩者所產製的正射影像成果之穩定性，此外，也與現地 RTK 測量資料進行平面誤差計算，得知透過 P4RTK 所產製出的正射影像之成果，全區均方根誤差約在 10 公分內，在此誤差規模下，透過 P4RTK 進行空拍建模的資料，將可直接應用於地表侵蝕差異分析及地表變動觀測等變動規模在公吋至公尺以上的項目上。

近期桃園市復興區光華地區一處農用道路有崩塌地持續滑動現象，此處過去因有發生崩塌滑動之虞，故將其範圍劃入桃園市山崩與地滑地質敏感區(L0011)，並於 104 年 12 月公告之；同時也於本所「潛在大規模崩塌精進判釋既補充調查」計畫中，完成崩塌特徵之調查。基於光華地區崩塌地近期有持續滑動現象，且已透過前期研究評估無人飛行載具空拍建模資料之可行性及應用性，故選定此處進行空拍建模及透過質點影像測速法進行分析，以此得知崩塌地整體移動方向及變量，作為崩塌調查參考資料。

中文關鍵字：無人飛行載具(UAV)、質點影像測速法(PIV)、山崩活動性觀測

Deformation pattern of landslide by long-term monitoring:

A dip slope case in northern Taiwan

Chia-Han Tseng¹、Yu-Chang Chan²、Ching-Jiang Jeng³、Ruei-Juin Rau⁴、
Yu-Chung Hsieh⁵

(1)Earthquake Disaster and Risk Evaluation and Management Center (E-DREaM), National Central University、(2)Institute of Earth Sciences, Academia Sinica, Taiwan、(3)Environmental and Hazards-Resistant Design Department, Huaan University、(4)Department of Earth Sciences, National Cheng-Kung University、(5)Central Geological Survey, MOEA, Taiwan

A natural hillslope developing into a landslide shows ground cracks and topographic deformation. Geomorphological and subsurface investigations using appropriate methodology are essential to understand the failure mechanisms and stability of a hillslope. Huaan University campus located on a dip slope in northern Taiwan is facing a potential landslide hazard. Slope movement was detected through the development of ground cracks and persistent deformation of campus buildings and facilities. To monitor the sliding behavior of the dip slope, a nail network consisting of 144 ground monitoring points was set in 2001, and its coordinates were measured using conventional traverse surveying twice a year until 2017. The 17-year surficial surveying results were presented as a time series of displacements with constraints of geometry and distribution of ground cracks and underground observations. The long-term surveying results reveal multiple potential sliding blocks within the Huaan University campus. A model of landslide movement with a listric sliding surface is proposed. Additionally, from the velocity field derived from the monitoring points, the horizontal strain rates of the slope are estimated. The pattern of strain rates indicates that a plausible fault passing through the campus may have affected the movement of the dip slope. The long-term surface monitoring of a potential landslide slope in this study provides a reliable and economical way to understand the mechanism of movement behavior of the slope and evaluate slope stability.

Keywords: dip slope, long-term monitoring, time series of displacement, listric sliding surface, landslide deformation

Constraining S-wave velocity structure of a complex large-scale deep-seated landslide at Chunlin, southern Taiwan using Rayleigh wave ellipticity inversion

Chin-Yao Huang¹、Hsin-Hua Huang²、Yih-Min Wu¹

(1)Department of Geosciences, National Taiwan University、

(2)Institute of Earth Sciences, Academia Sinica, Taiwan

Large-scale deep-seated landslides are one of the most catastrophic natural hazards which threaten lives and property in the world. The Chunlin landslide in southern Taiwan is one of such composed of complex morphology, showing multiple sub-blocks with different deformation behaviors, and cut through by possible fault zones. As a result, constraining its subsurface structure is crucial to understand the detailed geometry of sliding interface and fault zones, and potential weak zones prone to failure. For this purpose, a seismic network containing 15 stations was installed relatively uniformly across the Chunlin landslide area in July 2019 to provide comprehensive observations. We apply a method, named DOP-E (Berbellini et al., 2018), to estimate degree-of-polarization (DOP) in time-frequency domain to effectively extract and estimate the Rayleigh wave ellipticity information from seismic noise. We then invert the ellipticity measurements with neighborhood algorithm for each station to spatially map the subsurface velocity structure, so as to understand the possible sliding depth and layering structure of different sub-blocks. This method may also allow the temporal imaging of subsurface properties in the future.

Keywords: large-scale deep-seated landslides, Chunlin landslide, degree-of-polarization, Rayleigh waves, ellipticity curve

台灣中部廬山-能高板岩地區坡體重力量變形現象之探討

謝有忠¹、戴東霖¹、吳庭瑜¹、林錫宏¹、紀宗吉¹

(1)經濟部中央地質調查所

經濟部中央地質調查所推動「國土保育之地質敏感地區調查分析計畫」，運用空載光達技術，至民國 105 年底完成全臺高解析度數值地形資料建置與相關之地質災害調查分析工作。此為臺灣首次取得全島高解析度數值地形模型資料，其中一項工作是配合衛星影像與航空照片等資料，中央地質調查所據以自 99 年至 109 年於全臺坡地聚落與重要保全設施分布地區，約 4,500 平方公里範圍內，逐步累積判釋出 2,621 處具有重力邊坡變形現象的潛在大規模(10 公頃以上)崩塌地區，其中 188 處之區位可能會影響到 173 處聚落的安全，為國土計畫、保育規劃、防災應用與土地管理之重要參考資料。

坡面重力變形作用(deep-seated slope gravitational deformation, DSGSD)在 1940 年代開始提出(Agliardi et al., 2001)，主要為坡面上大規模岩體因重力作用造成岩體產生變形作用，常會出現張裂地形特徵如崩崖、陷溝、地塹、多重山脊等，以及壓縮地形特徵如坡面隆起(bulging)、挫曲褶皺(buckling folds)、高度破裂岩體等。過去國際間針對山崩或坡地土砂災害等現象之分類方法眾多，多以移動材料、移動方式、移動速度、發生規模等因子進行分類，常見的分類方法為 Varnes 之分類方法(Varnes, 1978)，以移動物質的材料及移動方式來分類，Hung 等在 2014 也針對 Varnes 的分類中，在移動方式中增加坡體變形(slope deformation)一類，並依照移動物質材料區分 Mountain slope deformation、Soil slope deformation、Rock slope deformation、Soil creep、Solifluction 等 5 細類 (Hung et al., 2014)。2009 年莫拉克風災時發生的大規模坡面土砂災害，也使得近年來大規模崩塌的調查研究越來越受關注，而臺灣板岩分布區域易受發達之劈理影響，岩體在長期重力作用下產生重力變形現象，多造成岩體破碎進而發生山崩現象，這些坡面重力變形區域極可能為潛在大規模崩塌之位置(Chen et al., 2015; Chigira et al., 2013; Lin et al., 2013)，所以對於這些坡面重力變形區域的調查研究，有助於對後續崩塌災害的了解，在國內地質災害上之研究也具有其重要性。自從莫拉克颱風災後，藉由空載光達測製技術，所獲得之臺灣全島高解析度數值地形資料，藉由進一步地形計測方法與視覺化加值處理後，專業地質人員可以判釋出植覆之下受崩塌作用影響所致的變形(地形)表徵，進而圈繪出潛在大規模崩塌之範圍，但對於其關鍵的地質本質仍所知有限，這些經由初步地質調查與資料判釋、分析，提供鄰近坡地聚落可能存在之不同規模大小的潛在崩塌的資訊，但如此多數量之潛在大規模崩塌在具有不同地質條件、崩塌類型、規模大小、水文地質等特性下，對於崩塌可能破壞的機制與活動性，仍有許多不確定位置的範圍而需進一步研究。好比缺少醫療專業的人，雖勉強可以察覺患者外觀的病徵，卻難以確認體內的病灶所在。由於空載光達數值地形測製是以鳥瞰的尺度與角度所進行的地形測繪，獲致的資

料有：去除或包含植覆與地表物之地形(DEM)或地表(DSM)面，對於滑動面深達岩體的潛在大規模崩塌的理解，仍缺乏個案場址的地下地質參考模型。對於坡面尺度下的潛在大規模崩塌的地質模型解釋，多受限於現階段板岩地區僅有的地質資料，主要為地質調查所出版之五萬分之一地質圖，此部分因資料尺度及精度限制下，已不敷現階段潛在大規模崩塌之應用。

中央山脈板岩地區地勢陡峭、交通不易，且受限過去之地形圖資精度及解析度有限，本研究以南投縣仁愛鄉廬山、清境地區，利用 1 米解析度空載光達數值地形資料，並結合高解析度三維地形判釋技術，初步完成區域尺度之地質資訊，圈繪出本區域大規模崩塌分布及細部地形特徵，配合野外調查，釐清區域構造作用抑或重力變形作用所造成之現象，並藉由對於這些地形特徵抑或坡面重力變形所致之岩體破壞狀況及可能機制進行研究，未來也可比對近年來已發生大規模崩塌，增進潛在大規模崩塌的判釋和調查，更能進一步探討坡面地質災害的可能成因和規模或影響範圍，做為未來坡地災害防救災策略上亟需的重要資訊。

中文關鍵字：空載光達、數值地形模型、坡體重力變形、三維地形判釋技術、
大規模崩塌



運用高精度 LiDAR 數值高程模型輔助區域地質調查 -

以台鐵侯硐崩塌為例

柳鈞元¹、黃韋凱¹、李璟芳¹、紀宗吉²、林錫宏²、GeoPort 團隊

(1)中興工程顧問社、(2)經濟部中央地質調查所

109 年 12 月初台鐵猴硐至瑞芳區間發生岩體滑動災害，大量岩屑材料與風化砂岩層從南北走向的邊坡上向東滑落掩埋台鐵宜蘭線，崩塌範圍呈現節理切割之楔型塊體，滑動塊體上的植生完整地下滑反映著岩體滑動的特徵。參考五萬分之一的雙溪圖幅地質圖，此次岩體滑動恰好位於侯硐背斜軸南翼，地層屬於大寮層下段岩層，層面為 27 度向南南東傾，但現地調查發現當地層面位態多為東北東傾約 15 度，與地質圖記載有所出入。

在沉積岩地區，層面與坡面的空間關係影響岩石邊坡的穩定性，然而五萬分之一的地質圖的尺度並不適用於單一邊坡場址，本團隊藉由高精度 LiDAR 數值高程模型來判釋猴硐地區的岩層跡，嘗試數化追蹤區域內的砂岩分布，並可協助判釋區域的斷層與褶皺構造，輔以現地調查驗證判釋成果。調查成果顯示猴硐地區可數化追蹤岩層跡達 6~12 條，搭配三維地形更可良好地展示侯硐背斜軸部與向東北東傾沒的型貌。

綜整現地調查與高精度數值地形判釋成果，此次台鐵侯硐崩塌的破壞機制較接近平面型滑動，但節理組主控滑動方向與邊界形貌。高精度數值高程模型有助於了解區域地層分布與構造型貌，更可增加現地調查的效率，使地質師與工程師能更全面地了解區域地質概況，降低邊坡場址的地質模型不確定性。

中文關鍵字：LiDAR 數值高程模型、台鐵猴硐崩塌、地質不確定性、岩層跡

使用參考案例建立離散裂隙網路地下水流模型

李在平¹

(1)臺灣電力股份有限公司

台電公司自 1995 年起依法執行用過核子燃料最終處置計畫，目前已完成第一階段我國潛在處置母岩的基本特性調查，並參考瑞典核燃料及廢棄物管理公司 (Swedish Nuclear Fuel and Waste Management Company, SKB) 所發展的 KBS-3 處置概念，以研究用參考案例的方式發展處置相關安全評估技術，於 2017 年提交「我國用過核子燃料最終處置技術可行性評估報告(SNFD2017 報告)」，並通過國際同儕審查。由於參考案例的處置母岩屬於較不透水的結晶岩體，本研究採用近年發展中的離散裂隙網路(Discrete Fracture Network, DFN)模型建置一簡化之區域地下水流模型，與 SNFD2017 報告中的分析結果進行比對。使用資料主要來自六口深度約 500 m 之鑽井以及地表測繪，裂隙分析統計則主要依據孔內地球物理井測與岩心紀錄。由於參考案例過去並未執行高精度之孔內水力試驗，缺乏對應離散裂隙網路模型所需之岩體透水關係式，本研究參考瑞典 Forsmark 花崗岩的現地調查數據，假設裂隙半徑與導水係數具半相關(semi-correlated)的冪律關係。模型全域共生成約 2100 萬個離散裂隙後，除了處置設施周圍保留 DFN，其他部分則使用升尺度方法轉換為等效孔隙介質(equivalent continuous porous medium, ECPM)進行地下水流分析，並選定一截切處置孔之導水裂隙進行質點追蹤，分析其向外的可能傳輸路徑。研究結果顯示區域地下水流的模擬結果與 SNFD2017 報告相近，採用混和 DFN 與 ECPM 的方法，是未來研究後續安全評估所需地下水流與傳輸途徑之可行方式，但尚需要搭配現地高精度的地層透水性試驗才能降低模型的不確定性。

中文關鍵字：裂隙岩體、離散裂隙網路、地下水、安全評估

水下文化資產與工程之間的取捨與共存

林瓚宏¹、羅立¹、柯斯曼¹

(1)中興工程顧問股份有限公司

台灣全島地狹人稠，經濟成長的代價是過度發展的土地使用，導致島上土地資源寸土寸金，在陸地上能開發的土地逐漸限縮下，也因此，想當然動念轉往擴張海域的土地，進行各項海上的工程開發，例如填海造陸工程、離岸風力機組工程等種種案例。在這樣條件下，水下文化資產保存法規也因應而生，於中華民國一百零四年十二月九日總統華總一義字第 10400143861 號令制定全文 44 條，並自公布日起開始施行。

其法規總則第一章第一條：「為保存、保護及管理水下文化資產，建構國民與歷史之聯繫，發揚海洋國家之特質，並尊重聯合國保護水下文化資產公約與國際相關協議之精神，特制定本法」，據此欲涉及海域之水體、海床及其底土，以及陸域內自然形成水域、人工湖庫及運河下之水體、水底及其底土，所有可能干擾與破壞水下文化資產的開發行為，都須依照水下文化資產保存法第 9 條：「應先行調查所涉水域有無水下文化資產或疑似水下文化資產…」。

本文將依據「水域開發利用前水下文化資產調查及處理辦法」，介紹常見於海域工程中，針對工程場址範圍內的水下文化資產調查方法，包含技術上的高精度水深、側掃聲納、地層剖面、磁力探測等調查，以及人文上的歷史資料文獻、了解周圍區域人文歷史環境、歷史的演變等等，進而探查可能被埋覆的水下文化資產與其存在的真實性，且在必要的情況下，甚至安排專業潛水考古人員，進行水下攝影、水下考古，建構完備的水下遺跡之分布與保存方式，融合了工程與人文之間的交流。

中文關鍵字：水下文化資產保存法、填海造陸、水下考古

Stochastic groundwater flow and land subsidence modeling in heterogeneous hydrogeological models in Huwei Town, Yunlin County

Duc-Huy Tran¹、Shih-Jung Wang¹

(1)Institute of Applied Geology, National Central University

Taiwan High Speed Rail (THSR) is an important infrastructure in Taiwan. It passes through the Choushui-River Alluvial Fan (CRAF), where has suffered land subsidence. The distribution of hydrogeological material plays a major role on heterogeneous aquifer system responded to groundwater flow and land subsidence. How to quantify the hydrogeological model uncertainty in the heterogeneous aquifer system is another challenge. Therefore, this study adopted the transition probability/Markov chain model to conduct the realization of 3D heterogeneous hydrogeology. Huwei Town located in the southern CRAF was chosen as the study area. 46 boreholes, collected from Central Geological Survey, multi-layer compaction monitoring wells, and irrigation association, were used to construct the heterogeneous hydrogeological models. Based on the realization number assessment results, 36 realizations were generated based on honoring the geological data. Monte Carlo simulations for groundwater flow and land subsidence were conducted to discuss how hydrogeological models reflects the geological model uncertainty. The result showed that the coefficient of variations at the 90th percentile of the CDF is 0.295 in the subsidence simulation. An appropriate realization was selected as the representative hydrogeological model and use to calibrate the groundwater flow model. A transient model of groundwater flow and land subsidence in the period of 2015-2020 was conducted based on the observation data. Different pumping scenarios were employed to assess the long-term land subsidence. The assessment results showed that after 50% cese of pumping, land subsidence quantity is largely improved, compared with the zero scenario. The proposed criterion for the selection of representative hydrogeological model can provide the best model for the simulations. The study results can be used for the safety assessment of THSR and a conscious groundwater management in Huwei Town, Yunlin County.

Keywords: groundwater flow, land subsidence, Markov Chain model, stochastic analysis, Choushui-River alluvial fan

地質保育發展史—科學、襲產、到整全的生態人文保育

紀權寬¹

(1)地創地質顧問有限公司、臺灣師範大學地理學系

地質保育(geoconservation)一詞在 1990 年代才被提出，其定義為保育地球的特徵與系統的多樣性，然而地質保育的概念在 19 世紀的英國已經開始萌芽，從具有特殊科學價值的地質景點或露頭開始產生保育的意識。日本 1919 年以及英國在 1949 年已制定法案針對其國內具有科學價值的地質與地形景點進行調查與保護，1970 年代起，澳洲與歐洲興起地質科學保育的風潮，1994 年由 IUGS 推動 Geosites 計畫使此風潮在達到最高峰，我國也這個時期推動全國的特殊地質與地形景觀普查。地質遺產保護的國際倡議始於 1972 年的《世界遺產公約》，同年我國也頒布《國家公園法》來保護珍貴的地質、地形自然遺產。1982 年《文化資產保存法》以自然保留區來保護特殊地形與地質的現象，至 2016 年二度修法，並增列自然紀念物(特殊稀有礦物、特殊地質地形現象)與地質公園等類別。1991 年歐洲地質遺跡保育協會發布「守護地球記憶權利宣言」，讓地質保育與全球的環境及社會議題開始對話，進而促成「地質多樣性(geodiversity)」概念的興起，以及 1997 年 UNESCO 推動世界地質公園計畫，將地質科學的重要性，連結到生態、文化與經濟的永續發展議題。國內雖已將地質保育的概念納入各項法規中，但仍缺乏地質科學為主軸的實務作為，地質僅被視為生態保育、觀光旅遊中的一個項目。30 年來國際地質學者努力開啟跨領域以及與社會的對話，如今國內的地質科學界應該一同思考如何突破國內的困境。

中文關鍵字：地質保育、地質遺跡、地質公園、地質多樣性、文化資產保存法

網路社群在地質知識推廣及民情反映之應用

王豐仁¹、林建緯²、郭麗秋³、侯進雄³

(1)臺灣省應用地質技師公會、勝田工程技術顧問有限公司、(2)臺灣省應用地質技師公會、
(3)經濟部中央地質調查所

網路社群是現今資訊時代生活中重要的一環。它是溝通的方式，也是社交的平台，更是推播教育的工具。經濟部中央地質調查所辦理之「地質知識網絡推動發展計畫」中，自 101 年開始利用臉書(Face Book)設立「地質知識網絡」臉書社群，由此作為傳遞地質知識、宣導地質觀念、協助推動地質法規、激發國人對於地質環境的認知。

而經由網路社群貼文地質知識議題的規劃，或圖文屬性的操作，可以發現對於讀者的點擊率、按讚數、留言回應數等，都有不同的效果，藉此，可以蒐集分析民眾對於不同地質議題或是地質法規的關注度差異，以及反應的強度。同時，經由民眾所屬地理位置的分析，可以進一步分析了解不同地區民眾對於該地質議題的關注度、或是對於該議題的民情反應趨勢，藉此，一方面將有助於地質知識的推廣，一方面亦有助於地質法規的意見蒐集與推動。

中文關鍵字：地質網路社群、傳遞地質知識



「創意地質旅遊」興起的社會參與及實用價值

郭麗秋¹、陳政恒¹、董英宏¹、黃芷馨¹、侯進雄¹

(1)經濟部中央地質調查所

地質旅遊(geotourism, tourism geology)，也稱作地景旅遊、地學旅遊等，是經常被用以探討地質資源利用的選項之一，在 Hose 於 1995 年提出地質和地貌可從審美的角度提供服務或設施而成為旅遊後，漸於全球發展。地質旅遊以地質為主角，搭配科學、文化、教育、價值、景觀、美觀、娛樂、威脅或風險、經濟、自然保護、管理等面向，帶入地方可提升旅遊品質、社區意識與特色環境的突顯；成為教學課程則能加深學生對地球起源、人類文化與環境現狀的洞察；對整體環境而言，有利於地質遺跡保育及地質災害事件借鏡。聯合國教科文組織(UNESCO)推動地質公園，地質旅遊便與地景保育、社區參與及環境教育等功能，並列四大核心價值。

臺灣「創意地質旅遊」一詞首先出現在 2012 年 9 月《地質》季刊，當時是地質法與環境教育法上路的第二年，推廣地質教育受到鼓舞正方興未艾，於是乎《地質》編輯委員會熱烈討論，想要催生給地科老師參考用的地質考察路線，也希望為民眾推薦輕鬆可及的地質知性旅遊景點。「創意」是時尚口號，激發編輯人員以「創意」套用在「地質旅遊」，規劃「北北基創意地質旅遊」12 條路線專題，並向地質從業喊話邀稿，最後由 11 位作者在被設定的段落、字數、順遊資訊、簡單文字、生動圖片等規格下寫作，呈現每 1 路線的地質景點及附近的名產或名勝等。北北基 12 條路線在《地質》專題被發行後，陸續搭配新聞稿及記者會露出，引發不少媒體報導；後於國際書展、旅展或機場展等場合，請作者在「地質小學堂」舞台上親口向民眾解說，既專業又知性的安排顯得新鮮有趣，而吸引眾多民眾駐足聆聽；如此一連串行銷也獲得地質與環境領域人士的關注與討論。「創意地質旅遊」從此順利發酵，至 2020 年時，已經依序出版中彰投 6 條、花東 10 條、恆春半島 7 條、高屏 9 條、雲嘉南 11 條、桃竹苗 10 條，未來加上離島地區，全國將會有至少百條地質賞析路線被推薦一遊。

「創意地質旅遊」可以說是傳統的地質圖、文資料重新包裝上市的地質產品，其實並未被局限於以此為名而規劃的地質路線，其他因地質遺跡地質敏感區、地質公園、步道地質、公路地質等主題而推薦的地區或景點，都是在表現臺灣原創的山、川、土、石、火、海、島之多樣性，均可以是創意地質旅遊之處。這些地質旅遊路線的圖文在著作授權後，跟著被導入到地質推廣的各個工作上，例如地質知識漂、地方特色地質輔導、地質主題網站、社群臉書貼文等，成為重要的教材與資料源，相當程度幫助了地質科學擴大社會參與並提升實用價值。

可惜因為成本投入有限，各分區的地質旅遊路線多在短時間內出版，可能有遺珠之憾；也還未形成足夠的影響力，讓更多生態、旅行、交通、路跑、健康或媒體等等業者，瞭解到其活動或報導所倚賴的山光水色根源於地質演化，因而漏

失不少異業連結、彼此互補的機會。這些美中不足之處，卻鋪陳了「創意地質旅遊」精進的藍圖，未來可透過盤點方式增修地質路線與周圍的生活資訊，再次包裝上市，加速降低各行各業與社會大眾普遍不認識地質環境之情況。

中文關鍵字：創意地質旅遊、地質產品、地質推廣、環境教育



東海岸寬闊河口區的河階地發育模式

陳佳宏¹、吳庭瑜²、齊士崢¹、顏君毅³

(1)高雄師範大學地理學系、(2)經濟部中央地質調查所、(3)東華大學自然資源與環境學系

在上個世紀中期，地形學者使用一個罕見名詞「thalassostatic terraces」，說明從 glacial minimum 到 interglacial climatic optimum 這段期間，因海水面快速上升，導致海岸地帶和流域下游被上漲的海水淹沒(或上漲海水面影響)而加積，由堆積作用形成寬闊的平原或河谷平原(對應於由侵蝕作用形成的準平原(peneplain))；然後從 interglacial climatic optimum 到 glacial minimum 期間，海水面下降，河川自堆積形成的平原面下切，殘餘的堆積平原面形成河階地。根據國家教育研究院雙語詞彙、學術名詞暨辭書資訊網將「thalassostatic terraces」翻譯為「海升期河階」，然所有河階地都生成於廣義的侵蝕基準面下降期，這樣的翻譯應該不易讓人理解這類型階地發育的含義；故猜測「海升期河階」的譯名原因應是強調階地面這個「平面」是海升期堆積或河谷埋積形成的。我們在港口溪、金崙溪、馬武窟溪、豐濱溪和水璉溪等等流域的研究中，發現在近河口區經常出現階地崖出露厚層沉積層的階地，部分階地崖底部以下可能還有厚層的沉積層，且這套沉積層的堆積開始時間大約就在末次冰河時期結束之後到全新世氣候最適宜期，或全新世高海水面時期，有一個明顯可以和「下切期」區隔的「堆積期」，或有「老的沉積物」和「年輕的階地面」。因此，這些階地似乎都是「thalassostatic terraces」，但階地沉積層的堆積開始時間與結束時間並不十分吻合於 glacial minimum 和 interglacial climatic optimum 時間點，或它們的發育並不完全反映海水面變化過程，所以這些階地並非典型的「thalassostatic terraces」。我們認為在台灣不容易出現典型的「thalassostatic terraces」的影響因素，包括地形發育過程中持續的海岸線位置變化、陸地抬升速率和河川供應沉積物特徵的種種差異。

中文關鍵字：海升期河階、河階地、冰期最小期、間冰期氣候最適宜期

以 COMCOT-SS 發展印度洋風暴潮系統

曾博森¹、吳祚任¹、林君蔚¹、莊淑君¹、許家鈞¹、莊美惠¹

(1)中央大學水文與海洋科學研究所

印度洋北方之孟加拉地區經常遭受熱帶氣旋侵襲。由於當地沿海人口密度高且多為河流及泥沼地，熱帶氣旋所引致之風暴潮往往對當地造成嚴重破壞。如發生於孟加拉灣之 1970 孟加拉風暴潮，造成近 50 萬人死亡，為人類史上死亡人數最高之熱帶氣旋；2020 年之氣旋 Amphan 與風暴潮事件，亦造成近 13 億美元之損失及 128 人死亡。本研究旨在以台灣 COMCOT 風暴潮預報系統為基礎，發展適用於印度洋之風暴潮速算系統。於印度洋所發展之熱帶氣旋，其結構與強度有別於太平洋之颱風與大西洋之颶風，因此適用於太平洋與大西洋之風暴潮模式是否適用於求解印度洋之熱帶氣旋型風暴潮為本研究之分析重點。本文以 2020 氣旋 Amphan 為研究案例，分析 5 種不同參數化風場與 NCEP 大氣模式於風暴潮生成之適用性，並利用歷史案例（2019 年氣旋 Fani 以及 2013 年氣旋 Phailin）進行模式準確度比較。分析結果發現，修正後之模式(Present Model)模擬之氣象場於風速剖面及時序潮位高程上與觀測資料有最佳之匹配。本研究所採用之 COMCOT 風暴潮預報系統求解球座標非線性淺水波方程式，搭配巢狀網格系統與移動邊界法，可於沿岸求解高解析度之風暴潮溢淹範圍。同時可結合 TPXO 全球天文潮模式，以掌握高低潮位對溢淹範圍之影響。本研究建立適用於孟加拉灣氣旋之 COMCOT 風暴潮速算系統，期待未來對於孟加拉灣地區風暴潮速報及災情掌控有實際之助益。

中文關鍵字：孟加拉灣氣旋、風暴潮、COMCOT 模式、參數化風場

發展 SSIIA 分析法並重建 1845 年雲林口湖風暴潮事件

許家鈞¹、吳祚任¹、林君蔚¹、莊淑君¹、曾博森¹、莊美惠¹

(1)中央大學水文與海洋科學研究所

西元 1845 年雲林口湖發生嚴重之風暴潮事件，造成萬人喪生，為台灣歷史上最嚴重之風暴潮事件。為重建 1845 口湖風暴潮事件，本文發展風暴潮影響強度分析法(SSIIA)。該法以現行於中央氣象局之 COMCOT 風暴潮模式為基礎，進行大量單元颱風之風暴潮模擬，以建立颱風位置對風暴潮與溢淹高程之 SSIIA 敏感關係圖。本研究為重建颱風路徑，發展颱風路徑對風暴潮影響分析法。該法透過 SSIIA 之分析結果，進行風暴潮潮高、溢淹高程與溢淹範圍之綜合評分，以求得可能之颱風路徑組合，並考慮颱風移動速度之差異性，得出最嚴重影響移動速度之路徑，並由該結果建立 1845 年事件之可能情境。透過上述之分析結果，本研究提出對雲林口湖風暴潮生成之颱風情境，以及該路徑所造成之風暴潮和溢淹範圍。本研究所建立之分析方法，可系統性分析沿海低窪地區之風暴潮溢淹潛在災情，有助於進行風暴潮風險評估及災防規劃。

中文關鍵字：風暴潮影響強度分析法 SSIIA、颱風路徑、移動速度、口湖風暴潮、COMCOT 風暴潮模式、風暴潮重建



Coupled OBS and MCS data processing to derive the stratigraphy and velocity of the middle Taiwan Strait

Sebastian Wege¹、Tan-Kin Wang²、Ren-Jie Wei²

(1)Institute of Earth Sciences, Academia Sinica, Taiwan; Institute of Earth Sciences, National Taiwan Ocean University、(2)Institute of Earth Sciences, National Taiwan Ocean University

In the last five years, many seismic datasets were acquired in the Taiwan Strait to understand the shallow stratigraphy of the foreland basin better. Recent seismic activity shows that the area is still active and ongoing offshore construction sites make it worth investigating. Ten ocean-bottom seismometers (OBS) were deployed in June 2017 in an area of 30x30 km and nine multichannel seismic (MCS) profiles were shot using a GI-gun. Supplementary seismic data have been acquired in the northwest of our main profile using two OBS and an MCS system from China. Coupled MCS and OBS data processing was used to make a stratigraphic line interpretation of the shallow sedimentary layers and faults. We picked and inverted refracted and reflected arrivals in the OBS data to obtain a P-wave velocity model consistent with the sedimentary interfaces interpreted in the MCS profiles. We integrated the sedimentary layers of the nine MCS profiles to construct an iso-depth model of the main unconformities. Further, the horizontal components of OBS data have been used to build a Poisson's ratio model. The sedimentary layers above the Break-Up unconformity were cut by nearly vertical normal faults that were occasionally reaching the seafloor. In profile E7 the faults form a flower structure and can hence be identified as part of a strike-slip system. To show the location and direction of the normal faults and strike-slip faults in the area, they have been picked and interpolated across our profiles. The P-wave velocity model has a low-velocity zone or a fracture zone in the northwest, caused by the faults across the basement between Wuchu Depression and Kinmen Rise. Below the Penghu Platform, we found relatively low Poisson's ratios in sedimentary layers caused by the normal faults softening the sediments. Based on the iso-depth model the depth of the Break-Up unconformity gradually becomes shallow from the southeast to the northwest.

Keywords: normal fault, Penghu Platform, Poisson's ratio, P-wave velocity, strike-slip fault, Taiwan Strait, Wuchu Depression

P-wave velocity structures of the sediment and crust across the northern Taiwan Strait imaged by using air-gun and GI-Gun recorded from MCS and OBS data

Sergaud Marseille¹、Sebastian Wege¹、Tan K. Wang¹

(1)Institute of Earth Sciences, National Taiwan Ocean University

In the northern Taiwan Strait, four multi-channel seismic (MCS) profiles with 8 ocean-bottom seismometers (OBS) shot by a GI gun and the northwestern portion of the OBS line shot by strong air guns were collected in 2018. About 60 km NE of 2018 survey area, ten MCS profiles with 6 OBS shot by a GI gun were acquired in 2019. The normal fault at SE side of the northernmost Nanjihtao Basin was identified as the boundary fault between the forebulge and the foredeep. However, most of the normal faults observed from the 2019 MCS profiles were near the central line of the northern Taiwan Strait where the Basal Foreland Unconformity (BFU) was at two-way travel times of 0.52-0.63 s. The northwestern part of the BFU is shallow while it is deep in southeastern part. The 2018 MCS profiles, after intersection with the 2019 OBS line, showed a flower structure generated by the strike-slip faults in the northeastern side of the Kuanyin Platform. On the other hand, the P-wave velocity model inverted from 6 OBS data collected in 2019 indicates a large lateral variation of the P-wave velocity (1.9-2.1 km/s) near the BFU while the P-wave velocity-interface model inverted from 8 OBS data recorded in 2018 shows the increasing thickness of the sediment. P-wave velocities of the upper crust (5-6.5 km/s), the middle crust (7-7.5 km/s) and the lower crust (7-8 km/s) across the Kuanyin Platform are greater than the previous result in the northern Taiwan Strait. However, near the Moho, the P-wave velocity (6-7 km/s) is slower than the previous study. The high-velocity zones of the upper, middle and lower crusts may have resulted in the Littoral Fault Zone NW of the northernmost Nanjihtao Basin near the boundary fault.

Keywords: basal foreland unconformity, faults, forebulge, Kuanyin Depression, Kuanyin Platform

太平地區車籠埔斷層的時空變化與在地球科學教育上的運用

鍾令和¹、黃豐昌²、陳榮原²

(1)國立自然科學博物館車籠埔斷層保存園區、(2)臺中市立建平國小

藉由持續觀察 20 年在太平地區 921 集集地震破壞的時空變化，將其歸納整理，分成四種類型：1. 地震破壞的演變 2. 斷層抬升 3. 地震相關的地質災害 4. 建築物的破壞與後續處理四大類。將這些災害的負面遺產融入鄉土教育與戶外教育課程，並配合車籠埔斷層保存園區與 921 地震教育園區的資源進行課程設計。藉此讓沒有經歷過規模七地震的新生代學生了解台灣的宿命，並進行相關的防救災知識與訓練，進而為下一次的大地震預作準備。

中文關鍵字：集集地震、車籠埔斷層、太平



操作型遊戲學習法應用於國小學童認識礦物之教學活動設計

李佩倫¹

(1)嘉義大學數位學習設計與管理學系

大部份教育者認為透過遊戲結合教材的方式可克服教室中枯燥的學習，研究結果亦顯示透過遊戲式學習其學習成效優於傳統授課的方式。「認識礦物的特性」為國小五年級自然科技與生活「岩石與礦物」的單元目標之一，過往教學活動設計除了教師圖片教學引導外，亦有學生觀看岩石和礦物標本，並進行特性觀察與描述之設計。然而，相較於物理、化學領域之教學活動，則較缺乏相關的操作實驗之設計，因此，應用操作型遊戲於此單元以增加學生的學習動機是本研究的主要目標。本操作型遊戲學習法分成二個階段，各約一節課：第一階段「尋寶活動」以認識礦物及學生能叫出礦物名稱為主要學習目標；第二階段「小小鑑定家」為利用礦物之物理、化學特性以辨認礦物為主要學習目標，相關之活動理念與設計如下：

在沙坑玩耍是每個小孩樂此不疲的活動，因此「尋寶活動」是結合沙坑與「Gem Hunting」的遊戲概念，讓學童在沙坑內挖掘出任務卡的礦物組合。因此除了沙坑外，主要設計為「礦物展示牆」以協助學童認識任務所需的礦物外型。活動過程中學童必須分辨不同的礦物及能說出其名稱才能過關，故必須在礦物展示牆上熟記礦物之晶型或特徵，如此反覆觀看及記憶，並及時在沙坑中尋覓，進而在遊戲之中便熟悉礦物特徵。本研究結果顯示本活動設計在認識礦物與名稱之學習成效，是不分年齡且均具正向的學習成效。「小小鑑定家」在活動前，教師需操作各種鑑定方法，如硬度、條痕、解理、斷口等等之示範及說明，之後給予學生一張鑑定流程及未知標本，讓學生依實驗流程進行測試。本活動研究結果顯示大部份學生都樂於挑戰，活動過程也會互相討論可能之礦物名稱。因此結合二節課程之後，大部份學生都能完成任務，亦同時在遊戲中認識礦物及理解其特性。

中文關鍵字：遊戲學習、礦物、教學活動設計

日月潭沉積物中的 Ca 指標顯示之自然災害與人類活動紀錄

陳惠芬¹、魏國彥²、黃致展²、林祈成¹、蘇志杰³、宋國士³、
李紅春²、李德貴⁴、宋聖榮²、潘惠娟¹

(1)臺灣海洋大學地球科學研究所、(2)臺灣大學地質科學系、(3)臺灣大學海洋研究所、
(4)中央研究院地球科學研究所

日月潭是 1934 年日治時期於臺灣建造的第一個水庫，也是主要的水力發電來源。在 1944-1945 年第二次世界大戰期間，發電廠曾遭遇美軍轟炸，接著又在 1999 年經歷 921 集集大地震的重創。本研究於 2016 年在日月潭鑽取湖泊沉積物岩芯，試圖從岩芯紀錄中尋覓這些天然災害或人類活動所留下的紀錄。首先我們在日月潭進行聲納震測底質剖面掃描，分析自 1934 年建壩之後的沉積物空間分佈，並決定鑽探岩芯的鑽取位置，然後以震盪岩芯採樣器取得 3 公尺以內的沉積物。我們使用 MSCL 分析磁感率、沉積物密度，也使用 X 光攝影、反射式可見光譜儀、X 光螢光掃描分析、X 光粉末繞射分析等方法，以了解沉積物中的組成變化和濁流層可能的位置。此外，定年方法採用沉積物的 ^{210}Pb 和 ^{137}Cs ，以及有機碳採用 AMS^{14}C 等方法以求得沉積物年代。結果發現在颱風頻繁與水庫快速沉積的環境下， ^{210}Pb 無法判斷沉積速率，僅有 ^{137}Cs 可以指示 1963 年的時間點。

對比沉積物中的黃色指標 b* 高峰、X 光攝影影像指示的濁流層，與 ^{137}Cs 高峰點，顯示出較大的濁流層訊號恰巧為發生在 1963 年的 Gloria 颱風。此外，高解析度的 XRF 掃描結果，顯示 Ca 含量低點可以完整對應到 1934 年以來重大的颱風災害事件所形成的濁流層，而 Ca 含量高峰也可以指出日月潭水庫建造初期、第二次世界大戰重建與 921 大地震災後重建的水泥使用訊號。未來近代沉積物的研究或歷史紀錄對比，可以思考使用類似的方法或手段進行相關研究。

中文關鍵字：人類活動、災害、地震、颱風、XRF、沉積物

Marine evidence for Holocene flooding and climate change off SW Taiwan (EAGER core MD18-3548/MD18-3552)

Pai-Sen Yu¹、Ting-Ting Chen¹

(1)Taiwan Ocean Research Institute, National Applied Research Laboratories

Taiwan, regularly affected by both climatic forcing (East Asian Monsoon, typhoons, and extreme climate/weather events) and tectonic origin (intense seismicity, and marine landslides), provides significant scientific topics and excellent material for testing past climate change and tectonic hypotheses. The EAGER's marine core MD18-3548/MD18-3552 (21.879°N; 119.953°E; water depth 1752 m) off SW Taiwan was investigated in order to reconstruct late Quaternary paleoceanographic changes and regional flooding events based on non-destructive technique. In contrast to traditional technique of stable oxygen isotope stratigraphy, the age model of core MD18-3552 was constructed using four AMS C¹⁴ dating and visible color reflectance data with/no MSCL physical properties. These extra-high sedimentation rates estimated for the top 16 m (equal to ~10 ka) could provide for clay mineral composition and associated paleoclimatic/paleoceanographic variations on centennial-to-millennial time scales. Besides, our results indicate that illite and goethite would represent a long-trend humid condition off SW Taiwan during the Holocene, which coincides with local insolation. The frequency of high illite would imply that heavy rainfall over SW Taiwan caused Holocene floodings. Moreover, we observed that Hematite existed large amplitude changes with ~1500 yr cyclical fluctuations, suggesting a plausible dynamic climate tele-connection between local process and extra-tropical forcing in the Holocene.

Keywords: EAGER cruise, off SW Taiwan, non-destructive technique, paleoceanographic changes, Holocene flooding events

Stalagmite-inferred hydroclimate in the northern rim of the Sahara over the past 300,000 years

Yun-Chuan Chung¹、Hatem Dhaouadi²、Hsun-Ming Hu¹、Emna Sbei³、
Hédi Ben Oueddou³、Mahjoor Ahmad Lone¹、Kuan-Jui Huang¹、
Chuan-Chou Shen¹

(1)High-Precision Mass Spectrometry and Environment Change Laboratory (HISPEC), Department of Geosciences, National Taiwan University、(2)Research Unity of Applied Chemistry and Environment, University of Monastir, Faculty of Sciences, Monastir, Tunisia、(3)University of Tunis, Faculty of Human and Social Sciences of Tunis, Laboratory of Geomorphological Mapping of Media, Environments and Dynamics, Tunisia

The Sahara Desert, located in northern Africa, is the largest desert in the world. The Sahara blocks the gateway from East Africa, hominin sites, to Eurasia; therefore, duration of green Sahara in the Quaternary is crucial for the studies of human evolution and distribution. However, lack of records with precise dates hampers us to investigate the link of local conditions with monsoonal and high-latitude climatic systems and to predict future regional hydroclimate. Here, we present absolute-dated stalagmite-inferred paleo-hydroclimate in Tunisia over the past 300,000 years. The stalagmite deposition intervals indicate history of wet conditions, receiving moist from the westerlies; instead, the hiatuses occurred during the arid periods. In other words, the dated stalagmite formations provide the timings of the alternation in desert and green periods. The results reveal the humid periods in the northern rim of the Sahara coincides with strong African monsoon windows and ²³⁰Th-normalized dust-inferred wet conditions. Our stalagmite records also suggest that the recurrence of wet-dry conditions in the northern Sahara should follow the insolation and/or glacial-interglacial cycle.

Keywords: stalagmite, the northern Sahara, hydroclimate

全新世東亞夏季風演變的貴州馬家坪洞石筍 $\delta^{18}\text{O}$ 記錄

梁明強¹、李紅春¹、米泓生²、李廷勇³、馬志邦⁴、Ludvig Löwemark¹、
林淑芬⁵

(1)臺灣大學地質科學系、(2)臺灣師範大學地球科學系、(3)雲南師範大學地理學部、
(4)中國科學院地質與地球物理研究所、(5)中央研究院歷史語言研究所

本研究基於中國貴州省馬家坪多種定年方法、高分辨率的石筍氧同位素記錄，利用通帶濾波、EEMD、Bernaola-Galvan 分割等方法，分析全新世東亞夏季風演變歷史。分析結果表明：1) 馬家坪石筍中整體死碳年齡較小，且相對穩定，因此可以利用 ^{14}C 定年技術對無法利用 $^{230}\text{Th}/\text{U}$ 定年的石筍進行精準定年。2) 從早全新世到晚全新世，馬家坪石筍 $\delta^{18}\text{O}$ 的長期演變趨勢受控於北半球夏季太陽輻射變化，並且與南亞季風(阿曼 Q5 石筍)、北非季風(ODP658 孔陸源百分含量)、及北美季風(ODP1102 孔 Ti 百分含量)變化一致，表明全新世長時間尺度 ITCZ 平均位置的南北移動與低緯度季風強度的變化同時受太陽輻射變化控制，支持“全球季風系統同步變化”的觀點。3) 在千年尺度，馬家坪石筍 $\delta^{18}\text{O}$ 在 8.6 - 1.6 ka 之間呈現了 8 次弱季風事件，其事件中心分別為 8.2 ka、7.3 ka、5.9 ka、5.5 ka、4.2 ka、3.4 ka、2.4 ka 和 1.9ka 事件，其中前 7 次事件都對應於於太陽輻射(Total solar irradiance-TSI)低值區，並在高緯格林蘭冰芯 NGRIP1 和北大西洋冰漂礫及低緯海溫(SST3.4)中響應，而 1.9 ka 事件發生在馬家坪 $\delta^{18}\text{O}$ 趨勢轉向之後(自 2.0 ka BP 起，石筍氧同位素逐漸偏負，與夏季太陽輻射變化相反)且僅存在低緯海溫記錄中，顯示該事件為地球系統內部波動，可能受控於低緯 ENSO 影響。4) 在年際-百年際尺度，馬家坪石筍 $\delta^{18}\text{O}$ 與低緯海溫(SST3.4)呈現顯著的負相關關係，與現代監測結果一致。當 El Niño 事件發生時，東亞夏季風減弱，貴州地區降水減少，導致石筍 $\delta^{18}\text{O}$ 偏重；當 La Niña 事件發生時，東亞夏季風增強，降水增多，石筍 $\delta^{18}\text{O}$ 偏重。

中文關鍵字：東亞夏季風、石筍氧同位素、千年事件、ENSO

中全新世早期台北盆地牡蠣的詳細 ^{14}C 定年以及氧碳同位素分析

李紅春¹、康素貞¹、劉聰桂¹

(1)臺灣大學地質科學系

2002 年 3 月在臺北盆地東緣，位於台北市政府東側的新光三越臺北信義天地 A11 館基地開挖時，發現早-中全新世台北盆地的沉積地層中有大量的貝殼和牡蠣堆積。剖面地面的海拔高度為 10 米，從地面往下 9.5 米處採集的窗貝 (Plancenta) 用貝塔液閃法 ^{14}C 定年得到的年齡為 7640 ± 60 yr BP。從地面往下 14.9 米處有一個 2 米見方的牡蠣礁體 (oyster reef)，在此礁體中採集了一枚長約 40 公分的牡蠣殼。在此牡蠣殼上採集了 8 處樣品進行 AMS ^{14}C 定年，年齡範圍從 8130 ± 200 yr BP 至 8435 ± 155 yr BP。雖然定年精度無法分別年齡層序，但可以確定這個牡蠣礁的形成年齡是在 8130~8435 年前，比上層貝殼年齡要老 800 年左右。從 ^{14}C 定年結果看，從 8435 年前到 7600 年前台北盆地遭受海侵。由於牡蠣為鹹水生物，判斷海平面較長時間停留在剖面之上。在該牡蠣殼的頭部（最老部分）沿著生長軸在 5.5 公分內鑽取了 79 個粉末樣品，進行碳氧同位素分析。在這 5.5 公分內，氧同位素值變化範圍是 $-6.03\text{‰} \sim -1.33\text{‰}$ (VPDB)，顯示大約 4 年的變化；碳同位素值變化範圍是 $-2.21\text{‰} \sim -0.31\text{‰}$ (VPDB)。碳、氧同位素都指示該牡蠣礁體的生長環境是鹽度較高的海水環境。本研究結果將對描述台北盆地早-中全新世的歷史提供新的證據。

中文關鍵字：台北盆地、早-中全新世、牡蠣殼、碳十四定年、穩定同位素

上帝之子(女)在搗蛋：台灣西半部乾旱的潛在因素？

林淑芬¹、陳添財²

(1)中央研究院歷史語言研究所、(2)慈濟大學通識教育中心

今年(2021 年)台灣正面臨嚴峻的缺水問題，究其原因，前一年(2020 年)沒有颱風登陸使得豐水期的儲水不足，又逢隨後的秋冬春季節降雨量減少，因此最終導致台灣西半部陷入缺水危機。台灣位在東亞季風區，除了颱風之外，冷暖季節轉換的鋒面(例如梅雨鋒面)也是重要的降雨機制，然而造成季風波動的原因十分複雜，聖嬰現象便是其中重要的大尺度長週期變化因素之一。

聖嬰-南方震盪(ENSO)主要發生在赤道太平洋附近，並透過大氣與海洋循環而對全球氣候造成影響。根據美國國家海洋暨大氣總署(NOAA)的監測資料顯示，在 2020 年夏秋之際赤道太平洋地區出現了強烈反聖嬰現象並持續至今，這次反聖嬰現象對於台灣降雨的實質影響值得關注。過去研究指出台灣在聖嬰現象期間的冬季至隔年春季往往出現降雨量多於平均的情形，在反聖嬰現象期間則台灣東北部經常降下秋季豪雨，然而對於 ENSO 事件與台灣乾旱現象的連結目前並無定論。過去筆者曾經透過宜蘭湖泊沉積物中的古氣候紀錄，指出台灣東北部豪雨事件與古代 ENSO 活動之間的對應關係，進而連結宜蘭秋季共伴豪雨與 ENSO 活動的遙相關，相對於今日台灣西半部的乾旱現象，除了利用近代儀器觀測紀錄之外，古氣候資料或許也能提供有用的線索。

中文關鍵字：乾旱現象、聖嬰-南方震盪、古氣候、台灣西半部

Identification and discrimination of two invasive cryptic species and development of methodology for environmental DNA (eDNA) barcoding

Pritam Banerjee¹、Gobinda Dey²、Raju Kumar Sharma³、
Caterina M. Antognazza⁴、Himani Kumari⁵、Michael W.Y. Chan⁵、
Jyoti Prakash Maity⁶、Chien-Yen Chen⁶

(1)Department of Earth and Environmental Sciences, National Chung Cheng University; Department of Biomedical Science; Graduate Institute of Molecular Biology, National Chung Cheng University、

(2)Department of Earth and Environmental Sciences, National Chung Cheng University; Department of Biomedical Science, Graduate Institute of Molecular Biology, National Chung Cheng University、

(3)Department of Chemistry and Biochemistry, National Chung Cheng University; Department of Chemistry and Biochemistry, National Chung-Cheng University、(4)Department of theoretical and applied science, University of Insubria, Varese, Italy、(5)Department of Biomedical Science, Graduate Institute of Molecular Biology, National Chung Cheng University、(6)Department of Earth and

Environmental Sciences, National Chung-Cheng University

Golden apple snails (*Pomacea* spp.) are the freshwater gastropod, were introduced during the 1980s in East and South-East Asia, are considered the top hundred destructive introduced species in the world. They are marked as a serious concern due to the destruction of agriculture by its excessive growth and overconsumption of plants (e.g. reduced rice production), spreading of life-threatening diseases by carrying pathogens, (e.g. intermediate host of *Angiostrongylus cantonensis*), and outcompeting native populations. However, few beneficial roles in food and fodder due to high protein content in tissue, use of the shell in production of cement, fertilizer, catalyst/ reagent of heavy metal removal, drug delivery, bone grafts, biofuel production, suggesting the potential utilization. Although, the lack of clear taxonomy and proper detection method affecting the control of invasiveness. Besides, misidentification can mislead researchers during application. Considering this background, present work focusses on the identification and discrimination of two cryptic invasive species, *Pomacea caniculata* and *P. maculata* from shell structure to molecular genetic level to maintain a clear taxonomy and emphasize on development of a standard protocol for detection of eDNA from both *Pomacea caniculata* and *P. maculata* in a mesocosm. Our study shows that in spite of failure in detection of those two species morphologically, a molecular level detection and monitoring can be used to detect species non-invasively. Nevertheless, as we found some minor differences in snail shell properties and structure, a strong need to distinguish species is obligatory. Furthermore, the development and validation of eDNA method for cryptic invasive species will be highly effective to survey the hidden biodiversity in the introduced places.

Keywords: environmental DNA, cryptic species, golden apple snail, molecular taxonomy, biodiversity monitoring



Methane rare isotopologue signals associated with methanotrophy in freshwater reservoir

Yeah-Ting Lin¹、Jhen-Nien Chen¹、Pei-Ling Wang²、Edward D. Young³、
Tzu-Hsuan Tu⁴、Li-Hung Lin¹

(1)Department of Geosciences, National Taiwan University、(2)Institute of Oceanography, National Taiwan University、(3)Department of Earth, Planetary and Space Sciences, University of California Los Angeles, USA、(4)Department of Oceanography, National Sun Yat-sen University

Methanotrophy plays an effective role in reducing the export of greenhouse methane from subsurface environments to the atmosphere over geological and contemporary time scales. In sediments or bottom water of freshwater lake, sulfate and oxygen are often scarce, thereby facilitating anaerobic methane oxidation potentially coupled to various electron acceptors. Quantifying the rates, pathways and regulatory factors of methanotrophy remains challenging as unique isotopic signatures associated with methane producing and consuming metabolisms are obscured by transport and mixing. Paired rare isotopologues of methane provide two dimensions in addition to bulk isotopes to describe isotopic re-equilibration and kinetics. In this study, we measured the abundances of rare methane isotopologues and companion characteristics derived from anaerobic incubation of sediments collected from the Feicui reservoir. Bulk isotope values of residue methane increased through time, generating fractionation factors of 1.01 for carbon and 1.07 for hydrogen. The $\Delta^{13}\text{CH}_3\text{D}$ and $\Delta^{12}\text{CH}_2\text{D}_2$ values were distributed in the proximity of the equilibrium line toward the high temperature end, a range greatly exceeding the incubation temperature (by hundreds of Celsius). Overall, the apparent equilibrium pattern suggests the unique kinetic control on the re-organization of rare isotopes in methane isotopologues during methanotrophy. Further deconvolution of mass balance is warranted.

Keywords: clumped isotopologues, methanotrophy, freshwater environments

菲律賓全新世珊瑚礁之微生物化

徐鈺婷¹、湯森林²、張英如¹、宮守業³

(1)臺灣海洋大學地球科學研究所、(2)中央研究院生物多樣性研究中心、(3)國立自然科學博物館

微生物岩(Microbolite)是由於底棲微生物群落在進行生理活動時，將碎屑沉積物凝聚、進行礦物沉澱或生物礦化等作用而產生生物沉積岩。菲律賓 Pararior 海岸之全新世(Holocene)岩芯中發現珊瑚礁與微生物岩交疊生長的狀況，而新生代珊瑚礁與微生物各指示著不同的環境條件，因此，其共生長的案例相當稀少，具有研究上的獨特性。Pararior 海岸珊瑚礁岩芯透過光學顯微鏡發現珊瑚礁最先被紅藻、有孔蟲覆蓋，接著是微生物岩生長，本研究試圖利用分析珊瑚、藻類及微生物岩之微生物群落，佐證藻類的存在可能改變珊瑚的生長狀態及其微生物菌相，進而促使微生物岩的生長。本研究萃取珊瑚礁岩芯之 DNA，進行 16s RNA 次世代定序，建立微生物群落庫。結果顯示岩芯 PAR 5 深度 15 與 15.1 公尺兩處微生物岩之微生物群落單元相似度為 97%，大多為兼性厭氧與厭氧菌。平均組成為 98.5%細菌(Bacteria)以及 1.42%古菌(Archaea)。細菌中占比最高為擬桿菌科(*Bacteroidaceae*)占 21.2%與理研菌科(*Rikenellaceae*)占 12.5%，分析結果多為厭氧與兼性厭氧之異營菌，而異營菌的生長及碳酸鹽沉澱會隨著有機質而遞增。珊瑚表面之肉質藻類與草皮藻類會釋放容易被微生物利用之溶解有機碳(Dissolved Organic Carbon, DOC)，促進對珊瑚有害之異營微生物生長，直接造成珊瑚微生物群落之改變。根據 Christophe Dupraz 和 Andre Strasser 所建立之珊瑚轉為微生物相之沉積環境，推論本研究可能處於低濁度營養相過度為高營養相之環境，以至於有利於微生物岩生長。本研究將繼續萃取岩芯中同深度之珊瑚、藻類、微生物岩與沉積物之 DNA，探討不同介質上之微生物菌相的轉變以及所代表的環境意義，建構珊瑚、藻類、微生物三者間之生長模式。

中文關鍵字：微生物岩、珊瑚礁、藻類、微生物化、次世代定序、全新世

The biofuel production by indigenous algae along with wastewater treatment

Pulipaka Naga Venkata Anootha¹、Pritam Banerjee²、Gobinda Dey²、
Raju Kumar Sharma³、Jyoti Prakash Maity¹、Chien-Yen Chen¹

(1)Department of Earth and Environmental Sciences, National Chung-Cheng University、
(2)Department of Earth and Environmental Sciences, National Chung Cheng University; Department of
Biomedical Sciences, National Chung Cheng University、(3)Department of Chemistry and
Biochemistry, National Chung-Cheng University

Enormous consumption of fossil fuels is unsustainable as a consequence of depletion of global reserves and increasing concerns about its contribution to global warming. Microalgae represent a viable alternative energy resource, which can produce large volumes of biomass, and subsequently biofuels, in much smaller geographic areas than first- and second-generation biofuels production. This study describes algal biofuel production, wastewater treatment using indigenous algae. Moreover, along with the production of biofuel, the study focuses on to optimization of biomass production (algal cultivation and operation under optimal conditions, biomass harvesting and lipid extraction) with different wastewaters using indigenous algae (*Chlorella sorokiniana*, *Scenedesmus*). Furthermore, the investigation focusses on the pollutant removal from wastewater. Result reflects that the production of biofuel was increased with the incubation time and biomass production. The pollutant concentrations in wastewater were decreased with the increasing time in presences of green algae and biomass concentration. Interestingly, the biofuel productions with wastewater treatment are the best mitigation option of replacing fossil fuels, safe wastewater disposal, carbon dioxide mitigation, and heavy metal removal.

Keywords: renewable energy, indigenous algae, biofuel, wastewater treatment, heavy metal removal

Isolation and characterization of indigenous rhizospheric salt tolerant phosphate solubilizing bacteria from Puzi Mouth Wetland in Taiwan

Gobinda Dey¹、Pritam Banarjee¹、Raju Kumar Sharma²、
Jyoti Prakash Maity³、Hsien-Bin Huang⁴、Chien-Yen Chen³

(1)Department of Biomedical Science, National Chung Cheng University; Department of Biomedical Science, Graduate Institute of Molecular Biology, National Chung-Cheng University、(2)Department of Chemistry and Biochemistry, National Chung Cheng University; Department of Chemistry and Biochemistry, National Chung-Cheng University、(3)Department of Earth and Environmental Sciences, National Chung-Cheng University、(4)Department of Biomedical Science and Graduate Institute of Molecular Biology, National Chung Cheng University

Soil salinity is one of the major abiotic stress all over the world due to the reduction of cultivated agricultural land and crop productivity compared to the growing population. In addition, last 50 years, due to fulfill our food demand the excessive use of chemical fertilizer, pesticides like fungicides, herbicides that make environmental problems including groundwater contamination, soil quality degradation, heavy metal contamination, biodiversity reduction, and increasing salinity of the soil. To counteract the adverse effects of salinity and chemical fertilizer on plants and soil, the use of salt-tolerant phosphate solubilizing bacteria (PSB) is an efficient and sustainable method in saline agriculture practice. Considering the background, In the present investigation, we have searched for efficient salt-tolerant phosphate solubilizing bacteria, which were isolated from the rhizosphere of *Avicennia* sp. and *Rhizophora* sp. of Puzi mouth wetland in Taiwan, a typical saline land. A total six isolates of PSB strains are identified by using of 16S rRNA gene and comparative analysis confirmed the taxonomic affiliation of PSB1, PSB2, PSB3, PSB4, PSB5, and PSB6 with *Bacillus velezensis* strain GD CCU TW1, *Enterobacter coloaecae* strain GD CCU TW2, *Bacillus licheniformis* strain GD CCU TW3, *Bacillus* sp. strain GD CCU TW4, *Kocuria arsenatis* strain GD CCU TW5 and *Bacillus* sp. strain GD CCU TW6 respectively. All PSB has a high potential for dissolving calcium phosphate $[Ca_3(PO_4)_2]$ within the range of 55.20-119.03 mg/L and showed phosphate solubilizing index from 2.21 to 2.88, but relatively weak ability to dissolve $AlPO_4$ and $FePO_4$ under salinity. Moreover, all the strains are produced IAA with ranges from 1.20 to 24.07 mg/L and well grown under Arsenite (AsIII) in 5 Mm concentration. This study characterized salt-tolerant PSB isolates can be used as bio inoculants that may be applied in saline agriculture and arsenic bioremediation practice.

Keywords: salt tolerant, phosphate solubilizing bacteria, IAA, arsenite, sustainable

110 年地質與地球物理學術研討會 B1-O-05
Biogeosciences 生物地球化學與地質（環境）微生物學
agriculture, bioremediation



A novel Bio-MCM-41 material: Synthesis using bacteria mediated biosurfactant and their characterization

Raju Kuma Sharma¹、Gobinda Dey²、Pritam Banerjee²、
Jyoti Prakash Maity³、Chien-Yen Chen³

(1)Department of Chemistry and Biochemistry, National Chung-Cheng University、(2)Department of Biomedical Science, Graduate Institute of Molecular Biology, National Chung Cheng University、
(3)Department of Earth and Environmental Sciences, National Chung-Cheng University

The mesoporous material synthesis has received a great attention in the field of material science due to their potential utilization as adsorbents, controlled drug delivery systems, sensors, catalyst in chemical reactions, acidic character, and cosmetics, etc. The different kinds of organic surfactants (e.g. CTAB, P123, F127, and CTAC, etc.) played an important role to synthesize the mesoporous material, where the material was introduced as less favorable in green nanotechnology due to their toxic effect. In the present study, a novel material Bio-MCM-41 was synthesized using a biological template as *Bacillus subtilis* BBK006 derived biosurfactant along with suitable precursor tetraethyl orthosilicate, which is a key objective to improve the green approach in nano-biotechnology. The material was prepared at room temperature with optimum pH and less time-consuming via sol-gel method. The key influence of synthesized material was studied at different calcinated temperatures such as 450 °C, 500 °C, 550 °C, and 600 °C respectively. The amorphous mesoporous silica characteristic was distinguished using low angle-XRD at d100, d110, d200 and wide angle-XRD at 22.59 (d100). The functional groups of calcinated material was observed at 3445 cm⁻¹ (-OH group), 802 cm⁻¹ (Si-O-Si). The FESEM and HRTEM micrograph of synthesized particle reflects the uniform spherical shape and specific particle diameter range of 250-300 nm. The TG-DTA result exhibits the removal of adsorbed surface water (30-210 °C), interlayered water molecules (210-307 °C), biological compound (307-468 °C), and formation of mesoporous silica nanoparticles (468-800 °C). The synthesized particles instituted a high surface area of 8.2616 m²/g and pore diameter of 14.8516 nm at calcinated temperature 550 °C. Thus, an eco-friendly novel material was synthesized using *Bacillus subtilis* and it can be applicable to the catalytic and environment research sector.

Keywords: mesoporous material, *Bacillus subtilis*, Bio-MCM-41, eco-friendly

Re-examine the active volcanoes in Taiwan

Sheng-Rong Song¹

(1)Department of Geosciences, National Taiwan University

Volcanic Hazards have been fitted into the Central Disaster Prevention and Response Council of the Central Emergency Operation Center (CEOC), which need to build up the warning system and emergent plans in 2018. It, thus, needs to know where the active volcano is for preventing volcanic disasters. Volcanologically, two criteria, the empirical and phenomenal have been used to define an active volcano. The former is a volcano having erupted during the last 10,000 yrs, while the latter is a magmatic plumbing system still being working underneath (Szakacs, 1994). Currently, two active volcanoes have been identified. One is the Tatun Volcano Group, while the other is the Kueishantao volcano. However, based on the geological information of inland and offshore of Taiwan, several potentially active volcanoes have been recognized. They are located in the offshore islands and submarine of north and east Taiwan. Historically, four submarine eruptive events have been recorded in captain log, which occurred in 1853, 1854, 1867 and 1916. Meanwhile, three volcanic islands, the Pengchiahsu, Mienhuahsu and Huapinghsu in north Taiwan and one, the Hsialanyu in the southeast offshore may also be the active ones, based on the preliminary field surveys, occurrences and dating. However, they still study in detail for building up the warning system and emergent plans in the future.

Keywords: active volcano, volcanic hazard, Taiwan

溫泉水之微量元素分析

畢如蓮¹、呂學諭¹、李曉芬²、吳雅文¹

(1)中正大學地球與環境科學系、(2)國家地震工程研究中心、大屯火山觀測站

溫泉水之地球化學研究是地熱流體探索的重要基礎，可提供區域的水文分布資訊—包括來源與傳輸；對於活躍的火山源(active volcanogenic)地熱區而言，則亦提供了岩漿源氣體的資訊，長期的溫泉水地化監測更是岩漿活動/氣體通道時空變化的重要證據；而上述地化研究首先需要的就是好的化學分析數據。本文即透過分析大屯火山區溫泉水的經驗，整理出溫泉水分析的流程與方法，分析項目包含主要元素與微量元素，微量元素包括 IA 族的 Rb, Cs、IIA 族的 Sr、Ba、IIIA~VIIA 的 B、Ga、Tl、Ge、Sn、Pb、As、Sb、Se，以及 B 族的 V、Cr、Co、Ni、Cu、Zn、Zr、Ag、Cd、Au 和稀土(REEs)元素，涵蓋的元素範圍很廣；透過光譜儀(e.g. ICP-OES)和質譜儀(e.g. ICP-MS)分析，擬定相關的 QA/QC(品管品保)程序，並依溫泉水特性做干擾的測試，以檢驗數據的正確性，訂定有效率的分析標準流程。

中文關鍵字：溫泉水、微量元素分析



利用高解析度數值地形模型精進火成岩與沉積岩混合區地質圖：

以玉里地質圖幅海岸山脈區為例

趙柏濂¹、詹瑜璋²、胡植慶¹、孫正璋³、謝有忠⁴

(1)臺灣大學地質科學系、(2)中央研究院地球科學研究所、(3)臺灣大學地質科學系、中央研究院
地球科學研究所、(4)經濟部中央地質調查所

過去繪製二維地質圖時，受限於台灣植被茂密與地形陡峭，在野外露頭能取得的資料有限，因此難以提高地質圖製圖解析度。近年來，光達技術產製的數值地形模型，能濾除覆蓋地表的植被，展示出精細裸露的地形。前人研究證實在台灣西部麓山帶與雪山山脈地質區，運用高精度與高解析度的數值地形模型，判釋岩層層跡與構造的地形特徵，具精進地質圖的潛力。本研究將以玉里地質圖幅海岸山脈區為例，進一步討論新的製圖方式是否適用於火成岩與沉積岩混合區，並且探知海岸山脈中段地質構造型態。海岸山脈出露岩層包含中新世中期到上新世早期的火成岩層：都鑾山層、上新世到更新世早期的沉積岩層：蕃薯寮層與八里灣層、以及中新世到更新世的利吉層。研究製圖流程分為四大步驟：首先，將數值高程模型套入 ArcGIS Pro，計算日照陰影圖與坡度圖。接著，在三維工作環境下，轉換不同視角與光源，觀察地形特徵，判釋岩層層跡與構造線。然後，運用位態計算工具，求出岩層位態資料，再到野外查核比對岩性與位態。最後，將資料整合成更高解析度的地質圖，且繪製剖面。研究結果顯示火成岩與沉積岩中，因為各岩層抗侵蝕能力不同，使得地形上坡度不同，所以得以精細的追蹤岩層層跡。本研究亦觀察到因植被覆蓋，而過去未發現的細微構造：高寮地區的正斷層系統為深層重力滑坡變形所致；花東山的都鑾山層為單斜構造；長濱地區都鑾山層與八里灣層邊界有清楚且延續性佳的構造線型，推測是小錯距的層間滑動。本研究為無法到達的地方補足地質資料，且在火成岩與沉積岩混合地區，提供高精度與高解析度的製圖方式。

中文關鍵字：高解析度數值地形模型、三維地質製圖、海岸山脈、差異侵蝕、火成岩

ArcGIS 地下地質三維模型建置 – 以桃園市地下水分層為例

賴俊瑋¹、陳鴻文¹、丁哲庸¹、林辰翰¹

(1)中興工程顧問股份有限公司

近年來，由於全球氣候快速變遷下，導致水庫蓄水量不定，造成工業、民生等用水極大問題與挑戰。長年以來，桃園市境內利用埤塘作為次要儲水使用外，而蘊藏之地下水是另一個相當重要的用水資源。從前人研究之水文地質剖面顯示，位於桃園地區之主要含水層分別位於晚更新世以來之階地礫石層及下伏之更新世楊梅層砂岩等，故為了解桃園地區之地下水分布，本研究蒐集且篩濾區域內 32 孔水文地質鑽孔，將岩心記錄中分為礫岩與砂岩之透水層，及粉砂岩與泥岩之阻水層，進行含水層判釋，參考既有平面地質圖及地質剖面圖，繪製 8 條岩性地層地質剖面，做為三維地質柵狀圖之依據。

而本研究則利用計畫區周緣設置三維模式邊界後，透過 ArcGIS 軟體將上述之岩性地質剖面圖，以三維空間處理模組建置三維地質柵狀圖，並擷取各透水層及阻水層面用以產製三維曲面資料，再依各曲面之空間分布狀況進行衝突修正後，建立實體水文地質模型。最後，此模型可將大量且複雜之地質資料以視覺化方式呈現，有利於地質專業人員進行判讀及檢核，更可以增進民眾及政府機關閱覽能力，並增進雙方溝通效率等益處，進而可即時且快速探討區域之水文地質架構。

中文關鍵字：三維地質模型、地理資訊系統(GIS)、水文地質

海床絕對壓力計的測試及初步資料分析

林慶仁¹、林豐盛¹、張坤輝¹、許雅儒¹、李炘旻¹

(1)中央研究院地球科學研究所

台灣位處於歐亞板塊和菲律賓海板塊的交界處，台灣東部海域不僅地震頻繁而且板塊聚合的速度也比其他的地方快很多，近幾年來中央研究院也在台灣周圍海域進行了一些使用聲波定位方法進行海床大地測量觀測的研究。為配合海床大地測量觀測，海底絕對壓力測量也是另一種測量的方法。

中研院自製的海床絕對壓力計(absolute seafloor pressure gauge, SAPG)是由 Paroscientific Inc. 出品的振動石英壓力傳感器，配合 RBR-Global Co. 出品的 OEM 資料記錄器 (<http://www.rbr-global.com/products/bpr>) 和 EdgeTech 海底聲納控制電路板…等元件所組成。目前已經完成六部 SAPG 的組裝，有三種不同的外觀設計，並且有 4 部佈放於台灣東部海域進行為期 11 個月的長期觀測。本文將介紹 SAPG 的儀器組裝、出海前的測試及海域資料的初步分析成果。

中文關鍵字：振動石英壓力傳感器、絕對壓力計、大地測量



跨井熱示蹤劑試驗結合分散式光纖溫度感測器量測特徵化裂隙岩體

之優勢水流路徑

邱永嘉¹、馬嵩哲¹、劉慶怡¹、戴迪墨¹、黃柏勳¹

(1)臺灣海洋大學地球科學研究所

地下水在裂隙岩體中之流動有別於在傳統孔隙介質之中，其流動行為不再遵循傳統的孔隙介質理論。裂隙岩體中的特定透水裂隙常被認定為地下水流及污染傳輸之主要優勢路徑，然而，由於裂隙本身之複雜性與外在不確定性因素，導致在調查裂隙岩體中之水流極具困難性，僅利用傳統之調查方式判釋地下水流向與流速，並推估透水裂隙之水文地質參數相當不易。本研究選用熱作為地下水示蹤劑，並搭配井下跨孔水力試驗，判釋透水裂隙位置及連通性，並同時推估其相對應之水力參數，用以特徵化透水裂隙之水力特性。研究區域選定於南投和社水文地質試驗場址進行現地試驗，選定一組跨孔觀測井作為試驗井，除了以傳統溫度陣列進行溫度量測之外，並同時利用高解析度之分散式溫度感測器（fiber optic distributed temperature sensor, FO-DTS）蒐集空間中連續性之溫度資料。本研究之試驗結果顯示，透過溫度變化分析及溫度破透曲線的描繪，可準確判釋井下導水裂隙之位置及連通性，而數值模式之模擬，則進一步量化導水裂隙之水力傳導係數。試驗結果亦顯示，在不同的流場條件下，對於裂隙位置判釋將產生差異，而導水裂隙與井下裸孔之交錯，將造成井內強烈的垂向水流。利用熱水搭配鹽水進行試驗，透過熱衰減（thermal attenuation）及熱與鹽水峰值之時間延遲（lag time），可更進一步推估導水裂隙之隙寬。本研究之成果顯示，熱-鹽水示蹤劑試驗搭配高解析度分散式溫度感測器量測，在特徵化裂隙岩體中的優勢水流極具潛力，可提供未來裂隙岩體中優勢水流路徑調查技術提供參考依據。

中文關鍵字：熱示蹤劑、鹽水示蹤劑、導水裂隙、分散式溫度感測器、南投和社

孔內多層式光纖光柵水壓與溫度感測系統研發與測試

何彥德¹、蔡瑞彬²、王子賓³、張良正⁴

(1)臺灣大學、(2)臺灣大學生物環境系統工程學系、(3)健行科技大學空間資訊與防災科技研究中心、(4)陽明交通大學土木工程學系

含水層常作為地下水使用的來源，一旦遭受地下水污染將立即影響供水安全性，同時地下水復育亦將面臨極大的挑戰。為了預測整治藥劑與污染團在深層含水層的移動路徑，了解地下水系統的狀態是很重要的(如地下水質、水位與水溫等)，然而傳統環保署觀測井多僅在特定深度開孔，且只能觀測含水層的平均狀態，因此提供的地下水相關資訊相當有限。有鑒於此，本研究使用光纖布拉格光柵(Fiber Bragg Grating, FBG)研發出多層地下水壓與溫度量測系統，可以在同一鑽孔內同時進行多個不同深度的水壓與溫度量測。光纖具有可遠距離穩定傳輸訊號、訊號不易受水與電磁波干擾與無火花安全性高等優點，而本研究所開發之 FBG 多深度水壓與溫度量測系統則進一步透過室內測試與現地測試，以展現本系統之觀測能力。

中文關鍵字：多層式光纖光柵感測系統、地下水壓、地下水溫



利用主動式光纖溫度感測器解析地下水污染場址之地下水流速

李雨軒¹、潘庭馨¹、劉慶怡¹、邱永嘉¹

(1)臺灣海洋大學地球科學研究所

傳統的水文地質調查方式，僅能針對大區域的環境進行試驗，在地下含水層極為複雜的情形下，由於現地資料空間解析度的不足，將導致水文地質狀況掌握不易，產生含水層透水區段及地下水流速、流向推估上的誤判。本研究利用分散式光纖溫度感測器（fiber optical distributed temperature sensing, FO-DTS）量測技術，針對台灣南部地下水污染場址，進行井下的高解析度（high resolution）水文地質調查，同時以複合式光纖纜線搭配主動式線性熱源加熱法，推估地下水流速在垂直方向上之分佈。分散式光纖溫度感測器之量測原理為藉由分析雷射光束在光纖中的雷曼散射（Raman scattering）訊號而獲得環境中的感測溫度，其最大優勢為在空間上與時間上的連續性量測。本研究針對場址內的 15 口監測井進行試驗，並透過熱傳輸的原理分析，解析井下透水區段及推估地下水流速在垂直上之分佈，細部的水文地質分層亦可透過上述資訊獲得進一步的解析。經由視熱傳導（apparent thermal conduction）的解析，可進一步將岩層的熱傳導與地下水流熱對流效應予以區分。本研究之成果顯示，利用分散式光纖溫度感測器在環境溫度感測上的高解析度優勢，搭配主動式的線性熱源加熱，可產出具有時間及空間上優勢的高解析度成果，提供地下環境細部分層狀況的進一步評析，未來土壤與地下水污染場址在水文地質調查、甚至污染整治成效評估之參考依據。

中文關鍵字：分散式光纖溫度感測器、熱示蹤劑試驗、井下水文地質調查、地下水流速

低衝擊開發之生態滯洪單元非飽和入滲形態對排水量之影響

許少瑜¹、蔡義誌¹、李榮棟¹、蘇昱豪¹、黃群展¹

(1)臺灣大學生物環境系統工程學系

低衝擊開發的理念已經廣為大眾所推崇，並落實於土地規劃及景觀設計，以友善環境的作法就源處理，透過入滲、過濾、滯留、蒸發延緩雨水排水量，達到消減洪峰流量、改善水質的目標。文獻指出透過設置生態滯洪單元能有效地減少逕流排出量，並且多以飽和入滲或穩定入滲率探討其效益。但是，生態滯洪單元內部的非飽和入滲過程及形態對於排水量，仍然缺乏相關研究。本研究在生態滯洪單元(槽池長 4m、寬 1.5m、深 2.3m)內部設置時域反射計(TDR)、張力計及溫度計觀測非飽和入滲過程之體積水分含量、基質勢能及土壤溫度之變化，並以地球物理探勘的地電阻技術測量入滲剖面，觀測入滲濕峰移動及水分分布，討論不同的供水方式(點源供水與降雨)所形成的入滲形態，以及影響生態滯洪單元的排水量。結果顯示，透過二維地電阻影像剖面能呈現出生態滯洪單元內部的非飽和入滲過程，入滲濕峰的移動受供水方式與地下水位的邊界條件所影響。再配合體積水分含量及溫度資料，發現剖面中層及深層高溫訊號落後於低溫訊號，顯示不同深度的濕峰移動，所混合的入滲新水及殘留舊水之比例明顯不同，而且舊水反應波速可達新水流速的兩倍以上。

中文關鍵字：入滲、體積水分含量、地電阻、新舊水互動

地震危害度分析之斷層幾何模型－觸口斷層與崙後斷層

陳冠宇¹、范秋屏¹、張毓文¹、張志偉¹、劉勛仁¹

(1)國家地震工程研究中心

地震危害度評估的第一要務便是建立斷層或孕震構造的幾何模型，斷層幾何形貌對於斷層上盤場址之地震危害度有極高的敏感度，除主控震源至場址的最短距離外，並掌控斷層破裂面積與其透過尺度公式(Scaling law)計算最大可能地震規模之結果。由此可知，斷層幾何在 earthquake 危害度評估中舉足輕重的地位。

因此，本研究之目的在蒐集斷層或孕震構造之相關資料，由地表地質調查、地下鑽井、平衡剖面、地電測量、反射震測等地質及地球物理資料之彙整到斷層幾何模型建立與不確定性評估之依據，並利用地理資訊系統(GIS)建立斷層三維模型，用以檢視幾何模型在各參數(長度、走向、傾角及深度)不確定範圍的組合內，向下延伸的斷層面是否會在特定位置產生非預期的截切，造成模型不合理之處。本研究之範圍北起三義斷層南至左鎮斷層，東側為雙冬-大茅埔斷層，西側至彰化斷層，而此簡報內容以觸口與崙後斷層為例，由三維方式呈現斷層幾何，並探討幾何參數組合之狀況。

觸口斷層長約 28 公里，崙後斷層由觸口地區至左鎮斷層長約 50 公里。最終幾何模型為觸口斷層向下之傾角分別為 25/40/50 度，深度停於下方的滑脫面(Décollement)。而觸口斷層與崙後斷層之破裂模型為：觸口斷層與崙後斷層個別單獨破裂(Individual ruptures)、觸口斷層與崙後斷層相連破裂(linked rupture)以及與大尖山斷層南段相連的全段破裂(Entire rupture)。

中文關鍵字：地震危害度、觸口斷層、崙後斷層、滑脫面、破裂模型

2006 年屏東外海地震誘發之恆春斷層慢滑移事件

蕭詩涵¹、景國恩¹、蔡佩京²、李劍珩³、張文和⁴、陳建良⁵

(1)成功大學測量及空間資訊學系、(2)綠環工程技術顧問有限公司、(3)K2 Management、

(4)中央大學地球科學系、(5)中央地質調查所

本研究藉由中央地質調查所於恆春半島設置之 7 個 GNSS 連續站、37 個移動站及 2 條精密水準測線 2002 年至 2016 年間之觀測資料發現，2006 年屏東外海 M_L 7.0 地震發生後，恆春半島之地表運動型態產生了明顯的轉變，且首次觀察到臺灣地區之慢滑移事件。為了釐清此區域慢滑移事件之活動型態及其在恆春斷層上能量累積與釋放的模式，本研究除了分析時間序列獲得地表速度場外，更透過基線反演模型與斷層錯位模型，推估斷層面上滑移虧損速率與滑移速率之分布型態及數值，再結合地質調查結果進行綜合探討。根據時間序列分析結果，恆春半島之地表速度場以 2006 年屏東外海地震及 2010 年 4 月為界，可區分為 3 個時期：相對於 S01R 測站，2006 年屏東外海地震發生前，西南側水平速度於約 53-58 mm/yr 向西北，垂直沉降速度約 8-15 mm/yr；東側水平速度於約 47-55 mm/yr 向西北西，垂直沉降速度約 5-18 mm/yr。2006 年屏東外海地震發生後至 2010 年 4 月，西南側水平速度於約 53-56 mm/yr 向西南西，垂直沉降速度約 3-10 mm/yr；東側水平速度於約 45-53 mm/yr 西北西，垂直速度轉為抬升為主約 3-9 mm/yr。2010 年 4 月至 2016 年，西南側水平速度於約 50-54 mm/yr 向西南西，垂直沉降速度約 3-8 mm/yr；東側水平速度於約 43-53 mm/yr 西北，垂直速度轉回沉降為主約 1-6 mm/yr。基線反演模型與斷層錯位模型結果則指出，恆春斷層為具有左移分量之逆衝斷層，其於 2006 年屏東外海地震發生前，具有南北兩個地栓 (Asperity)；且地震發生後，能量並未停止釋放，而是持續於此兩個地栓由南往北遞進釋放。此外，根據地質調查研究結果，鄰近恆春斷層區域直至 2017 年仍有地表裂隙產生，亦為此區域震後持續潛移之佐證。綜上所述，本研究推論：(1) 恆春半島地表運動型態的改變是由 2006 年屏東外海地震所誘發；(2) 恆春斷層上盤垂直速度之變化與地質調查研究結果顯示，斷層面上所累積之能量於地震後仍持續緩慢釋放中，亦即此區域有慢滑移事件之發生；(3) 恆春斷層之位置可能位於目前劃定範圍之東側約 1-2 公里之位置。

中文關鍵字：恆春斷層、2006 年屏東外海地震、慢滑移事件、斷層滑移虧損速率

Ground deformation along the Chegualin fault between 2018 and 2020 from SBAS DInSAR observation

Cheng-Han Lin¹、Jyr-Ching Hu²、Ming-Lang Lin¹

(1)Department of Civil Engineering, National Taiwan University、

(2)Department of Geosciences, National Taiwan University

The Chegualin fault in southern Taiwan is the major active fault within the Gutinkeng formation in the fold-and-thrust belt. According to Central Geological Survey in Taiwan, the Chegualin fault is considered as the category two active fault documented it as a thrust fault striking N-S in the north and gradually striking NE-SW to the south with various dipping angle. However, several investigations have shown that the southwestern segment of the Chegualin fault is recently dominated by right-lateral movement with minor thrusting component. This fault also shows creeping behavior which could gradually affect the functions of the infrastructures across the Chegualin fault. This study aims to reveal the surface deformation rate relevant to the Chegualin fault zone from 2018 to 2020 by using multi-temporal InSAR analysis. For this purpose, the Small Baseline (SBAS) DInSAR technique was adopted, which allows efficiently analyze the temporal deformation on the small temporal and spatial baselines interferogram network over a wide area. The reliability of the observation and qualities of the procedures in the SBAS DInSAR workflow were quantitatively evaluated based on the results of continuous GPS measurements. We further remark that this study follows the work of Lin et al. (2021) where a numerical workflow for assessing the fault rupture-engineering structure interaction problems was present. The results of this study could provide reliable free-field ground deformation data for the calibration of the numerical simulations in the future.

Keywords: Chegualin fault, ground deformation, SBAS DInSAR analysis, multi-temporal observation

Numerical tectonic escape models of southwest Taiwan

Fang-Yi Lee¹、Eh Tan²、Emmy T.Y. Chang¹

(1)Institute of Oceanography, National Taiwan University、

(2)Institute of Earth Sciences, Academia Sinica, Taiwan

This study investigates the tectonic escape in SW Taiwan. The studying area in this research ranges from the Pingtung Plain to the east bound of the Peikang High. GPS data show a counterclockwise rotation in the velocity field in the inland part of the studying area. The velocity vectors are around 5 cm/yr westward in the east of the Pingtung plain and around 5 cm/yr southwestward at the coast of Pingtung and Kaohsiung. Previous studies suggest that Peikang High may act as a western backstop and play a crucial role for the tectonic escape here.

Our experiments are 3D dynamic models under elastoplastic deformation regime with the program DynEarthSol. To construct the circumstances of SW Taiwan, field observation with fault map, Cenozoic sediment isopach and GPS data are considered for model settings. Our model is under lateral shortening in E-W direction with a ramp under Chishan fault, and have a southern open boundary, where materials can escape through. The frictional strength and the orientation of the open boundary are varied in our experiments. Common features in all models are: (1) a counterclockwise rotation in surface velocity field, (2) subsidence around the open boundary, and (3) a dextral thrust along the “Chishan” fault. The strength of the decollement controls the width of the fault zone and the degree of rotation in the velocity field. With a high-strength decollement, the rotation in velocity field is small and the fault zone is narrow. Only when the basal friction is low enough and the open boundary is parallel to the coastline between Kaoping river and Chaochou fault, the velocity field would be able to rotate that much as the observation.

Keywords: numerical simulation, southwest Taiwan, tectonic escape

分析環境背景雜訊探查恆春半島速度構造

黃有志¹、林哲民¹、謝宏灝¹、張志偉¹、張議仁¹、溫士忠²

(1)國家地震工程研究中心、(2)中正大學地球與環境科學系

恆春半島位於中央山脈最南端，往南連接巴士海脊，是板塊碰撞所形成的增積岩體，以覆瓦狀褶皺逆衝斷層帶為主，所代表的是臺灣造山帶形成初期之地質構造，亦即現今西部麓山帶之地質雛形。恆春斷層為一向東傾斜的逆斷層，呈北北西-南南東走向，大致位於山麓與平原區交界，斷層兩端可能往海域延伸，認為有較高之斷層活動潛勢。因此，國震中心於恆春半島南端架設 12 個臨時寬頻地震站，測站間距約 5 公里，進行恆春半島斷層活動監測。

近年來，分析環境背景雜訊探求地下速度構造，在經過理論方法驗證，有標準化的資料處理程序，也證實研究結果的可靠性，已經被廣泛接受應用。本研究試著將恆春半島的 12 個測站，結合國震中心 SANTA 寬頻地震網，位於南臺灣的 14 個測站，及 4 個監測萬丹泥火山活動的臨時寬頻地震站，總共約有 30 個寬頻地震站，試著解析恆春半島之淺部地殼速度構造。初步分析西元 2018-2020 年的連續紀錄，取樣率降至 20 Hz，選定的分析週期為 0.5-10 秒。把所有測站對疊加平均的交對比函數，依照測站對距離遠近排列，隱約可見時間域經驗格林函數訊號，大致以視速度 2.1 公里/秒傳播。再進一步試著挑選每組測站對，0.5-10 秒的雷利波相速度頻散曲線。接下來進行三種棋盤格解析度測試，確定側向解析度後，層析成像選擇以 0.05 度格點，獲得 1-5 秒的雷利波相速度分布圖。相關的速度分布特性，與活動斷層及地質構造等資訊相互比對及分析討論。

中文關鍵字：恆春半島、環境背景雜訊、層析成像、速度構造

台灣山脈地形研究(I)：被遺忘的緩起伏地形

謝孟龍¹、陳展懋¹

(1)中正大學地球與環境科學系

日據時期即已報導，台灣山脈主要稜脊存在「緩起伏地形」，從丘陵到海拔>3000 m 的高山；其中緩溪流與緩坡遍布，常見窪地(或積水成池)。在彼「地形循環」學說盛行的年代，緩起伏地形被視為地殼運動「休止」的證據，相對爾後地殼「快速抬升」、河流「回春」產生的陡坡。地形循環學說已走入歷史，並被「地形穩態」的概念所取代：當造山達到一定規模後，其侵蝕將抵銷隆升，從此山脈高度不再增加。此「地形穩態」的概念最早由 J. Suppe 引入台灣—配合其「斜碰撞」的造山模式，認為中央山脈最高、最寬的北—中段(立霧溪—新武呂溪或知本溪)已達到「地形穩態」。從此，該概念深入學界。由於達到地形穩態的山脈「不應」出現緩起伏地形，該地形或因此被忽略，或如 S.D. Willett 之模型，被視為水系變遷過程中次要的產物(因流域上源被侵蝕或被襲奪，導致河流失去下切力而逐漸形成)。本研究以為，上述台灣山脈「地形穩態」的達成(包括「斜碰撞」造山模式)至今仍處於假說階段，並無直接證據支持(或支持之證據也不違背其它假說)，吾人或應重新正視緩起伏地形存在的意義：(1)這些地形，絕大多數並無法用 S.D. Willett 之模型解釋。(2)這些地形的分布是全島性，其規模(面積)約與海拔高度呈負相關(抬得越高越難被保存下來)。(3)這些地形常見風化嚴重的土壤或崩積層(顯示其形成時代久遠)。以上，本研究認為，所見之緩起伏地形乃生成於低海拔、地殼隆升緩慢的環境；之後被抬升，遭河流切割、山崩侵蝕，最終「殘存」在中、高海拔山區；殘存於高海拔的緩起伏地形有利冰雪堆積，間接促成末次冰期冰河的發育。在此模式下，台灣山脈應曾經歷一段漫長緩慢隆升的階段(山脈整體一起抬升)，當時「緩起伏地形」遍布；之後地殼隆升加速(特別是山脈今日較高的區段)，直到今日。

中文關鍵字：緩起伏地形、地形穩態、台灣山脈

台灣山脈地形研究(II)：緩起伏地形之於山脈隆升歷史與形態的應用

謝孟龍¹、李元希¹

(1)中正大學地球與環境科學系

咸信台灣山脈曾經歷一段緩慢隆升的階段，當時「緩起伏地形」遍布(如今日之恆春半島)；之後地殼隆升加速，被抬升的緩起伏地形遭河流切割、山崩侵蝕，最終殘存在中、高海拔主要稜脊上。檢視這些緩起伏地形高程系統性的差異(反映不等量抬升)，及其保存的程度(透露侵蝕狀況)，再配合分水嶺的位置(應為，或曾經為流域隆升最快處)，或能推斷山脈隆升的歷史與形態。主要論點包括：(1)沿山脈(主稜)走向，緩起伏地形高程越高、越窄(保存越差)，則地殼抬升量越大；海拔最高，但無緩起伏地形殘留的地帶地殼抬升量最大。(2)垂直山脈走向，若河流中、下游流域有較高的緩起伏地形(即流域最高的緩起伏地形並非保存於主要分水嶺上)，則代表地殼隆升中心已由分水嶺轉移至流域中、下游。本研究由此兩論點出發，計畫檢視台灣山脈所有的緩起伏地形。已得到的結論(初步)包括：(1)中央山脈沿主稜計有五個抬升較快的區段，由北至南：南湖—中央尖山(向西對應雪山聖稜)，奇萊山區，馬博、秀姑巒山區(向西對應玉山山塊)，向陽—關山，南、北大武山區；續向南，山脈抬升速率遞減，直到恆春半島。(2)中央山脈中段濁水溪流域，抬升中心已由主要分水嶺(安東軍山—丹大山)向西移至東郡大—千卓萬山區。(3)恆春半島楓港溪、四重溪流域抬升中心已由山脈主要分水嶺向西移至流域下游。

中文關鍵字：緩起伏地形、山脈隆升歷史、山脈隆升中心遷移

台灣山脈地形研究(III)：緩起伏地形邊緣超高瀑布的生成與其意義

吳純然¹、謝孟龍¹

(1)中正大學地球與環境科學系

台灣山區圍繞緩起伏地形的陡坡常見瀑布，落差可達數百公尺(以下稱「超高」瀑布)，具名者如阿里山區的「蛟龍瀑布」(落差六、七百公尺；號稱台灣最高的瀑布)，濁水溪支流丹大溪的「九華瀑布」。瀑布一般被視為「遷急點向上游遷徙」的產物，無論這「遷急點」是如何形成(岩性差異，斷層活動，侵蝕基準面下降，主、支流下切速率不同等)。然而，此傳統「遷急點遷徙」的模式並不易解釋所見「超高」瀑布的生成—這些瀑布下游河道皆平緩，距主要溪流匯口(或任何可能產生遷急點的地帶)亦有相當的距離。本研究經地圖、影像分析以及野外實察後，認為該類型瀑布的生成與其下游集水區廣泛的山崩有關：(1)山崩產生充足的岩屑，有利河道岩盤的下切(無論藉由河流或土石流作用)，岩盤的下切使坡地變陡，進一步促成山崩，如此循環，逐漸擴大瀑布上、下游河道的起伏。(2)當岩性許可、崩塌產生垂直岩面(硬岩，具垂直節理，且層面水平或其傾向與坡向相反)，則山崩活動降低(因植被的移除，風化減弱，岩屑來源減少)；垂直岩面持續擴大後將使坡地趨近穩定，瀑布因而成形。以上地形的正、負回饋作用不只解釋了「超高」瀑布的形成，也說明為何緩起伏地形能殘存於台灣隆升、侵蝕快速的山脈中。須知，「超高」瀑布也常見於世界其它地區，特別是構造運動並不活躍的高原邊緣。由於發育瀑布需要冗長的時間，不易研究，台灣的觀察或為這些瀑布的成因提供了看法。

中文關鍵字：緩起伏地形、瀑布、遷急點、台灣山脈

台灣山脈地形研究(IV)：檢視河階碳十四定年得到的岩盤下切速率

檢視台灣由河階碳十四定年得到的岩盤下切速率

陳奕豪¹、謝孟龍¹

(1)中正大學地球與環境科學系

河流下切岩盤使坡地變陡，若河流下切岩盤能與山脈隆升同步，則山脈的侵蝕或能抵銷其隆升，使之達到地形「穩態」。換言之，若山脈已達到地形「穩態」，則或能利用河流岩盤的下切，及其相關地形特徵(如河流縱剖面形貌)，來一窺山脈隆升的細節(速率、空間變化)。台灣山區已產出超過六百筆碳十四年代(大多<20 ka cal BP)，適以用來檢視河流岩盤下切的控因，及其與山脈隆升的關聯。本研究將階地「岩盤面比高」(E，相對現生河床面)除以階地「沉積物的碳十四年代」(A，取最大者)，來定義「岩盤下切速率」($U = E/A$)，用來代表河流長時間岩盤垂直方向上被侵蝕的速率(期間河流可反覆堆積、下切、側蝕)。主要結果包括：(1)當 E 沿河道橫剖面存在顯著變異時(即存在古河道)，U 最大值可達每年數公分(平均千年，切蝕砂頁岩)，顯示台灣河流下切岩盤的巨大潛能；產出這些高 U 值的河流(如荖濃溪、立霧溪)，也皆有間歇性大規模堆積的紀錄。(2)由較年輕階地($A < 10$ ka)所計算的 U 有很大的離散性，從零(岩盤未出露)至每年數公分，其中僅少部分能用地殼不等量隆升來解釋。(3)由較老階地($A > 20$ ka)所計算的 U (< 4 mm/yr)與台灣山脈長時間的剝蝕速率較為接近。(4)所有河流最上游河段得到的 U 皆為零(A 從<0.2 ka 至 50 ka)；這些河段上源皆缺乏山崩、土石流。以上，配合現生河流環境觀察及坡地運動資料，得到以下結論：(1) U 強烈受控於礫質沉積物的供應(因此與山崩、土石流息息相關)。(2)所見整體 U 值的增加應反映全新世以來洪水頻率的增加—導致河流水與礫質沉積物流量的增加；後者相當部分來自末次冰期時的坡地堆積。(3)在碳十四定年的時距下，台灣山脈並未達到地形「穩態」，因此並不適合利用 U 及其相關地形特徵來推論地殼隆升。

中文關鍵字：河流岩盤下切、坡地作用、地形穩態、台灣山脈

台灣山脈地形研究(V)：山崩控制下的河流地形－

以乾坑溪(嘉義豐山)為例

梁凱鈞¹、謝孟龍¹、郭昱廷¹

(1)中正大學地球與環境科學系

山區河流地形的模擬一般以「水力」的觀點出發，並假設「地形穩態」(河流下切岩盤與地殼隆升同步)。如此，在岩性、地殼隆升均一的流域，流量向下游的增加，或主流流量大於支流流量的事實，解釋了為什麼河流一般向下游變寬、變緩，且支流河道陡於主流河道。本研究則提出不同的看法，認為至少在千年、萬年的尺度下，台灣山區河流地形主要受控於山崩、土石流的規模與頻率，並非「水力」(流量)，位於嘉義豐山村的「乾坑溪」即為一例。此溪於 1996 年賀伯颱風時發生土石流，1999 年九二一地震誘發上源大規模山崩；之後，凡颱風必有土石流肆虐，直到今日。由於山崩(及爾後的土石流)主要發生於支流，造成主、支流截然不同的形貌：主流較窄(多<20 m 寬)，支流較寬(50 – 70 m)；主支流交匯處，主流較陡，支流較緩，並因支流下切較快，使主流下游產生明顯的遷急點；匯流口以下，河道寬度、坡度皆與支流者相同。以上地形特徵極易使匯流口以上的支流被誤認為「主流」。乾坑溪「主流」兩側也發育十、二十公尺高的土石流階地(豐山村即位於其溪口之土石扇上)，其中漂木破十四定年(n=9)可將此間山崩、土石流的活動追溯至 1800 年前。至此，本研究強調沉積物供輸對河流形貌的重要性，此結論支持「沉積物磨蝕」學說(認為河流下切岩盤主要依賴底床沉積物的磨蝕，並非水力)。

中文關鍵字：山區河流地形、山崩、土石流、沉積物供輸

台灣山脈地形研究(VI)：高山冰河消退後的侵蝕－以南湖山區為例

彭冠箏¹、謝孟龍¹

(1)中正大學地球與環境科學系

南湖大山(主峰海拔 3742 m)，擁有中央山脈北段最高峰群，為台灣少數發育末次冰期圈谷與 U 形谷的區域。這些地形保存的狀況正適以用來檢視冰川消融後山脈的侵蝕。本研究發現：(1)所有切蝕硬岩(變質砂岩、礫岩或石灰岩)產生的圈谷與 U 型谷皆完整保存，包括其間冰緣作用產生的「碎石坡」(在空照圖或衛星影像上或被誤認為山崩地)。(2)雖然陡坡遍布，但僅北峰北坡(和平北溪上源)、東南稜一向西的坡地(陶塞溪上源)、以及巴巴山東坡有較大規模的山崩。(3)出露於南峰、東南峰稜脊之石灰岩皆有明顯溶蝕的現象。(4)和平南溪上源之 U 形谷不乏石灰岩巨礫漂石(來自東南峰)，但現生溪床上幾無石灰岩礫石。以上證據顯示，冰川消融後南湖山區，除前述山崩地外，侵蝕量極低(石灰岩稜脊物理侵蝕速率近乎零)。本研究在東南峰南側海拔~3200 m 之草坡土層中採得炭屑(野火產生)，得到兩筆碳十四年代：8032±21 BP 與 8106±21 BP (樹輪校正後~9000 cal BP)，顯示在距今九千年前，此間冰川不僅已完全消融，且曾發生野火事件—即至少東南峰一帶地形的穩定可追溯至距今九千年前或更早。至此，本研究結果與一般台灣山脈「隆升快、侵蝕快」的模式不合。推測台灣高山侵蝕的緩慢(山崩較不頻繁)乃反映此間大地震的稀少(主要地震斷層皆位於山脈周圍)。在這樣的背景下，台灣高山將持續增高，直到永久被冰川覆蓋。

中文關鍵字：冰川地形、山崩、侵蝕、台灣高山

Global distribution of chemical weathering rate: potential shift from erosion and climate change

Jr-Chuan Huang¹、Meng-Chang Lu¹、Pei-Hao Chen¹、Shih-Chien Chan²、
Ying-San Liou³、Chien-Sen Liao⁴、Min-Hui Lo⁵

(1)Department of Geography, National Taiwan University、(2)Department of Geography, National
Changhwa University of Education、(3)Department of Natural Resources and Environmental Studies,
National Dong-Hwa University、(4)Department of Civil and Ecological Engineering, I-Shou
University、(5)Department of Atmospheric Science, National Taiwan University

Chemical weathering, which draws much attention due to its capacity of atmospheric CO₂ drawdown, exhibits a tight interplay between physical erosion and runoff, but its global distribution remains unclear due to its (de) coupling with physical erosion. Here we use data from 211 rivers globally and a modified hydrologic regulation model to quantitatively simulate global distributed SiO₂ yield. Modeling results infer that the sediment concentration of 100 mg L⁻¹ could separate coupling between chemical weathering and physical erosion reasonably and applicably. Under climate scenarios, kinetically-limited weathering in high- and low-mountains account for 29.3 and 24.3% of the increased SiO₂ export, whereas supply-limited weathering in high- and low-mountains contribute 13.4 and 23.0%, respectively. Conclusively, kinetically-limited weathering in mountains predominately responds to SiO₂ increase under climate change, even solely enhanced by runoff; however, the chemical weathering in low-mountains, where both supply- and kinetically-limited weathering are accelerated simultaneously, are more efficiently responsible to climate change.

Keywords: chemical weathering, physical erosion, supply-limited, kinetically-limited, atmospheric CO₂ drawdown

Behavior of radiogenic and stable Sr isotopes of river water and groundwater collected from Hsinwulu River

Hung-Chun Chao¹、Chen-Feng You²、Hou-Chun Liu²、
Chuan-Hsiung Chung²

(1)Department of Earth and Environmental Sciences, National Chung-Cheng University、

(2)Department of Earth Sciences, National Cheng Kung University

Traditional radiogenic Sr isotope is a robust tool as a tracer for water mass in the hydrosphere. However, the variation of stable Sr isotope in the surface water is presently considered controlling by the source, incongruent weathering, and secondary mineral precipitation. River water from main stream and major tributaries of Hsin-wulu River and groundwater were collected and measured their major constitution and dual Sr isotopes. The results of major elements indicate fresh upstream water with high sulfate, calcium, and sodium tributary (Da-Lun River). Ca/Na ratio also indicates a carbonate dominated river water at upstream and shifted to silicate dominated river water after converge with Da-Lun River. Radiogenic Sr isotopes ($^{87}\text{Sr}/^{86}\text{Sr}$) indicate that all tributaries has higher $^{87}\text{Sr}/^{86}\text{Sr}$ than main stream but only Da-Lun River is big enough to increase the main stream significantly. Groundwater in Site DL shows decreasing $^{87}\text{Sr}/^{86}\text{Sr}$ ratio with depth and deep groundwater has the lowest $^{87}\text{Sr}/^{86}\text{Sr}$ ratio among all samples. Stable Sr isotopes ($\delta^{88}\text{Sr}$) show relatively small variation, possible resulting from incongruent weathering and/or minor carbonate precipitation. The limited data indicates the complexity end member of river water in Hsinwulu River and more samples from springs, tributaries, and different seasons are needed to get better understanding of the catchment.

Keywords: Sr isotopes, chemical weathering, river water

The fate of petrogenic organic carbon in Beinan River catchment

Li-Hung Lin¹、Wan-Yin Lien¹、Pei-Ling Wang²、Chih-Tung Chen³

(1)Department of Geosciences, National Taiwan University、(2)Institute of Oceanography, National Taiwan University、(3)Department of Earth Sciences, National Central University

Petrogenic organic carbon (OC_{petro}) had been regarded as non-degradable and excluded from carbon cycle due to its graphite-like structure. Recently, OC_{petro} was inferred to be oxidized by microbial activities in large river systems, hence contributing CO_2 to atmosphere. However, the fate of OC_{petro} in small mountainous river systems where fresh bedrocks rapidly expose to weathering front but with short transport distance is still uncertain. To provide additional constraints, Raman spectroscopy was applied to rocks, soils and river sediments in Beinan catchment and marine sediments alongside Taitung submarine canyon. The degree of graphitization of OC_{petro} was distinguished based on the peak metamorphic temperature versus total full widths (at half maximum). Data derived from bedrocks clustered mostly between lower- and mildly-graphitized level and some in highly-graphitized level. The graphitization degrees of suspended loads and most of bedloads were similar to bedrocks, indicating mechanical mixture of detritus without substantial alteration. However, data points from bedloads in the estuary and soil samples scattered towards disordered level. For marine sediments, the graphitization degrees of samples increase with the travel distance from land. Comparison of Raman parameters demonstrates the impact of long residence time on OC_{petro} in soils and bedload sediments in the estuary, causing degradation of graphitized OC_{petro} . Contrarily, disordered OC_{petro} is preferentially consumed during long transporting; therefore, graphitized OC_{petro} remains in marine sediments at distant location.

Keywords: petrogenic organic carbon, Raman spectroscopy, weathering process

卑南溪流域地下變質岩層破碎帶之化學風化作用

郭欣諾¹、林立虹¹、王珮玲²、邱永嘉³、柯建仲⁴

(1)臺灣大學地質科學系、(2)臺灣大學海洋研究所、(3)臺灣海洋大學地球科學研究所、

(4)中興工程顧問社大地工程研究中心

化學風化為岩石與水的交互作用，得以調節大氣二氧化碳含量。過去關於化學風化的研究主要聚焦於大河系統，透過量測河水的溶質濃度，建立流域尺度的化學風化速率，並探討不同因素對風化速率的影響。除了近地表環境外，化學風化作用亦可能藉由地表水流經裂隙或破裂帶入滲，與地下岩石反應。然而透過河水反推的風化機制並無法解析風化作用進行的確實位置，更鮮有研究探討以變質岩為主之活動造山帶地下化學風化作用。

有鑑於此，本研究藉由大崙溪流域(卑南溪上游)鑽取的岩心，進行岩心產狀的觀察、淋溶試驗、岩石元素豐度的分析，探討於造山帶、片岩為主體的小河流域之地下化學風化作用。透過岩心產狀得知，岩性變化由淺至深依序為地表至 10 公尺深的土壤與崩積層、10 至 60 公尺區段屬黑色片岩夾雜多處厚度不等、破碎、未膠結、粒徑不一的岩屑構成的破碎帶、60 公尺以下以緻密綠色或矽質片岩為主。元素分析顯示破碎帶的總有機碳含量高於圍岩；由淋溶實驗溶質分析結果顯示 SO_4^{2-} 是最主要的陰離子成分，破碎帶樣本平均濃度達 $5.12 \pm 4.5 \text{ mmol g}^{-1}$ ，為相鄰圍岩產率的 2 倍以上。破碎帶與圍岩的淋溶產生的陽離子組成有顯著差異，由 $\text{Ca}^{2+}/\text{Na}^+$ 和 $\text{Mg}^{2+}/\text{Na}^+$ 的關係圖顯示，圍岩產生的溶質多集中於矽酸鹽礦物風化的端成分，而破碎帶淋溶得到的溶質則介於矽酸鹽礦物與碳酸鹽礦物的端成分間。綜合上述，本研究推測大崙溪地下的風化作用主要由黃鐵礦氧化產生的硫酸根所驅動，又因構造作用形成地層的破碎帶，增加礦物與地下水的反應面積，由此可知地下破碎帶對化學風化作用有重要的貢獻，並影響碳循環的收支。

中文關鍵字：卑南溪、化學風化、硫酸根、破碎帶、變質岩

山區裂隙岩層風化帶之水文地質特性

劉慶怡¹、黃柏勳¹、邱永嘉¹、林立虹²、王珮玲³、柯建仲⁴

(1)臺灣海洋大學地球科學研究所、(2)臺灣大學地質科學系、(3)臺灣大學海洋研究所、
(4)中興工程顧問社

台灣位於造山運動活躍的板塊交界處，山區的岩層多經板塊擠壓而破裂，這些破裂及風化帶常是山區地下水存在之處。本研究選定卑南溪流域上游支流之新武呂溪及大崙溪為研究地點，該區沿主流設置數個河川水位與流量測站、雨量站及地下水位站，提供了新武呂溪集水區域之降雨、河川水位、河川流量與地下水位變化情形之紀錄。此外，於大崙溪與新武呂溪之匯流處，建置了大崙水文地質試驗井場，井場內設有四口深度範圍介於 45 公尺至 150 公尺不等的試驗井。該區地表下崩積層深度範圍約小於 10 公尺，岩盤之岩性以片岩為主，依據岩芯資料，特定深度有明顯的裂隙構造存在，推測是地下水流動的主要通道。本研究分析大崙水文地質井場選定井位的長期地下水位資料，探討地下水位變化和集水區域降雨量之間的相關性，並透過抽水試驗，推估大崙水文地質試驗井場的水力參數，分析地下水在岩層風化帶或裂隙中的可能流動路徑。此外，針對新武呂溪流域的河川流量進行基流分離（baseflow separation），初步推估地下水對於河川之補注量，以增進對該區域的水文特性的瞭解。本研究嘗試使用多種水文資料探討山區裂隙岩層風化帶的地下水變化，建立中、小尺度的高山水文地質特性。

中文關鍵字：高山水文地質、地下水、抽水試驗、基流分離、裂隙岩層